

4D-A078 836

ILLINOIS UNIV AT URBANA-CHAMPAIGN DEPT OF CIVIL ENGIN--ETC F/G 13/2  
LONGITUDINAL JOINT SYSTEMS IN SLIP-FORMED RIGID PAVEMENTS. VOLU--ETC(U)  
NOV 79 A M TABATABAIE / E J BARENBERG DOT-FA-11-8474

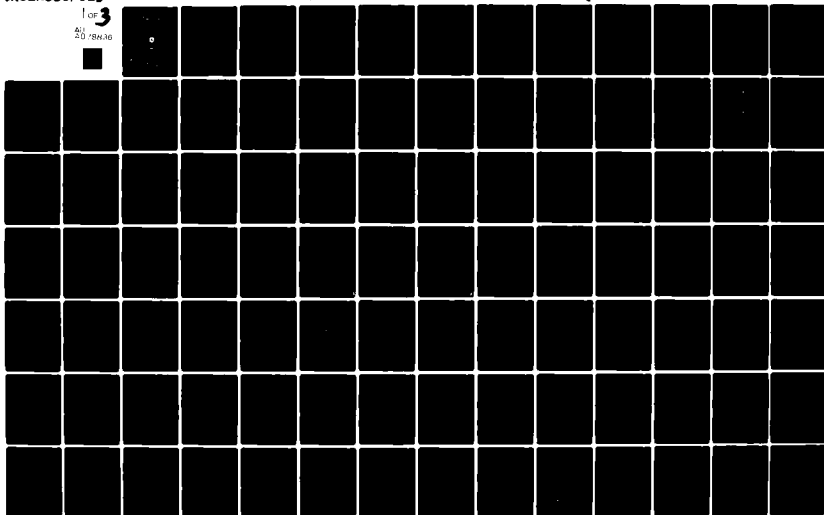
UNCLASSIFIED

FAA-RD-79-4-2

NL

1 OF 3

4/1 20 1984/10



18  
Report No. FAA-RD-79-4-2

12  
11066-20

6  
**LONGITUDINAL JOINT SYSTEMS IN  
SLIP-FORMED RIGID PAVEMENTS.**

**Volume II - Analysis of Load Transfer Systems  
For Concrete Pavements.**

ADA 078836

10  
A.M. Tabatabaie E.J. Barenberg  
R.E. Smith

University of Illinois  
Urbana, Illinois

15 DOT-TH-11-8474

12 193



9 Interim Report  
11 November 1979

Document is available to the U.S. public through  
the National Technical Information Service,  
Springfield, Virginia 22161.

DDC FILE COPY

Prepared for

**U.S. DEPARTMENT OF TRANSPORTATION**  
**Federal Aviation Administration Federal Highway Administration**

Washington, D.C. 20590

3-4-1  
-176 010  
Jm

NOTICE

This document is disseminated under the sponsorship of the Department of Transportation in the interest of information exchange. The United States Government assumes no liability for its contents or use thereof.

1. Report No. <b>FAA-RD-79-4-II</b>	2. Government Accession No.	3. Recipient's Catalog No.	
4. Title and Subtitle <b>Longitudinal Joint Systems in Slip-Formed Rigid Pavements Vol. II Analysis of Load Transfer Systems for Concrete Pavements</b>		5. Report Date <b>November 1979</b>	6. Performing Organization Code
7. Author(s) <b>R. M. Tabatabaie; E. J. Barenberg &amp; R. E. Smith</b>		8. Performing Organization Report No.	
9. Performing Organization Name and Address <b>Department of Civil Engineering University of Illinois Urbana, IL 61801</b>		10. Work Unit No. (TRAIS)	11. Contract or Grant No. <b>DOT-FH-11-8474 MOD #4</b>
12. Sponsoring Agency Name and Address <b>U.S. Department of Transportation Federal Aviation Administration Federal Highway Administration Washington, DC 20590</b>		13. Type of Report and Period Covered <b>Interim</b>	
14. Sponsoring Agency Code <b>ARD-431</b>		15. Supplementary Notes <b>The use of dowels and ties at joints for load transfer methods appears to be both effective and economical and is recommended for use with both slip-form and fixed form type pavers. The authors feel that the problems usually associated with these types of methods can generally be attributed to inadequate design standards rather than to basic deficiencies in the system.</b>	
16. Abstract <b>This report covers the development of rigid pavement joint models, the theoretical evaluation of joint systems and the results and conclusions reached from these studies. This is Volume II of a three volume series on the design and construction of longitudinal joint systems in slip-formed concrete pavements. Volume I - Literature Survey and Field Inspection - dated January 1979, was issued earlier. Volume II - User's Manual is now being printed. This report emphasizes the theoretical evaluation of joint systems. Although the study was primarily for the analysis of longitudinal joint systems for use with slip-formed pavements, the data is applicable to the analysis/design of other types of joints in rigid pavements. The study has been divided into 4 phases. Part 1, Extensive Literature Review; Part 2, Development of Rational Structural Analysis Methods; Part 3, The Finite Element Computer Model is compared with other theoretical Methods; Part 4, Studies Were Made to Define the Interaction of Joint Components and How They Affect the Stresses and Deflections of the Pavements. Cost data are given for the various alternate systems considered.</b>			
17. Key Words <b>Pavement Design, Pavement Construction, Rigid Pavements, Slip-Formed Pavements, Concrete, Joints in Concrete Pavements, Load Transfer</b>		18. Distribution Statement <b>Document is available to the Public through the National Technical Information Service, Springfield, Virginia 22151</b>	
19. Security Classif. (of this report) <b>Unclassified</b>	20. Security Classif. (of this page) <b>Unclassified</b>	21. No. of Pages <b>182</b>	22. Price

1700 010

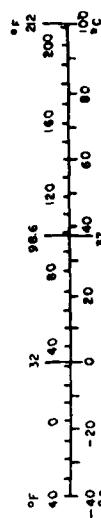
# METRIC CONVERSION FACTORS

## Approximate Conversions to Metric Measures

Symbol	When You Know	Multiply by	To Find	Symbol
<b>LENGTH</b>				
in	inches	2.5	centimeters	cm
ft	feet	30	meters	m
yd	yards	0.9	kilometers	km
mi	miles	1.6		
<b>AREA</b>				
m <sup>2</sup>	square inches	6.5	square centimeters	cm <sup>2</sup>
ft <sup>2</sup>	square feet	0.09	square meters	m <sup>2</sup>
yd <sup>2</sup>	square yards	0.8	square meters	m <sup>2</sup>
mi <sup>2</sup>	square miles	2.6	square kilometers	km <sup>2</sup>
	acres	0.4	hectares	ha
<b>MASS (weight)</b>				
oz	ounces	28	grams	g
lb	pounds	0.45	kilograms	kg
	short tons (2000 lb)	0.9	tonnes	t
<b>VOLUME</b>				
ts	teaspoons	5	milliliters	ml
Tsp	tablespoons	15	milliliters	ml
fl oz	fluid ounces	30	milliliters	ml
c	cup	0.24	liters	l
pt	pint	0.47	liters	l
qt	quart	0.95	liters	l
gal	gallon	3.8	liters	l
cu ft	cubic feet	0.03	cubic meters	m <sup>3</sup>
yd <sup>3</sup>	cubic yards	0.76	cubic meters	m <sup>3</sup>
<b>TEMPERATURE (exact)</b>				
°F	Fahrenheit temperature	5/9 (after subtracting 32)	Celsius temperature	°C

## Approximate Conversions from Metric Measures

When You Know	Multiply by	To Find	Symbol
<b>LENGTH</b>			
millimeters	0.04	inches	in
centimeters	0.4	inches	in
meters	3.3	feet	ft
meters	1.1	yards	yd
kilometers	0.6	miles	mi
<b>AREA</b>			
square centimeters	0.16	square inches	in <sup>2</sup>
square meters	1.2	square yards	yd <sup>2</sup>
square kilometers	0.4	square miles	mi <sup>2</sup>
hectares (10,000 m <sup>2</sup> )	2.5	acres	
<b>MASS (weight)</b>			
grams	0.035	ounces	oz
kilograms	2.2	pounds	lb
tonnes (1000 kg)	1.1	short tons	
<b>VOLUME</b>			
milliliters	0.03	fluid ounces	fl oz
liters	2.1	pints	pt
liters	1.06	quarts	qt
liters	0.26	gallons	gal
cubic meters	35	cubic feet	ft <sup>3</sup>
cubic meters	1.3	cubic yards	yd <sup>3</sup>
<b>TEMPERATURE (exact)</b>			
°C	Celsius temperature	9/5 (then add 32)	Fahrenheit temperature



\* 1 in = 2.54 centimeters. For other exact conversions, use and more detailed tables. See NBS Special Publication 400-1, Units of Measurement, Price \$2.25, SO Calif. of No. C-110-246.

# TABLE OF CONTENTS

## CHAPTER

Page

1	INTRODUCTION . . . . .	1
	1.a General . . . . .	1
	1.b Joint Functions . . . . .	2
	1.b.(1) Contraction Joints . . . . .	4
	1.b.(2) Expansion Joints . . . . .	4
	1.b.(3) Construction Joints. . . . .	4
	1.b.(4) Longitudinal Joints. . . . .	5
	1.c Load Transfer Systems . . . . .	5
	1.d Analysis of the Problem . . . . .	9
	1.e Scope of the Study of Methods of Analysis . . . . .	9
2	PERFORMANCE OF JOINTS AS RELATED TO EXISTING METHODS OF DESIGN AND ANALYSIS OF CONCRETE PAVEMENTS. . . . .	12
	2.a General . . . . .	12
	2.b Existing Methods of Analysis and Design . . . . .	13
	2.a.(1) Bending of Plates on Winkler Foundation. . . . .	13
	2.b.(2) Bending of Plates on Elastic Solid Foundation. . . . .	16
	2.b.(3) Finite-Element and Discrete-Element Models . . . . .	17
	2.b.(4) Analysis and Design of Dowel Bars. . . . .	23
	2.b.(5) Aggregate Interlock as a Load Transfer Mechanism. . . . .	40
	2.b.(6) Keyed Joints . . . . .	44
	2.c Limitations of Present Methods of Analysis and Design . . . . .	44
3	DEVELOPMENT OF THE ANALYTICAL MODELS FOR ANALYSIS OF JOINTED CONCRETE PAVEMENTS AND PAVEMENT JOINTS . . . . .	46
	3.a General . . . . .	46
	3.b The Finite-Element Method . . . . .	47
	3.b.(1) Finite-Element Modeling of the Jointed Concrete Pavement and Pavement Joints . . . . .	47
	3.b.(2) Development of Stiffness Matrix for Rectangular Plate Element for Concrete Slab, Stabilized Base, and Overlay. . . . .	54
	3.b.(3) Stiffness Matrix for Beam Element for Dowel Bar. . . . .	63
	3.b.(4) Stiffness Matrix for Spring Element for Aggre- gate Interlock System and Keyway . . . . .	65
	3.b.(5) Overall Stiffness Matrix . . . . .	65
	3.b.(6) Computer Program . . . . .	66

CHAPTER		Page
3.c	Verification of the Finite-Element Model. . . . .	66
3.c.(1)	Comparison with Westergaard's Solutions. . . . .	67
3.c.(2)	Comparison with Influence Charts . . . . .	67
3.c.(3)	Comparison with AASHO Road Test Results. . . . .	69
3.c.(4)	Comparison with Public Roads Test Results. . . . .	73
3.d	Summary . . . . .	75
4	APPLICATION OF THE METHOD TO ANALYSIS OF JOINTED CONCRETE PAVEMENTS AND PAVEMENT JOINTS. . . . .	79
4.a	General . . . . .	79
4.b	Doweled Joints. . . . .	79
4.c	Joints with Aggregate Interlock . . . . .	105
4.d	Keyed Joints. . . . .	112
4.e	Butt Joints on Stabilized Bases . . . . .	128
4.f	Thickened Edge Slab with Butt Joints. . . . .	129
4.g	Example Problem . . . . .	134
5	SUMMARY AND CONCLUSIONS. . . . .	143
5.a	General Summary . . . . .	143
5.b	Cost Analysis . . . . .	152
5.c	Recommendations for Design. . . . .	155
6	RECOMMENDATIONS FOR FURTHER STUDY. . . . .	164
	LIST OF REFERENCES. . . . .	167
	APPENDIX A - TABULATION OF STIFFNESS MATRIX AND LOAD VECTOR . . . . .	172

## LIST OF FIGURES

Figure	Page
1-1 Joint Types. . . . .	3
1-2 Tie Bars . . . . .	8
2-1 Comparison of Winkler Foundation with Elastic Solid Foundation . . . . .	14
2-2 Discrete-Element Model of Concrete Pavement Slab (Ref. 24) . .	18
2-3 Specialized Finite-Element Representation of Joints with Partial Moment Transfer (Ref. 30). . . . .	21
2-4 Pressure Exerted on a Loaded Dowel Bar . . . . .	26
2-5 Effect of Dowel Size on Progressive Failure Load (Ref. 38) . .	32
2-6 Data on Initial Dowel Looseness (Ref. 35). . . . .	33
2-7 Effect of Load Magnitude and Number of Load Cycles on Dowel Looseness (Ref. 35). . . . .	34
2-8 Relation between Dowel Diameter and Dowel Looseness (Ref. 35). .	35
2-9 Relation between Length of Dowel Embedment and Dowel Looseness (Ref. 35). . . . .	36
2-10 Relation between Width of Joint Opening and Dowel Looseness (Ref. 35). . . . .	37
2-11 Relation between Dowel Looseness and Loss in Initial Load Transfer (Ref. 35) . . . . .	38
2-12 Effect of Repeated Loadings on Joint Efficiency (Ref. 16). . .	42
2-13 Influence of Joint Opening on Effectiveness of Aggregate Interlock (Ref. 53). . . . .	43
2-14 Nomograph for Design of Aggregate Interlock Joints for a Specified Long-Term Efficiency (Ref. 53) . . . . .	43
3-1 A Typical Longitudinal and a Typical Transverse Section of a Jointed Concrete Pavement System . . . . .	48
3-2 A Typical Finite-Element Mesh Used for Two-Dimensional Analysis . . . . .	49
3-3 Finite-Element Model of Pavement System. . . . .	51



Figure	Page
3-4 A Typical Finite-Element Mesh Used for Three-Dimensional Analysis. . . . .	53
3-5 Comparison of Finite-Element Solutions with Westergaard's Equations . . . . .	68
3-6 Influence Chart for the Moment in a Concrete Pavement Due to Interior Loading (Ref. 3). . . . .	70
3-7 Influence Chart for the Moment in a Concrete Pavement Due to Edge Loading (Ref. 3). . . . .	71
3-8 Comparison of Finite-Element Solutions with those Computed by Pickett's Influence Charts . . . . .	72
3-9 Comparison of Edge Stresses Computed with Finite-Element Program and those Measured at the AASHO Road Test . . . . .	74
3-10 Comparison of Slab Deflections Computed with Finite-Element Program and those Measured at the Public Roads Test . . . . .	76
3-11 Comparison of Joint Deflections and Stresses Computed with Finite-Element Program and those Measured at the Public Road Test . . . . .	77
4-1 Various Loading Cases . . . . .	81
4-2 Comparison of Dowel Shear Forces Computed with Finite-Element Program with Conventional Analysis. . . . .	84
4-3 Effect of Dowel Spacing and Load Position on the Maximum Dowel Shear Force . . . . .	85
4-4 Effect of Dowel Bars in Reducing Maximum Tensile Edge Stresses. . . . .	87
4-5 Effect of Dowel Bars in Reducing Maximum Edge Deflections . . .	88
4-6 Effect of Multiple Loads on Maximum Tensile Edge Stresses . . .	90
4-7 Effect of Multiple Loads on Maximum Edge Deflections. . . . .	91
4-8 Effect of Multiple Loads on Maximum Dowel Shear Forces. . . . .	92
4-9 Comparison of the Finite-Element Solutions with Timoshenko's Solution for Dowel Deflections. . . . .	94
4-10 Comparison of the Finite-Element Solutions with Timoshenko's Solution for Concrete Bearing Stresses. . . . .	95

Figure	Page
4-11 Effect of Concrete Modulus, Slab Thickness, Dowel Diameter and Subgrade Modulus on Maximum Concrete Bearing Stress . . . .	96
4-12 Effect of Concrete Modulus, Slab Thickness, Dowel Diameter and Subgrade Modulus on Maximum Dowel Deflection. . . . .	97
4-13 Design Chart for Dowel Bars, for Various Load Positions . . . .	99
4-14 Design Chart for Dowel Bars for Various Concrete Modulus. . . .	100
4-15 Relation between Concrete Bearing Stress and Dowel Looseness, after 600,000 Load Applications . . . . .	103
4-16 Joint Faulting on Plain Jointed Concrete Pavements at the AASHO Road Test Site (Ref. 58). . . . .	104
4-17 Relation between Concrete Bearing Stress and Joint Faulting .	106
4-18 Relation between Joint Efficiency (Eff) and Spring Stiffness (Agg) . . . . .	108
4-19 Effect of Aggregate Interlock in Reducing Maximum Tensile Edge Stresses. . . . .	109
4-20 Effect of Aggregate Interlock in Reducing Maximum Edge Deflections . . . . .	110
4-21 Combined Effect of Bonded Stabilized Base and Aggregate Interlock in Reducing Maximum Tensile Edge Stresses . . . . .	111
4-22 Effect of Slab Thickness on Maximum Shear Stresses at Joint Interface . . . . .	113
4-23 Effect of Keyway in Reducing Maximum Tensile Edge Stresses. .	114
4-24 Effect of Keyway in Reducing Maximum Edge Deflections . . . .	115
4-25 A Typical Finite-Element Mesh Used for Analysis of Keyed Joints. . . . .	117
4-26 Distribution of Nodal Forces Normal to the Contact Boundaries for Different Key Designs . . . . .	118
4-27 Tensile Stress Contours for a Standard Key in a 16 in. (40.6 cm) Slab, Male Side . . . . .	119
4-28 Tensile Stress Contours for a Standard Key in a 16 in. (40.6 cm) Slab, Female Side . . . . .	120
4-29 Tensile Stress Contours for a Round Smooth Key in a 16 in. (40.6 cm) Slab, Male Side . . . . .	121

Figure	Page
4-30 Tensile Stress Contours for a Round Smooth Key in a 16 in. (40.6 cm) Slab, Female Side. . . . .	122
4-31 Tensile Stress Contours for a Standard Key in a 12 in. (30.5 cm) Slab . . . . .	123
4-32 Tensile Stress Contours for a Standard Key in a 12 in. (30.5 cm) Slab on a 10 in. (25.4 cm) Cement Stabilized Base. .	124
4-33 Effect of Bonded Stabilized Base in Reducing Maximum Tensile Edge Stresses. . . . .	130
4-34 Effect of Bonded Stabilized Base in Reducing Maximum Edge Deflections. . . . .	131
3-35 Effect of Thickened Edge Slab in Reducing Maximum Tensile Edge Stresses. . . . .	132
4-36 Effect of Thickened Edge Slab in Reducing Maximum Edge Deflections. . . . .	133
4-37 Possible Joint Designs for the Example Problem . . . . .	135
4-38 Possible Layout of Joints with French Keying Device. . . . .	138
4-39 Effectiveness of French Keying Device on Joint Efficiency. . .	139
5-1 Equivalent Pavement Systems Based on Maximum Edge Stress Criterion. . . . .	146
5-2 Figure Eight Steel Load Transfer Device (Schematic). . . . .	147
5-3 Alternate "Z" Joint for Longitudinal Joints with Slip-Form Paving Operations. . . . .	148
5-4 Alternate Construction Procedure for Installing Dowels at Longitudinal Joints with Slip-Form Paving Operations . . . . .	149
5-5 Typical Failure Patterns in Pavement Sections of O'Hare Airport. . . . .	158
5-6 Recommended Load Transfer Devices for Airport Pavements Designed for 727 Class Aircraft. . . . .	160
5-7 Recommended Load Transfer Devices for Airport Pavements Designed for DC-8 Class Aircraft . . . . .	161
5-8 Recommended Load Transfer Devices for Airport Pavements Designed for Wide-bodied Aircraft. . . . .	162

# LIST OF TABLES

Table		Page
1-1	Dowel Size and Spacing (Ref. 1). . . . .	7
2-1	Range of Modulus of Dowel Reactions from Various Sources (Ref. 43). . . . .	28
2-2	Ratio of Concrete Bearing Stress to Compressive Strength of Concrete (Ref. 44). . . . .	30
2-3	Progressive Failure Loads (Ref. 38). . . . .	30
2-4	Loss in Joint Efficiency (Ref. 16) . . . . .	41
4-1	A Typical Result of Maximum Slab Stress and Deflection and Maximum Dowel Shear Force Due to Various Load Position . . . .	82
4-2	Dowel Looseness Resulting from 600,000 Cycles of a 10 Kips (44 KN) Load (Ref. 35) . . . . .	102
4-3	Effect of Key Design on Maximum Tensile Stress in the Slab . .	125
4-4	Effect of Slab Thickness on Maximum Tensile Stress in the Slab . . . . .	126
4-5	Effect of Cement Stabilized Base on Maximum Tensile Stress in the Slab. . . . .	127
5-1	Loads and Bearing Stresses at Transverse Joints at O'Hare. . .	159

## CHAPTER 1

### INTRODUCTION

#### 1.a General

This report along with an earlier report entitled "Longitudinal Joint Systems in Slip-Formed Rigid Pavements: Vol. I, Literature Survey and Field Inspection," (63) and Vol. III, User's Manual, are presented in fulfillment of the requirements of this phase of the contract DOT-FH-11-8474 (Mod #4). This report covers the development of models, the theoretical evaluation of alternate joint systems, findings and conclusions from this study, plus recommendations for implementation of the findings and conclusions from this study, plus recommendations for implementation of the findings and for further studies. Background of the specific problem and its seriousness were presented in the earlier report (63).

This report emphasizes the *theoretical evaluation of the joint system*. While the major emphasis of this study was the analysis of longitudinal joint systems for use with slip-formed pavements, it is obvious that the findings and conclusions reached have much wider implications. In fact, the models presented in this report, should logically form the basis for significantly improved design procedures for rigid pavements. As a minimum, these models and analysis techniques will provide the tools for the design and analysis for various pavement systems with both longitudinal and transverse joints systems.

Field studies and field verification of these models were not part of this modification of the contract. Tools are presented for the detailed analysis of pavement systems with various types of longitudinal and transverse joints, but actual performance of these systems are being validated through testing of field installations.

### 1.b Joint Functions

Concrete structure members are subjected to changes in volume due primarily to changes in moisture content, and temperature. If volume change in concrete is excessively restrained, then cracking, distortion, or crushing due to excessive stresses (or strains) can occur.

Joints are placed in concrete pavement slabs to control cracking and provide space and freedom of movement. Joints may also be required to facilitate construction, such as longitudinal joints, without serving any other structural purpose. Although joints are introduced in concrete slabs partially to control cracks, problems associated with joints continue to exist, result from pavement use, improper joint design and improper construction methods.

Load is transferred across a joint principally by shear. Some moment may be transferred through some types of joints, particularly doweled joints, or across joints with the French connectors described later. The amount of moment transfer is negligible however, and should not be relied upon in pavement design calculations. Thus, joints are structural weaknesses in the pavement system and stresses and deflections at the joints should be of major concern to the designer. Lack of attention to such structural weakness in concrete pavement slabs causes most of the problems usually lamented by the maintenance engineer.

To minimize the effect of planes of weakness, adequate load transfer capability must be built into a joint, or the pavement system must be strengthened in some other manner such as by improving the slab support or by increasing slab thickness.

Concrete pavement joints may be designed as contraction, expansion, construction, or longitudinal joints according to their construction and function.

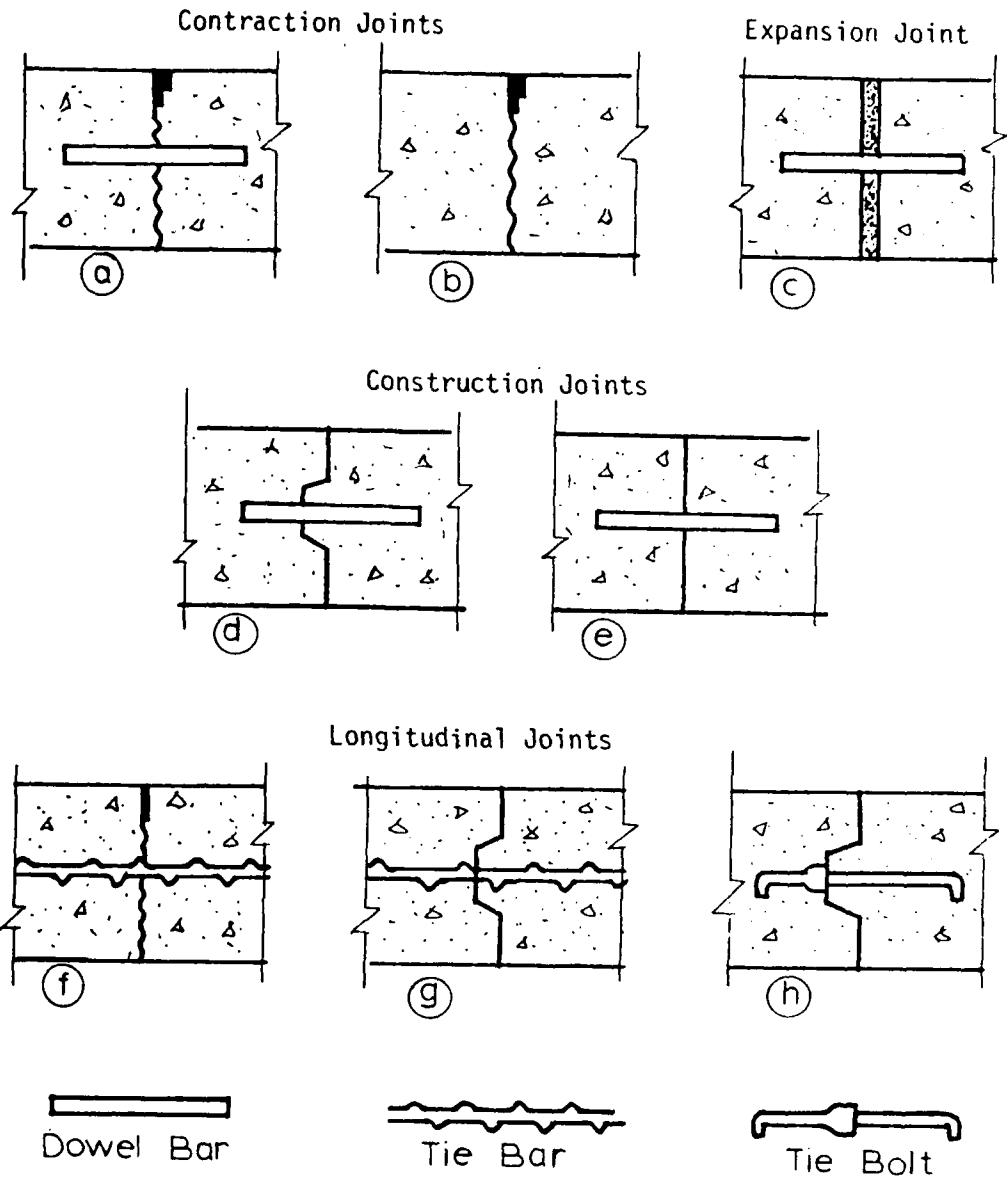


Figure 1-1. Joint Types

#### 1.b.(1) Contraction Joints

Contraction joints are designed to prevent intermediate transverse random cracking of concrete slabs due to slab shortening (Figures 1-1-a, 1-1-b). Under normal warm-weather construction conditions the pavement slab attains its greatest length soon after placement due to high temperatures associated with the hydration of the cement. As temperature decreases and hydration heat diminishes, resulting in contraction of the concrete, which combined with some drying shrinkage, causes slab to shorten significantly at early ages. Contraction joints are placed in concrete slabs to permit unrestrained movement, thus reducing frictional drag stresses induced in the concrete to tolerable values. Contraction joints are usually formed by weakening the pavement cross section, either by grooving the fresh mix, embedding an insert strip, or sawing a groove as soon as the concrete has attained sufficient strength to allow sawing without raveling but before shrinkage occurs. Contraction joints may or may not be fitted with load transfer devices. If load transfer devices are not provided then the entire load transfer at these joints must be by aggregate interlock.

#### 1.b.(2) Expansion Joints

Expansion joints are intended to provide space for concrete slab expansion (Figure 1-1-c). Expansion of slabs may result from temperature or moisture increase, or from some unusual condition that causes abnormal growth or lengthening of the concrete. The joints are built by placing a compressible filler material throughout the full depth of the concrete slab. Expansion joints always have load transfer devices, or are strengthened by thickening the pavement edge or both.



### 1.2.(3) Construction Joints

Construction joints are used at planned interruptions of paving operations such as at the end of each day's work, at leave-outs for bridges, at intersections, and where emergency interruptions suspend operation for 30 minutes or more. Often transverse construction joints fall at planned locations for expansion or construction joints and are built to conform with the specifications for those joints (Figures 1-1-d, 1-1-f).

### 1.b.(4) Longitudinal Joints

Longitudinal joints are located between paving lanes and are either weakened-plane joints as shown in Figure 1-1-a or construction joints (Figure 1-1-g, 1-1-h). They may have dowels in place of ties.

Weakened-plane joints are normally used at the center of a two or more pavement lanes when cast in a single operation. The purpose of such a joint is to reduce stresses due to combined effect of temperature curling, moisture warping and loading. Construction joints are used where adjacent pavement lanes constructed separately join to form a continuous pavement. These are full-depth joints with abutting plain faces or with formed keys and keyways. Horizontal movement of these joints can be restrained by tie bars or tie bolts. Figures 1-1-g and 1-1-h show longitudinal construction joints with tie bar and tie bolt, respectively. Wide runway pavements usually have a combination of different longitudinal joints allowing lateral movement in some joints while preventing movement in others.

### 1.c Load Transfer Systems

The high stresses and deflections at slab edges can be reduced by providing load transfer systems across the joint. Load transfer across the joint is developed by one or a combination of:

- (1) Aggregate interlock,
- (2) Dowel bars, and
- (3) Keyways.

Aggregate interlock is the simplest means of load transfer system. The irregular faces of the cracks that form below the groove or saw cut provide some load transfer when the resulting joint opening is small such as when short joint spacing is used. Aggregate interlock is normally used as the only load transfer mechanism only when traffic volume is low, and the pavement has a firm support such as a stabilized subbase.

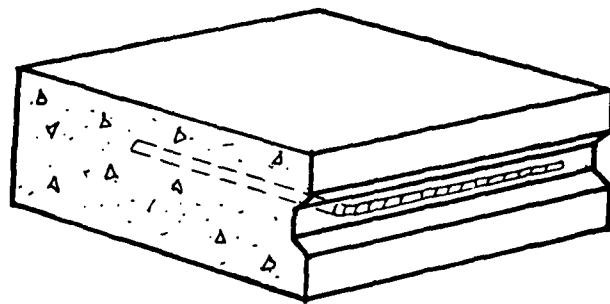
Mechanical load transfer devices are used world-wide in the joints of concrete pavements. Many alternative designs have been used, some of which are simple structural shapes, others quite elaborate. Currently, however, smooth, round, dowel bars are the most popular devices and are used by most of the agencies because their performance, simple structural shape and low cost. Table 1-1 gives the typical suggested dowel size and spacing for concrete pavements. Dowels are normally installed in a single row at mid-depth of the slab.

Keyed joints have long been used in the longitudinal joints of paving lanes, where slab thickness is 8 in. (20 cm) or greater are specified. Pavement slabs can be cast with either female keyway containing bent tie bars or threaded inserts (Figure 1-2), or male keyway cast first and the mating slab cast adjacent thereto. To complete the joint, when the female side with bent tie bars are cast first the bent bars are straightened or sections are threaded into the inserts prior to placement of the adjacent slabs.

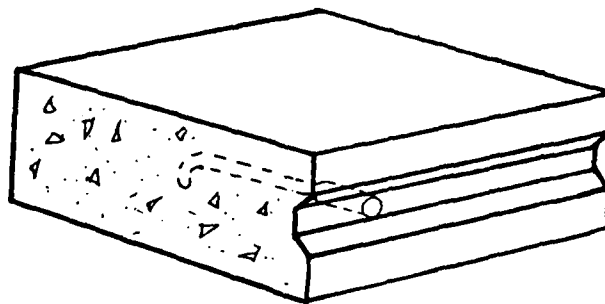
Tie bars of 1/2 or 5/8 in. (13 or 16 mm) diameter, 24 to 48 in. (61 to 122 cm) long and spaced at 18 to 48 in. (46 to 122 cm) intervals are normally

Table 1-1. Dowel Size and Spacing (Ref. 1)

Slab Depth	Dowel Diameter		Dowel Length		Dowel Spacing	
in. (cm)	in.	(mm)	in.	(cm)	in.	(cm)
5-6 (13-15)	3/4	(19)	16	(41)	12	(30)
7-8 (18-20)	1	(25)	18	(46)	12	(30)
9-11 (23-28)	1-1/4	(32)	18	(46)	12	(30)
12-16 (30-41)	1-1/2	(38)	20	(51)	15	(38)
17-20 (43-51)	1-3/4	(44)	22	(56)	18	(46)
21-25 (53-64)	2	(51)	24	(61)	18	(46)



a) Bent Bar



b) Threaded Bolt

Figure 1-2. Tie Bars

used as ties to restrain lateral movement at keyed joints or joints with aggregate interlock. Installation of load transfer systems along the longitudinal joints when casting pavement with slip form pavers is often a serious construction problem.

#### 1.d Analysis of the Problem

To achieve a balanced design of the jointed concrete pavement system, that is a design in which the pavement near the joint performs as well as the interior of the slab, it is necessary to be able to analyze the response of the pavement system under the expected loading conditions with the appropriate joint systems. Therefore, the structural analysis of the system with regard to the evaluation of the stresses, strains, and displacements within the critical regions of the system is of major concern. Based upon the reliability of the structural analysis method, parts of the system may be over-designed or under-designed. Thus, for a balanced design of jointed concrete pavement system, it is required that a rational structural analysis of the system be completed. Most concrete pavement slabs are designed by assuming continuous slabs, infinite in extent, calculating the stresses and deflections for the continuous slab and then superimposing the selected joint system on the slab. However, pavement joints and load transfer systems which are an integral part of the pavement structure effect all pavement components, should be taken into consideration in a rational analytical model used for concrete pavement analysis.

#### 1.e Scope of the Study of Methods of Analysis

The purpose of this study was to develop a structural analysis method for jointed concrete pavements and pavement joints that would adequately characterize the structural response of the jointed system to applied load.

Special emphasis for this study was to develop models which would permit the analysis of joint systems which could be used with either slip form or fixed form pavers. This portion of the study was divided into 4 phases.

Phase 1 was an extensive literature review and evaluation that considered the methods of analysis and design of concrete pavement joint systems. The results of theoretical approaches as well as laboratory and field investigations were included. The structural failure modes of jointed concrete pavements as influenced by the characteristics of the joint system were also reviewed. Results from Phase 1 are presented in Chapter 2.

Phase 2 emphasized the development of a rational structural analysis method for jointed concrete pavement systems. Phase 1 findings indicated the desirability of developing a finite-element model for the structural analysis of these systems, and the analysis and the modeling was broken down into a two-dimensional and a three-dimensional analysis stages.

The two-dimensional analysis is based on a finite-element model developed from the classical theory of medium-thick plate on Winkler foundation. Various types of load transfer systems such as dowel bars, aggregate interlock, keyways, or a combination thereof could be considered at the pavement joints. Dowel bars at the pavement joints were treated as linearly elastic beam elements located at the neutral axis of the slab. Linearly elastic spring elements were employed for modeling aggregate interlock or keyways for load transfer system at the pavement joints. The model developed is capable of analyzing pavement slabs supported by a stabilized base or slabs with flexible or rigid overlays.

A three-dimensional finite element model was developed for analysis of the concrete pavement in the vicinity of the joint. Input to the three-dimensional model was linked to the two-dimensional analysis to

to provide appropriate boundary conditions for the analyses. Phase 2 results are presented in Chapter 3.

In Phase 3, the structural models developed in Phase 2 were validated by comparing the finite-element solutions with available theoretical solutions (Refs. 2, 3), and the results of previous experimental studies (Refs. 4, 5). No field investigations were carried out to validate the structural analysis models developed. Phase 3 results are presented in Chapter 3.

In Phase 4, the structural models were used to perform a parameter studies to define the interaction among the various factors affecting the stresses and deflections of the concrete pavements at or near the joints. Other applications of the model to concrete pavement analysis and design are illustrated in several example problems presented in Chapter 4. Chapter 5 presents a comparison of various joint systems compatible for use in longitudinal joints for slip formed rigid pavements. Comparative cost data are presented for several of the alternate systems as available. Design recommendations for longitudinal and transverse joints, based on the current technology, are also presented in Chapter 5.

Chapter 6 gives recommendations for validation of the findings from this study.

## CHAPTER 2

### PERFORMANCE OF JOINTS AS RELATED TO EXISTING METHODS OF DESIGN AND ANALYSIS OF CONCRETE PAVEMENTS

#### 2.a General

In reviewing the results from the field surveys for this project, and from discussions with pavement engineers, it can be concluded that the performance of concrete pavements is controlled by the performance of the joints, and of the concrete slabs in the immediate vicinity of the joints. Several engineers visited as well as the evidence seen by the project staff on pavements in service, clearly indicates nearly all distress in concrete pavements occurs near the joints and is directly related to the behavior and performance of the joint system. If realistic designs procedures are to be developed for concrete pavements the design of the joints must be an integral part of that procedure, and not something to be added at a later time.

The primary thrust of this study was to evaluate alternate joint systems for longitudinal joints for use with slip formed pavements. While it is apparent that the design of a joint system for the longitudinal joints for use with slip formed pavements will give restraints to the type of joint system which can be installed, once a joint system is installed whether it is a longitudinal or transverse joint will have little effect on how the joint system affects the behavior of the pavement. For purposes of this study all joints were considered on the same basis for evaluating their performance and their effect on pavement behavior. A doweled joint system for example, is considered in the same manner whether used as a longitudinal joint between paving lanes or as load transfer for a transverse joint. There



may be some differences in the performance of the two joints because of the repetitive nature of the loads but not in the behavior of the joints under a given load.

## 2.b Existing Methods of Analysis and Design

The determination of stresses and deflections in concrete pavement slabs, due to loading, has been a subject of major concern for several years. Several theories for analyzing pavement slabs have been developed, but the classical bending theory of a medium-thick plate, because of its simplicity and validity, has been the most popular. Development of the classic differential equation for a medium-thick plate is presented in many standard references, including Reference 20, and will not be repeated here. The partial differential equation (2-1), forms the basis of the method of analysis considered most realistic by most investigators.

$$\frac{Eh^3}{12(1 - \mu^2)} \left( \frac{\partial^4 w(x, y)}{\partial x^4} + 2 \frac{\partial^4 w(x, y)}{\partial x^2 \partial y^2} + \frac{\partial^4 w(x, y)}{\partial y^4} \right) = p(x, y) - q(x, y) \quad (2-1)$$

where:

$E$  = modulus of elasticity of the concrete slab

$\mu$  = Poisson's ratio of the concrete slab

$h$  = thickness of the concrete slab

$w(x, y)$  = deflection of the slab at point  $(x, y)$

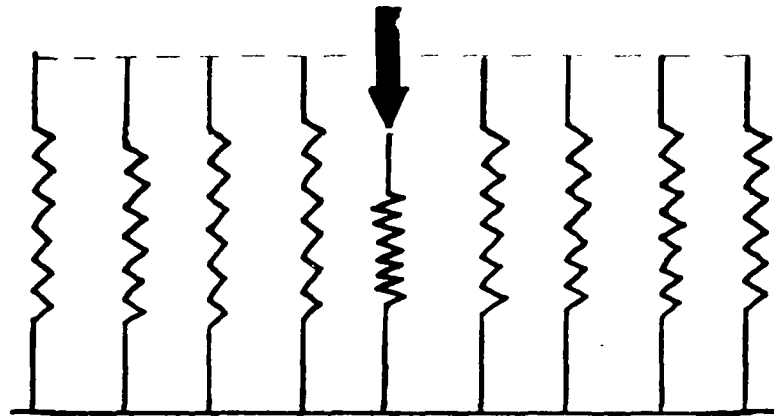
$p(x, y)$  = externally applied load

$q(x, y)$  = reaction of the idealized subgrade

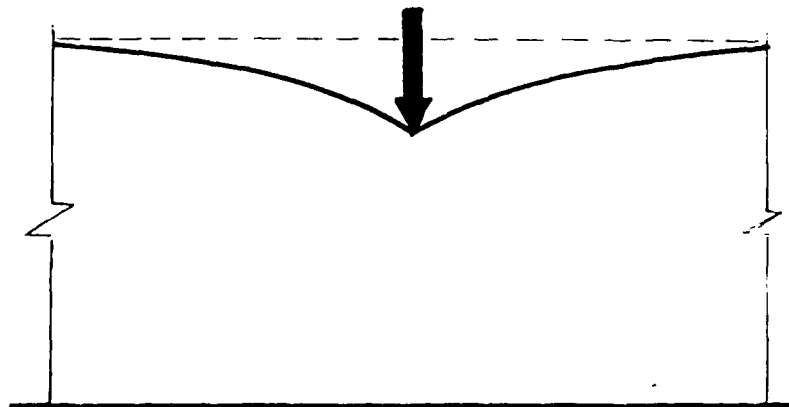
In this method it is assumed that the plate is continuously and uniformly supported, and the subgrade provides only vertical reaction to the slab.

### 2.b.(1) Bending of Plates on Winkler Foundation

In 1926 Westergaard (Ref. 2), assuming that the reactive pressure



a) Winkler Foundation



b) Elastic Solid Foundation

Figure 2-1. Comparison of Winkler Foundation with Elastic Solid Foundation

between subgrade and slab at any given point to be proportional to the deflection at that point (Winkler foundation, see Figure 2-1-a), developed some mathematical models for determining the critical stresses in an infinitely large concrete slab, under a single load, for three cases of loadings, namely, corner, edge, and interior. The equations shown below were developed by Westergaard to give the maximum stresses and deflections in the concrete slab for the specified loading cases.

Case 1. Interior load

$$\sigma = 0.275 (1 + \mu) \frac{P}{h^2} (4 \log \frac{\ell}{b} + 1.069) \quad (2-2)$$

$$\Delta = \frac{P}{k\ell^2} \left[ \left(1 - \frac{a^2}{\ell^2}\right) (0.217 - 0.367 \log \frac{a}{\ell}) \right] \quad (2-3)$$

Case 2. Edge load

$$\sigma = 0.497 (1 + \mu) \frac{P}{h^2} (4 \log \frac{\ell}{b} + 0.359) \quad (2-4)$$

$$\Delta = \frac{1}{\sqrt{6}} (1 + 0.4 \mu) \frac{P}{k\ell^2} \quad (2-5)$$

Case 3. Corner load

$$\sigma = \frac{3P}{h^2} \left[ 1 - \left( \sqrt{2} \frac{a}{\ell} \right)^{0.6} \right] \quad (2-6)$$

$$\Delta = \frac{P}{k\ell^2} (1.1 - 0.88 \sqrt{2} \frac{a}{\ell}) \quad (2-7)$$

where:

$\sigma$  = the maximum bending stress at the extreme faces of the slab

$\Delta$  = the maximum deflection of the slab

P = applied load

a = radius of a circular loaded area

$b = \sqrt{1.6 a^2 + h^2} - 0.675 h$ , for  $a < 1.74 h$

$b = a$ , for  $a > 1.74 h$

k = modulus of subgrade support

$\ell$  = radius of relative stiffness of the pavement with respect to subgrade given by

$$\ell = \sqrt[4]{\frac{Eh^3}{12(1 - \mu^2)k}} \quad (2-8)$$

To extend the method for analysis of slabs with multiple loads, Pickett and Ray (Ref. 3) developed influence charts, which have been employed by the Portland Cement Association (PCA) (Ref. 1) for the design of concrete pavements.

#### 2.b.(2) Bending of Plates on Elastic Solid Foundation

In 1938 Hogg (Ref. 21) and Holl (Ref. 22) by assuming the subgrade to behave as an elastic foundation of infinite depth developed mathematical equations for determining the critical stress and deflection in infinitely large slabs under a single load applied at an interior point on the slabs. The significant difference between an elastic solid subgrade and the Winkler foundation is shown in Figure 2-1. The following equations give the maximum stress and deflection in the slab due to a symmetrical load applied at the interior of the slab. Note that equations for an elastic slab on an elastic solid subgrade have not been solved for edge and corner loading conditions.

$$\sigma = -\frac{6P}{h^2} (1 + \mu) \left( 0.1833 \log \frac{a}{\ell_e} - 0.049 - 0.0120 \frac{a^2}{\ell_e^2} \right) \quad (2-9)$$

$$\Delta = \frac{P\ell_e^2}{3\sqrt{3} D} \left[ 1 - \frac{a^2}{\ell_e^2} (0.144 - 0.238 \log \frac{a}{\ell_e}) \right] \quad (2-10)$$

where:

$$\ell_e = 3\sqrt{\frac{2D}{C}} \quad (2-11)$$

$$D = \frac{Eh^3}{12(1 - \mu^2)} \quad (2-12)$$

$$C = \frac{E_s}{2(1 - \mu_s^2)} \quad (2-13)$$

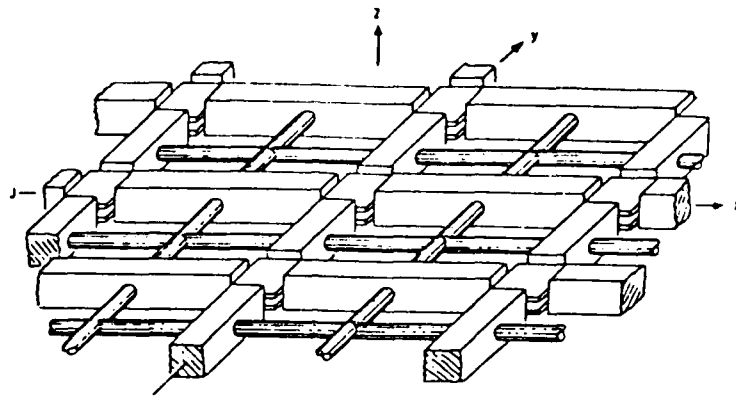
$E_s$  = modulus of elasticity of the subgrade

$\mu_s$  = Poisson's ratio of the subgrade

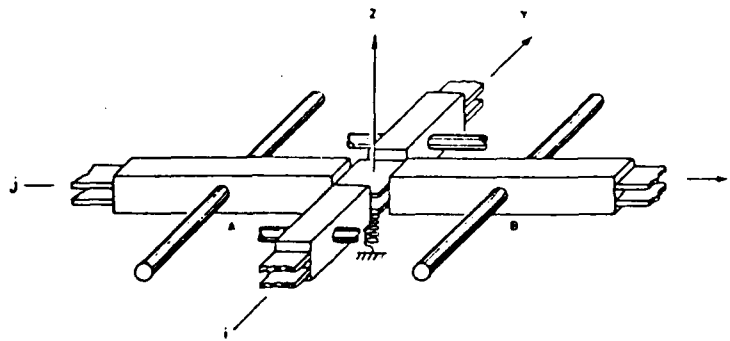
### 2.b.(3) Finite-Element and Discrete-Element Models

The theoretical solutions discussed heretofore were based on an assumed infinitely large slab with no discontinuities, with a load at the corner, on the edge, or at an interior position. These analyses may not be applicable to a finite slab with most traffic moving at a short distance from the slab edges. Furthermore, these methods were developed for ideal cases where there are no joints or cracks, and for slabs with uniform thickness, and uniform subgrade support. With the development of high speed computers and the powerful finite-element and discrete-element methods, it is now possible to analyze concrete pavements in a more realistic manner.

Use of discrete-element method for structural analysis of plates was pioneered by Newmark (Ref. 23) and Ang and Newmark (Ref. 61). Later this method was employed by various investigators, Hudson and Matlock (Ref. 35), and Vesic and Saxena (Ref. 25) for analysis of concrete pavement slabs. In



a) Discrete-Element Model of a Plate or Slab



b) A Typical Joint Taken from Discrete-Element Model

Figure 2-2 Discrete-Element Model of Concrete Pavement Slab (Ref. 24)

developing a discrete-element model to simulate pavement slabs as, for example, by Hudson and Matlock, the concrete slab was considered as an assemblage of elastic joints, rigid bars, and torsional bars as shown in Figures 2.2. This model is helpful in visualizing the problem and forming the solution. The model consists of:

- (1) Infinitely stiff and weightless bar elements to connect the joints.
- (2) Elastic joints where bending occurs, made of an elastic, homogeneous and orthotropic material which can be described by four independent elastic constants.
- (3) Torsion bars which represent the torsional stiffness of the plate.
- (4) Elastic support springs which provide foundation support. These springs can either support the forces exerted by the slab to the subgrade or can restrain the slab from lifting, but cannot sustain or transmit lateral forces.

The basic equation of equilibrium developed from application of the model shown can be presented in generalized matrix form (Ref. 26) as:

$$[K] \{w\} = \{F\} \quad (2-14)$$

where:

$[K]$  = stiffness matrix

$\{w\}$  = displacement vector

$\{F\}$  = load vector

A computer program to solve the above equation has been developed (Refs. 24, 26).

The effect of joints and shrinkage cracks is taken into consideration

with the discrete element model by reduction of bending stiffness of the slab at those stations where a joint or crack are assumed to exist. The effect of transverse shrinkage cracks on the longitudinal bending rigidity of continuously reinforced concrete pavements was studied in Texas (Ref. 27) using this procedure. It was found that a significant drop (80 to 90 percent) in the bending rigidity of concrete slab is encountered at these crack locations.

The primary source of error associated with the use of the discrete element model is in approximating a continuum with a lumped parameter model. The error can be reduced by decreasing the size of the mesh used, but this increases the computer time and cost required to solve the problem. Since the increased number of increments generally affects the solution only near points of abrupt or rapid changes in load, support condition, or stiffness of the slab, Pearre and Hudson (Ref. 28) have described a method which permits using two different element sizes in the model. Further improvements of this model were made by Vera and Matlock (Ref. 29) for analysis of anisotropic skew plates and grids.

Finite-element methods for analysis of concrete pavement slabs has been used by several investigators, including Eberhardt (Refs. 30, 31), Huang and Wang (Refs. 32, 33, 34). In contrast while with the discrete element model in which the concrete slab is considered as an assemblage of elastic joints, rigid bars, and torsional bars (Figure 2.2), the finite-element method is based on plate theory in which the entire slab is comprised of a series of small (finite) slab elements jointed together at the nodes. This is presented in detail in Chapter 3.

The finite-element models developed by Eberhardt (Refs. 30, 31), and Huang and Wang (Refs. 32, 33, 34), were based on rectangular plate elements



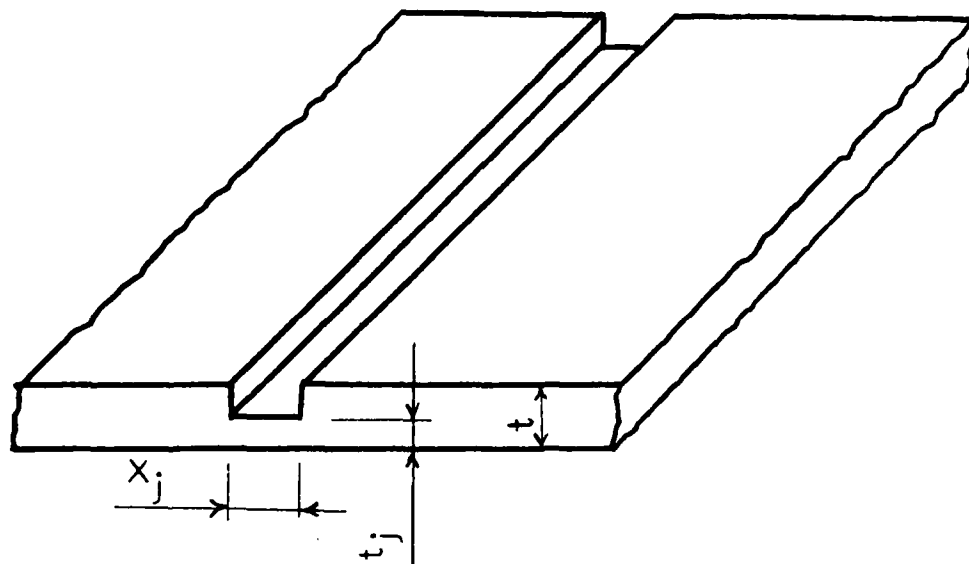


Figure 2-3. Specialized Finite-Element Representation of Joints with Partial Moment Transfer (Ref. 30)

originally developed by Melosh, each having three degrees of freedom per node (Ref. 59). The subgrade was assumed to behave as Winkler foundation in References 30, 32, and 33, and Reference 34 idealized the effect of subgrade on the concrete pavement as an elastic half space solid.

In these finite-element models the slab is divided into a number of rectangular elements, and a rectangular stiffness matrix (Ref. 46), relating the nodal displacements to nodal forces is utilized to represent each element. By assembling the stiffness matrices for all elements in the system, the force-displacement relationship for the system as a whole is developed. The force-displacement relationship in generalized matrix form is of the form given in Equation 2-14, which is then solved for unknown displacements, strains and stresses at any point in the slab.

For the model developed by Eberhardt (Refs. 30, 31), the physical characteristics of the joints were taken into consideration through reduction of slab stiffness at the joints. Figure 2.3 shows the specialized element with conceptual dimensions ( $X_j$  by  $Y$  by  $t_j$ ), where  $S_j$  is the joint opening,  $Y$  is the normal element length, and  $t_j$  is the thickness required for a given percentage of moment transfer across the joint, and is determined from the following equation:

$$t_j = \sqrt[3]{R_m/100} t \quad (2-15)$$

where:

$R_m$  = percentage of the moment transferred across the joint

$t$  = thickness of the basic slab

For the finite-element model developed by Huang and Wang (Refs. 32, 33, 35) the effect of doweled joints was taken into consideration by imposing a specified value for deflection efficiency across a joint expressed as the

ratio of deflections of two adjacent slabs along the joint. The efficiency of doweled joints was defined as

$$L = \frac{W_r}{W_\ell} \times 100 \quad (2-16)$$

where:

$L$  = efficiency of doweled joint in percentage

$W_\ell$  = deflection of the loaded slab

$W_r$  = deflection of the unloaded slab

Assuming the discontinuity of the two adjacent slabs, equilibrium equations for each slab, in terms of unknown displacements, are developed. In this step it is assumed that there is neither moment nor shear transfer across the doweled joint. By assuming no moment transfer across a doweled joint, the addition of dowels affects only those equations that represent vertical forces at the nodes. Finally, by equating the sum of the every two equations corresponding to vertical forces at adjacent nodes along the joint to the externally applied force at these nodes the number of equations is reduced. However, at every two adjacent nodes, one equation (efficiency equation) is added to the set of the equilibrium equations, resulting in the total number of equations remaining unchanged (Ref. 32).

#### 2.b.(4) Analysis and Design of Dowel Bars

The use of smooth, round steel bars across transverse joints in concrete pavements for the purpose of transferring load was reportedly first used in a pavement built in 1917-1918 between two army camps near Newport News, Va. In this installation four 3/4 in. (19 mm) diameter bars were used in the 20 ft. (6.1 m) pavement width (Ref. 3). In the years that followed World War I the use of steel dowels spread rapidly, and by 1930 nearly half of the states required use of dowels in transverse joints

(Ref. 35). However, the requirements of dowel diameter, length, and spacing varied widely.

In 1932 Bradbury (Ref. 36) attempted to determine analytically the required diameter, length, and spacing of dowels. His studies indicated the need for larger diameter dowels than had previously been used, and closer dowel spacing. Through the application of the Timoshenko's equations (Ref. 37) for the bending of bars embedded in an elastic body, Bradbury developed a formula for estimating the required dowel length. In 1938 Friberg (Ref. 38) analyzed the dowel equations by means of the same equations (Timoshenko) and reported on an experimental study of the support afforded dowels by the surrounding concrete. Friberg also emphasized the advantages of increasing dowel diameter and decreasing dowel spacing. He concluded that the length of dowels could be reduced below the 24 in. (61 cm) length then in common use. Westergaard (Ref. 39) in his analytical studies of dowel reactions, concluded that the major part of the load transfer is accomplished by the 2, or at most, the 4 dowels nearest to the wheel load.

In 1940 Kushing and Fremont (Ref. 40) published a theoretical analysis of the distribution of reactions among the several units of a doweling system in which the authors assumed an elastic deflection of the dowels. Results of this study indicated a wider distribution of reactions than was indicated by Westergaard's study in which the dowels were assumed to be rigid. In a discussion of the results and conclusions of this study, Sutherland (Ref. 41) presented the results of a series of experimental studies that supported the conclusions of Westergaard and his assumption of rigid dowels and indicating that only the dowels near the load were effective in the load transfer.

The conventional analysis for distribution of dowel shear forces along the joint was presented by Friberg (Ref. 42). It was observed that according to the theoretical analysis presented by Westergaard, maximum negative moment occurs at a distance  $1.8 \ell$  from the point of applied load, where  $\ell$  is the radius of relative stiffness of the concrete slab with respect to subgrade as was defined in Equation 2-8. Thus it was assumed that the dowel bar immediately under the applied load carried full capacity and those on either side carried a load which decreased linearly from full capacity at the point of load to zero at a distance of  $1.8 \ell$  from the center of the loaded area. Because of lack of viable analytical tools to establish this load transfer distribution, it was assumed that the distribution of transferred load was linear.

Stresses in dowel bars result from shear, bending, and bearing. These stresses can be determined analytically to determine those factors which affect load-transfer characteristics of the dowels. All of the mathematical analyses of dowel design have been based upon the principles of elasticity first presented by Timoshenko (Ref. 37). According to Timoshenko, a dowel bar encased in concrete can be modeled as a beam on a Winkler type foundation (Figure 2-4). The following differential equation forms the basis of the method.

$$EI = \frac{d^4 y}{dx^4} = - Kby \quad (2-17)$$

where:

$EI$  = flexural rigidity of the dowel bar

$K$  = modulus of dowel support

$b$  = diameter of the dowel

The solution of the above equation gives the moment, shear and deflection at any point in the dowel, which are:

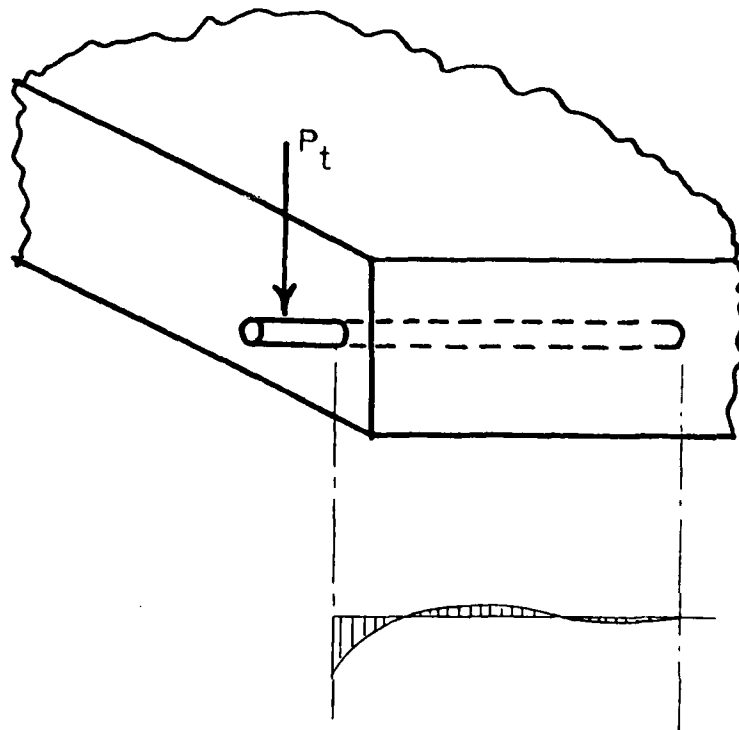


Figure 2-4. Pressure Exerted on a Loaded Dowel Bar

$$y = \frac{e^{-\beta x}}{2\beta^3 EI} [P_t \cos \beta x - \beta M_0 (\cos \beta x - \sin \beta x)] \quad (2-18)$$

$$M = \frac{e^{-\beta x}}{\beta} [P_t \sin \beta x - \beta M_0 (\sin \beta x + \cos \beta x)] \quad (2-19)$$

$$V = -e^{-\beta x} [(2 \beta M_0 - P_t) \sin \beta x + P_t \cos \beta x] \quad (2-20)$$

$$\sigma = Ky \quad (2-21)$$

where:

$$\beta = \sqrt[4]{\frac{Kb}{4EI}} \quad (2-22)$$

$P_t$  = transferred load by dowel

$M_0$  = bending moment on dowel at face of concrete

$\sigma$  = bearing pressure on the concrete

Assuming the two adjacent slab faces at the joint remain parallel to each other, then a point of counterflexure exists at the center of the doweled joint and Equation 2-23 gives the moment in the dowel as a function of joint opening and load transferred as:

$$M_0 = 1/2 w P_t \quad (2-23)$$

where  $w$  is the width of joint opening.

The rate at which the concrete reacts against deflection of the dowel bar, is referred to as modulus of dowel support ( $K$ ), which appears in Equations 2-17 through 2-22. Therefore, shear and bending stresses in the dowel bar, and bearing stress on concrete, which is usually the controlling parameter for dowel design, are functions of  $K$ .

One of the problems involved in this analysis is the proper selection of this modulus of dowel support ( $K$ ). For convenience the value for  $K$  has

often been considered a constant equal to 1,500,000 pci ( $406,500 \text{ N/cm}^3$ ). Table 2-1 (Ref. 43) indicates that test results have produced a wide range of values for this parameter. Testing procedures have varied between investigators, but it appears that K is also susceptible to variation between specimens tested in a prescribed manner. A study of the results from these investigations seems to indicate that K is not a constant but varies with the concrete properties, dowel diameter, slab depth, dowel length and dowel looseness.

In reality, the interaction between a loaded dowel bar and surrounding concrete is in three-dimensional state of stress, dependent upon dimensions, elastic properties, boundary conditions of the dowel bar and the concrete slab, and this interaction cannot be modeled as a single quantity such as K.

#### Dowel Bending and Shear Stresses

Equations 2-19 and 2-20 were employed for determination of bending and shear stresses in the dowel. Maximum bending stress in a dowel, according to Equation 2-19, occurs at a point slightly inside the face of concrete; whereas the maximum shear stress in the dowel occurs at the face of concrete (Equation 2-20). For design of dowels, these stresses should be limited to the allowable bending and shear stresses for the steel in the dowel bars. The recommended allowable bending and shear stresses suggested for steel dowels are respectively 0.60 and 0.40 times the yield strength of the steel.

#### Concrete Bearing Stresses

Bearing pressure of the dowel on the concrete is usually the controlling factor in design of dowel bars, and it is determined by use of Equation 2-21. The American Concrete Institute (ACI), subcommittee 325 (Ref. 43)



recommended the following relationship for determining the allowable bearing stress on concrete.

$$f_a = \left( \frac{4 - b}{3} \right) f'_c \quad (2-24)$$

where:

$b$  = diameter of dowel bar

$f'_c$  = compressive strength of concrete

Based on this equation, allowable bearing stress on concrete for a 1 in. (25 mm) dowel bar is equal to compressive strength of concrete. However, concrete has been observed to withstand higher bearing stresses, and values, in the range of about 2 to 3 times the 28 day compressive strength of concrete have been observed. Marcus (Ref. 44) reviewed the results of tests performed by the National Bureau of Standards to determine the resistance of concrete to uniformly distributed bearing stresses by dowels of different diameter placed on prismatic concrete blocks of depths 6, 12, and 18 inches (15, 30, and 46 cm). The ratio of the ultimate bearing stress to the compressive strength of concrete ( $f_b/f'_c$ ), are presented in Table 2-2. It can be seen that from the results of these tests concrete withstood bearing stresses equal to 1.73 - 3.43 times the compressive strength of concrete. Initial failure of concrete usually accompanied by small cracks and/or spalls, before the ultimate load was applied.

In a series of tests conducted by Friberg (Ref. 38) on loaded dowels embedded in concrete blocks initial and ultimate loads were measured. Dowel bars of three sizes, 3/4, 1, and 1 1/4 inches (19, 25 and 32 mm) were embedded 3, 6, and 9 times of their diameter in prismatic concrete blocks 6, 7, and 9 inch (15, 18, and 20 cm) thicknesses. Table 2-3

Table 2-2. Ratio of Concrete Bearing Stress to  
Compressive Strength of Concrete  
(Ref. 44)

Dowel Size in. (mm)	Depth of Concrete Block in. (cm)		
	6 (15)	12 (30)	18 (46)
3/4 (19)	3.43	2.61	2.76
1 (25)	3.15	2.34	2.40
1-1/2 (38)	2.51	1.83	1.99
2 (51)	2.16	1.78	1.73

Table 2-3. Progressive Failure Loads (Ref. 38)

Dowel Size in. (mm)	Ave. Failure Load, Kips (KN)	
	Initial	Ultimate
3/4 (19)	4.3 (19.1)	6.8 (30.2)
1 (25)	5.9 (26.2)	9.1 (40.4)
1-1/4 (32)	7.0 (31.1)	12.0 (53.3)

and Figure 2-5 illustrate the average failure loads of all specimens for various dowel sizes. From these test results it is seen that initial failure of concrete occurs with loads about 2/3 of the ultimate failure loads.

#### Dowel Looseness

Dowel looseness is defined as the space between the dowel bar and the surrounding concrete. When a load is applied on one slab near a joint with a loose dowel, the loaded slab will first deflect an amount equal to the dowel looseness before the dowel bar starts to bear on concrete. Therefore, a dowel can function at its full efficiency only after this looseness is completely taken up by the relative slab deflection.

Dowel looseness consists of two parts, initial looseness and looseness caused by elongation of the socket caused by repetitive loads. Causes of initial dowel looseness are summarized in Reference 24, as:

1. Coating applied to dowels to prevent bond and/or to protect dowels against corrosion.
2. Water or air voids in the concrete around the dowels due to improper vibration.
3. Shrinkage of concrete during hardening.

Figure 2-6 shows the effect of dowel diameter, slab depth, joint width, and length of dowel embedment on the initial dowel looseness, measured by Teller and Cashell (Ref. 35). Based on this investigation dowel looseness was found to be about 0.002 to 0.004 inches (0.05 to 0.10 mm).

The high-bearing pressure between the dowel and the concrete, particularly in the region above and below the dowel near the face of the joint, tend to break down or wear the concrete during repetitive loading, and increase the dowel looseness. Teller and Cashell also investigated the

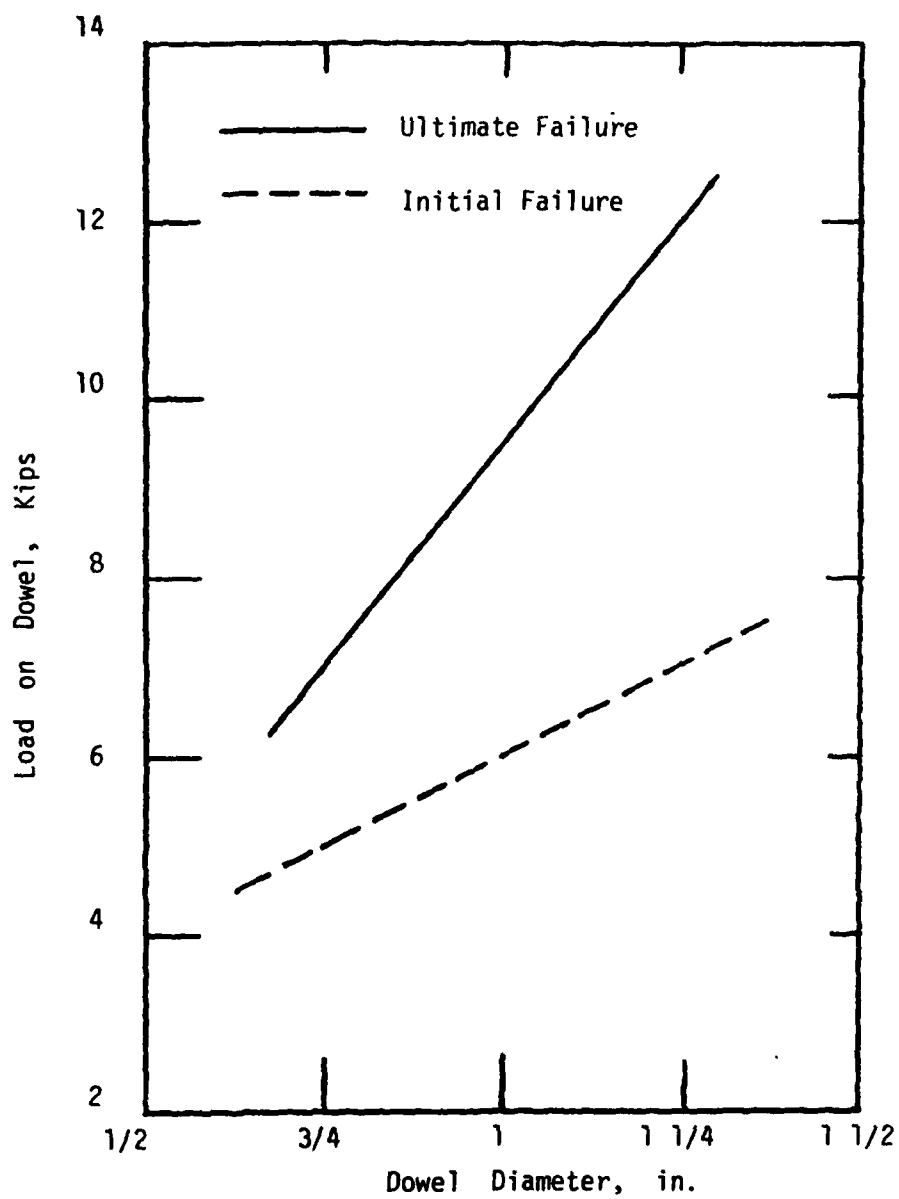


Figure 2-5. Effect of Dowel Size on Progressive Failure Load (Ref. 38)

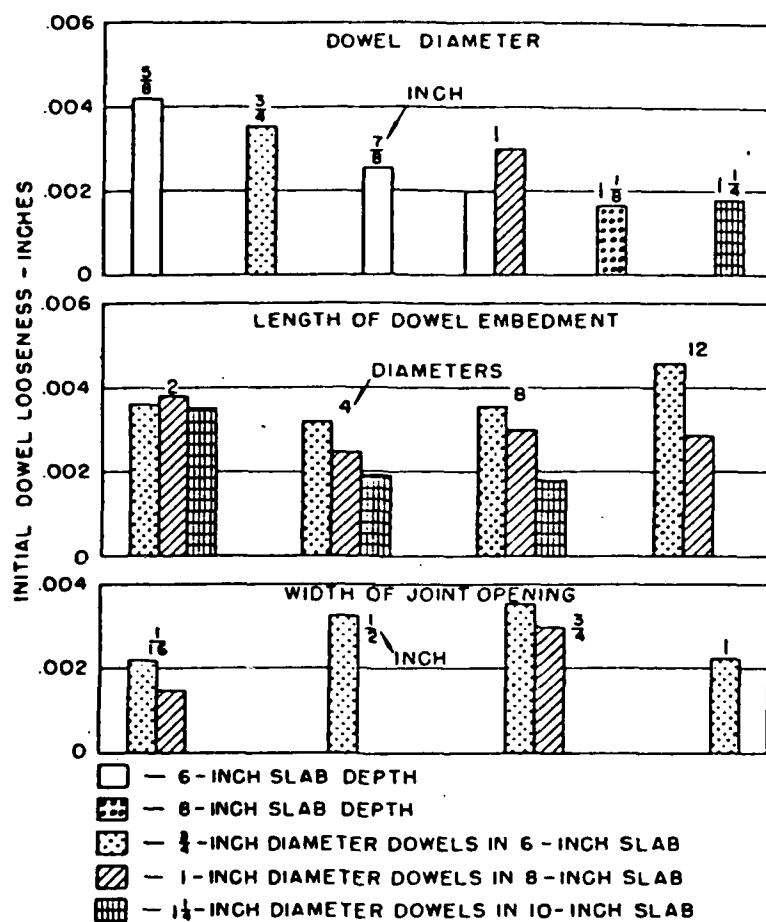


Figure 2-6 . Data on Initial Dowel Looseness (Ref. 35)

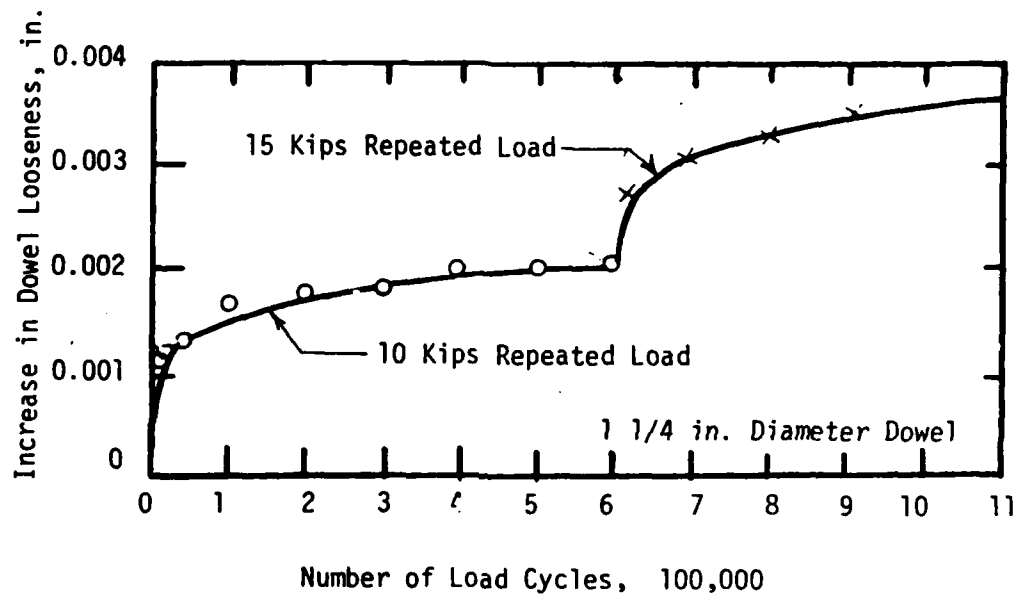


Figure 2-7. Effect of Load Magnitude and Number of Load Cycles on Dowel Looseness (Ref. 35)

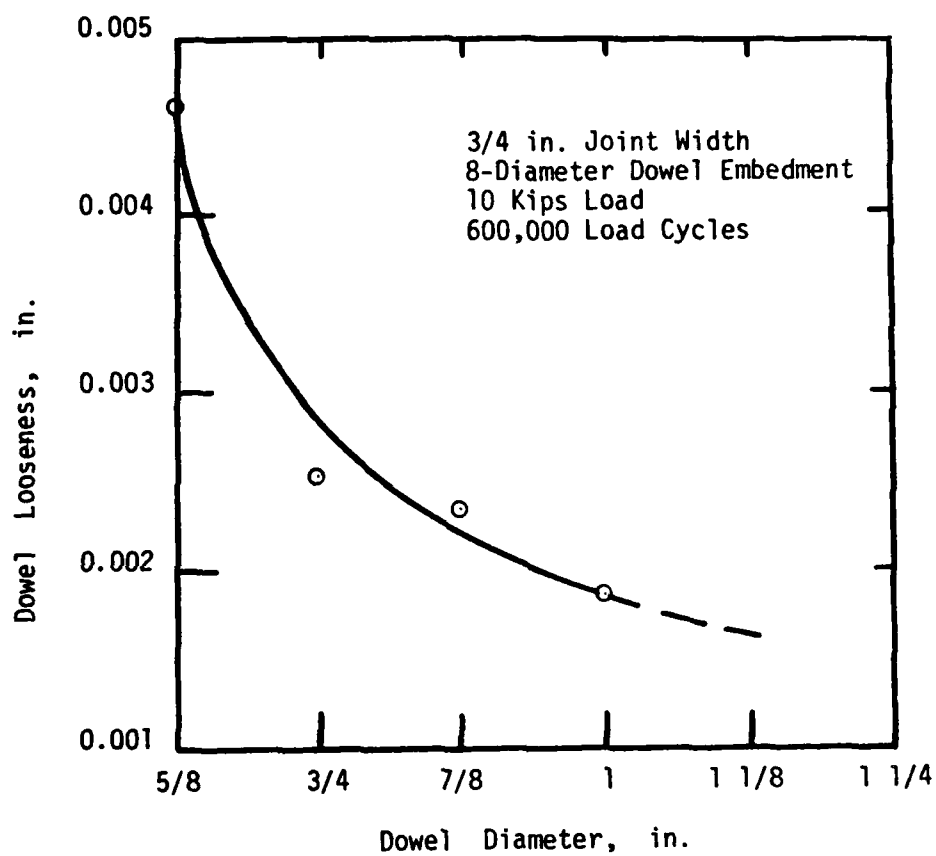


Figure 2 - 8. Relation between Dowel Diameter and Dowel Looseness (Ref. 35)

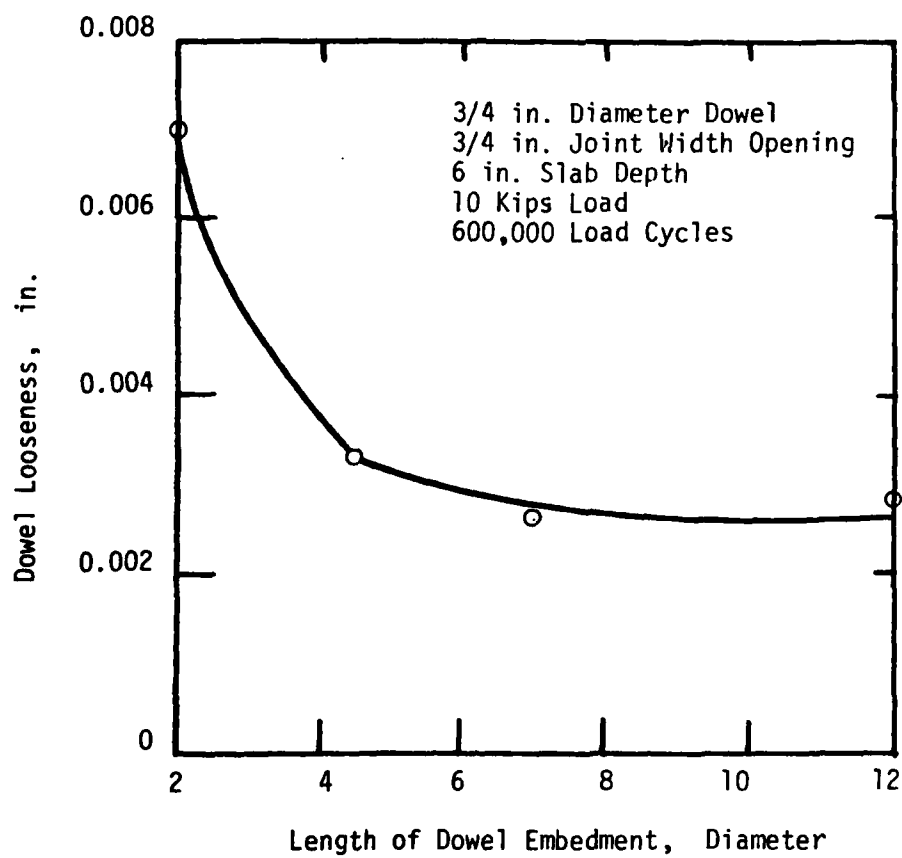


Figure 2 -9. Relation between Length of Dowel Embedment and Dowel Looseness (Ref. 35)



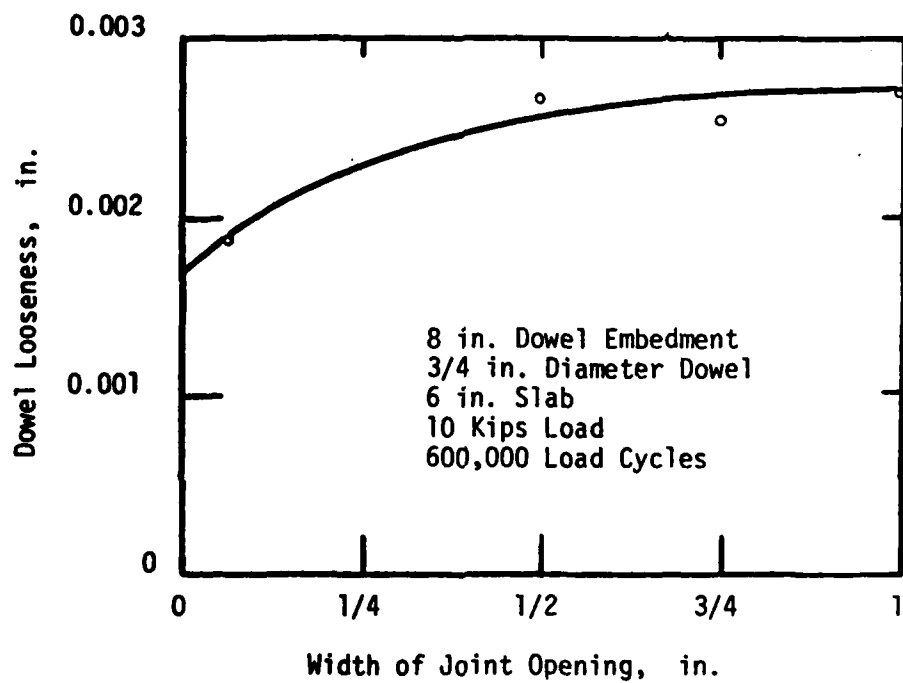


Figure 2-10. Relation between Width of Joint Opening and Dowel Looseness (Ref. 35)

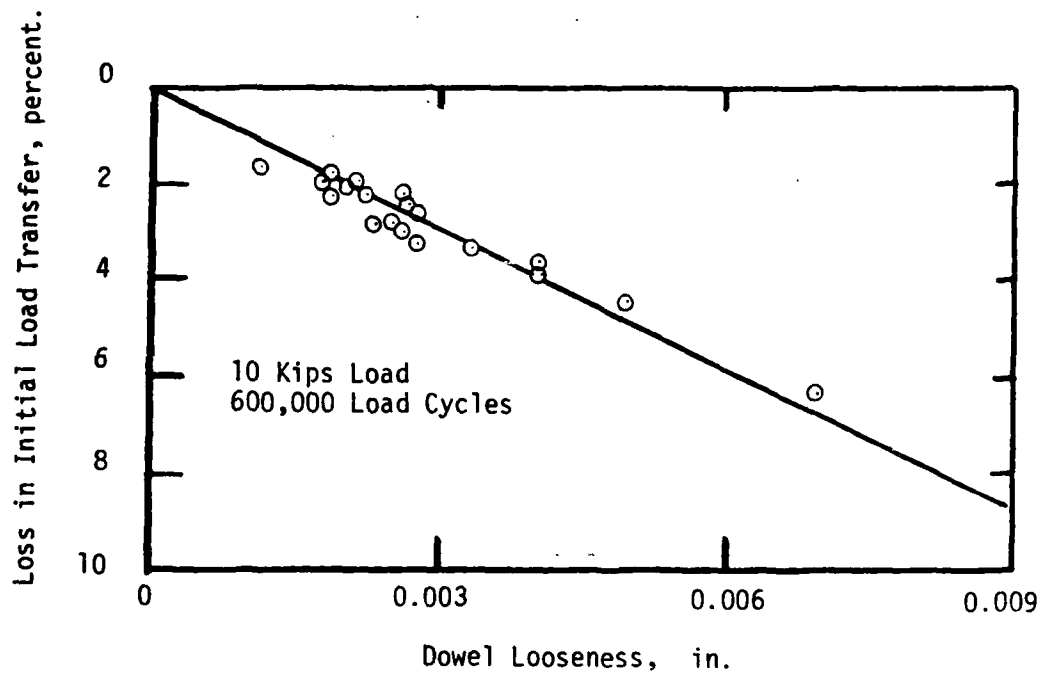


Figure 2-11. Relation between Dowel Looseness and Loss in Initial Load Transfer (Ref. 35)

effect of repetitive loads on dowel looseness. Figures 2-7 through 2-10 illustrate the effect of load magnitude, number of load applications, diameter of dowel, length of dowel embedment, and width of joint opening on the dowel looseness.

Effectiveness of dowels for load transfer progressively reduces as the dowel looseness increases. Figure 2-11 shows the relationship between dowel looseness and loss in load transfer, after 600,000 cycles of a 10 kips (55.56 KN) load (Ref. 35). The load transfer in this study was calculated using the following expression:

$$LT = \frac{1}{2 + \frac{\Delta_D}{\Delta_F}} \times 100 \quad (2-25)$$

where:

$\Delta_D$  = dowel deflection

$\Delta_F$  = free-edge deflection of the slab with no dowels

LT = load transfer, percent

Since dowel looseness reduces load transfer capability of a doweled joint, it is therefore essential that looseness be kept at an absolute minimum. To do this concrete should be vibrated very thoroughly around the dowels, the thickness of any bond breakers be kept to a minimum, and the value of bearing stress on the concrete be kept at a realistic value by using dowels of adequate diameter, length, and spacings. value of bearing stress on the concrete be reduced by using dowels of adequate diameter, length, and spacings.

The effect of load repetitions on joint efficiency (relative deflection of unloaded slab to loaded slab), was investigated by PCA (Ref. 16). In this study concrete beams containing doweled joints with 3/4 and 1 inches

(19 and 25 mm) diameter dowel bars were tested under repetitive loading. Results of the dynamic tests on these jointed beams indicated that the joint efficiency of the doweled joints decreased as the number of load applications increased. Figure 2-12 shows the trend in loss of joint efficiency, and Table 2-4 summarizes these results.

#### 2.b.(5) Aggregate Interlock as a Load Transfer Mechanism

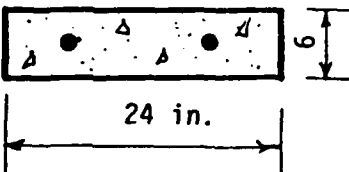
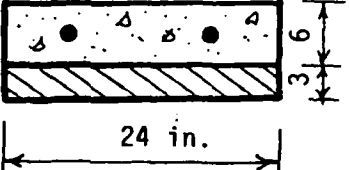
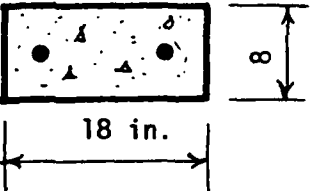
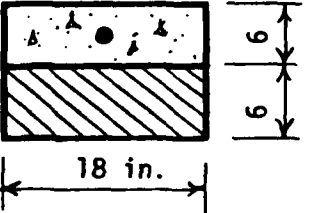
Aggregate interlock as a mechanism for load transfer across a joint is not normally used with longitudinal construction joints. This mechanism is frequently used, however as the basic load transfer mechanism for joints formed at the center of paving lanes to reduce the slab width. If joint location with respect to location of wheel loads is to be considered in optimizing the pavement joint systems then the performance of the joints with aggregate interlock must also be given consideration.

As with doweled joints, performance of joints with aggregate interlock can be evaluated in two phases; the initial efficiency of the joints, and the long-term efficiency. Tests reported by Colley and Humphrey (Ref. 53) indicate both the initial and long-term efficiency of joints with aggregate interlock are functions of joint opening. Results in Figure 2-13 indicate that as long as the joint opening is less than about .045 inches (1.15 mm) the initial efficiency of the joints for load transfer would be high. As the joint opening is increased above about .050 inches (1.25 mm) the joint efficiency decreases significantly with increasing joint opening.

As can also be seen in Figure 2-13 increased joint openings have a significant effect on the long-term load transfer performance of the joints. To achieve good long-term performance of these joints, a joint opening of .025 inches (0.62 mm) or less must be maintained.

Design criteria for joints with aggregate interlock were developed by Colley and Humphrey (Ref. 53). Figure 2-14 shows the relationship between

Table 2-4. Loss in Joint Efficiency (Ref. 16)

Joint Type	Dowel Diameter in.	Initial Load Kips	Load Cycles Millions	Joint Efficiency %	
				Initial	Final
	3/4	6.3	2.66	94	68
	3/4	8.5	3.21	98	74
	3/4	8.0	2.06	96	70
	1	8.5	2.36	96	78

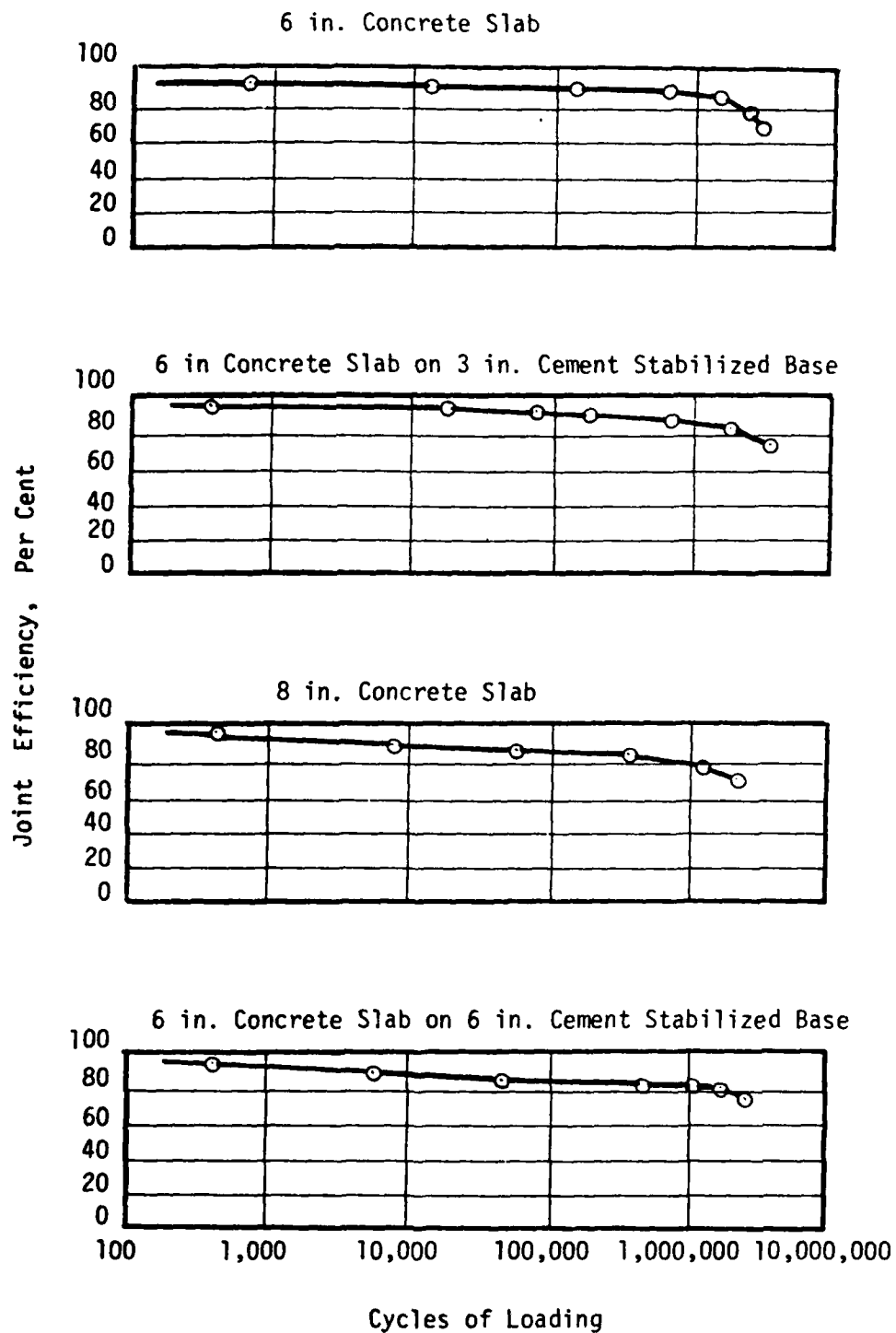


Figure 2-12. Effect of Repeated Loadings on Joint Efficiency (Ref. 16)

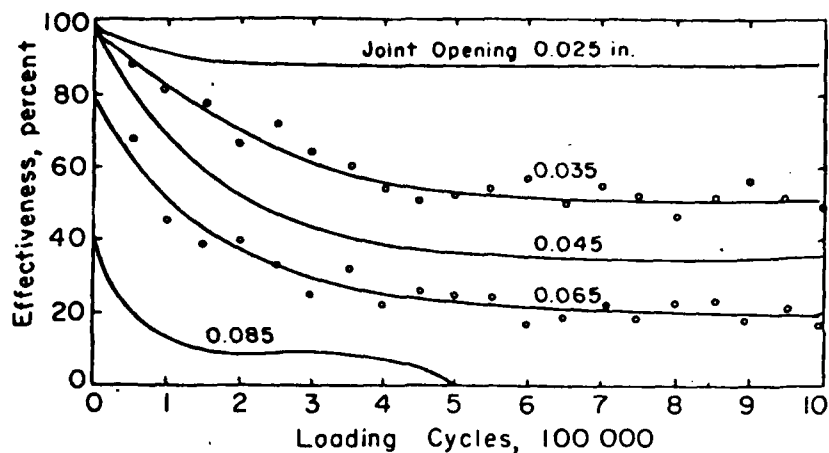


Figure 2-13. Influence of Joint Opening on Effectiveness of Aggregate Interlock (Ref. 53).

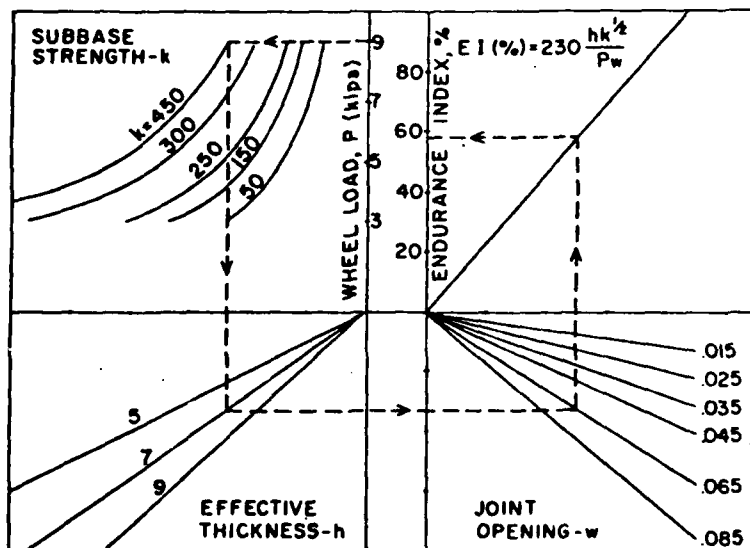


Figure 2-14. Nomograph for Design of Aggregate Interlock Joints for a Specified Long-Term Efficiency (Ref. 53).

subgrade support, slab thickness, joint opening and long-term load transfer efficiency of the joints based on the simulated tests conducted on the beam samples by PCA.

From the parameters involved in the design nomograph, it is apparent that the long-term effectiveness of joints with aggregate interlock is a function of the shear stresses across the joints. To develop the necessary design criteria for pavements with this type of joint it is necessary to evaluate the critical stresses across the joints for typical pavements with normal loading conditions.

#### 2.b.(6) Keyed Joints

Keyed joints are the most common type joint used for load transfer across longitudinal construction joints. It is because of the specific problems associated with this type joint and the problems in constructing keyed joints with slip formed pavements which has spurred this study. A more detailed discussion of the keyed joint problems and their performance is presented in an earlier report from this study entitled "Longitudinal Joints for Slip Formed Rigid Pavements; Vol. 1, Literature Survey and Field Inspection."

#### 2.c Limitations of Present Methods of Analysis and Design

In the current design procedures jointed concrete pavements are analyzed and designed by assuming continuous slabs, infinite in extent, calculating the stresses and deflections for the continuous slab and then superimposing the selected joint systems on the slab. However, various types of joints with different load transfer systems and their different effectivenesses affect the structural response of the jointed concrete pavements under load, and to be valid the structural model used should be



able to consider the entire pavement system with all the pavement components such as joints, load transfer systems, type of subbase, uniformity of support including loss of subgrade support, non-uniform slab thickness, etc. The major limitations of present methodology and models used for analysis and design are summarized below:

- (1) The primary mechanisms of concrete pavement joint failure is not well understood.
- (2) A comprehensive model for analysis of jointed concrete pavement considering all the pavement components has not been developed.
- (3) Structural analysis of various joint types is still in a state of development.
- (4) There are no provisions for economic or performance comparisons of different joint alternatives.

## CHAPTER 3

### DEVELOPMENT OF THE ANALYTICAL MODELS FOR ANALYSIS OF JOINTED CONCRETE PAVEMENTS AND PAVEMENT JOINTS

#### 3.a General

For many pavement structures it has been virtually impossible to obtain analytical (closed form) solutions because of the complexity of geometry, boundary conditions, and material properties, unless certain simplifying assumptions were made which result in a change or modification of the characteristics of the problem. With the advent of high speed digital computer methods, solution of these complex structural problems has been greatly facilitated. One of the most powerful methods that has evolved is the "finite-element method." This method of analysis is applicable to a wide range of complex, boundary value problems in engineering.

To be effective the analytical model for the jointed concrete pavement should be capable of handling the following parameters on an integral basis.

- (1) Concrete pavement with a stabilized base or an overlay,
- (2) Concrete pavement with non-uniform slab thicknesses and non-uniform subgrade support,
- (3) Effect of the loss of subgrade support,
- (4) Effect of different load transfer joint systems,
- (5) Localized stresses at the joints,
- (6) Effect of slippage and/or separation at the joints, and
- (7) Partial shear or moment transfer at the joints or cracks.

With proper application, the finite-element method is capable of analyzing all of the foregoing situations.

### 3.b The Finite-Element Method

Basically, with the finite element method approach the system to be analyzed is represented by an assemblage of subdivisions or discrete bodies called finite-elements. These elements are interconnected at specified locations which are called nodes or nodal points. Functions are developed to approximate the distribution or variation of the actual displacements over each finite element, and such assumed functions are called displacement functions or shape functions. Relationships are then established between these generalized displacements (usually denoted as  $\{d\}$ ) and generalized forces (usually denoted as  $\{p\}$ ) applied at the nodes using the principle of virtual work or some other variational principle. This element force-displacement relationship is expressed in the form of element stiffness matrix (usually denoted as  $[k]$ ) which incorporates the material and geometrical properties of the element, viz.,

$$[k] \{d\} = \{p\} \quad (3-1)$$

The overall structural stiffness matrix,  $[K]$  is then formulated by superimposing the effects of the individual element stiffness using the topological or the element connectivity properties of the structure. The overall stiffness matrix is used to solve the set of simultaneous equations of the form:

$$[K] \{\Delta\} = \{P\} \quad (3-2)$$

where:

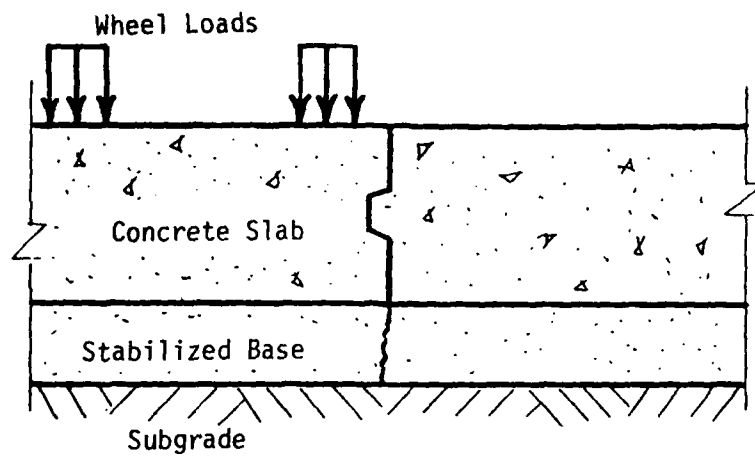
$\{P\}$  = applied nodal forces for the whole system

$\{\Delta\}$  = resulting nodal displacements for the whole system

#### 3.b.(1) Finite-Element Modeling of the Jointed Concrete Pavement and Pavement Joints

A typical longitudinal section and a typical transverse section

a) A Typical Longitudinal Section



b) A Typical Transverse Section

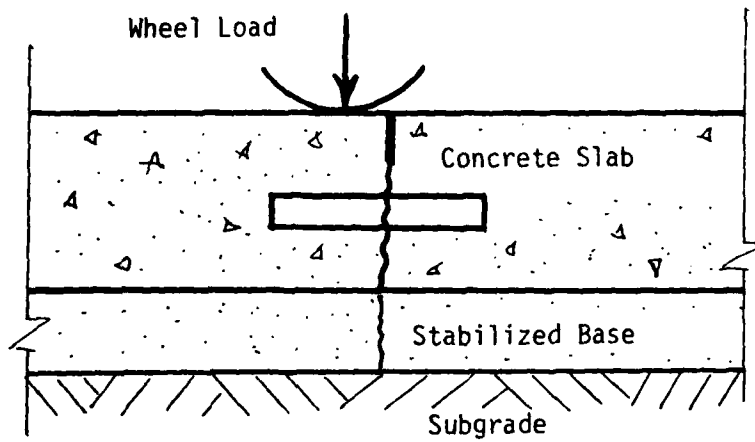


Figure 3-1. A Typical Longitudinal and a Typical Transverse Section of a Jointed Concrete Pavement System

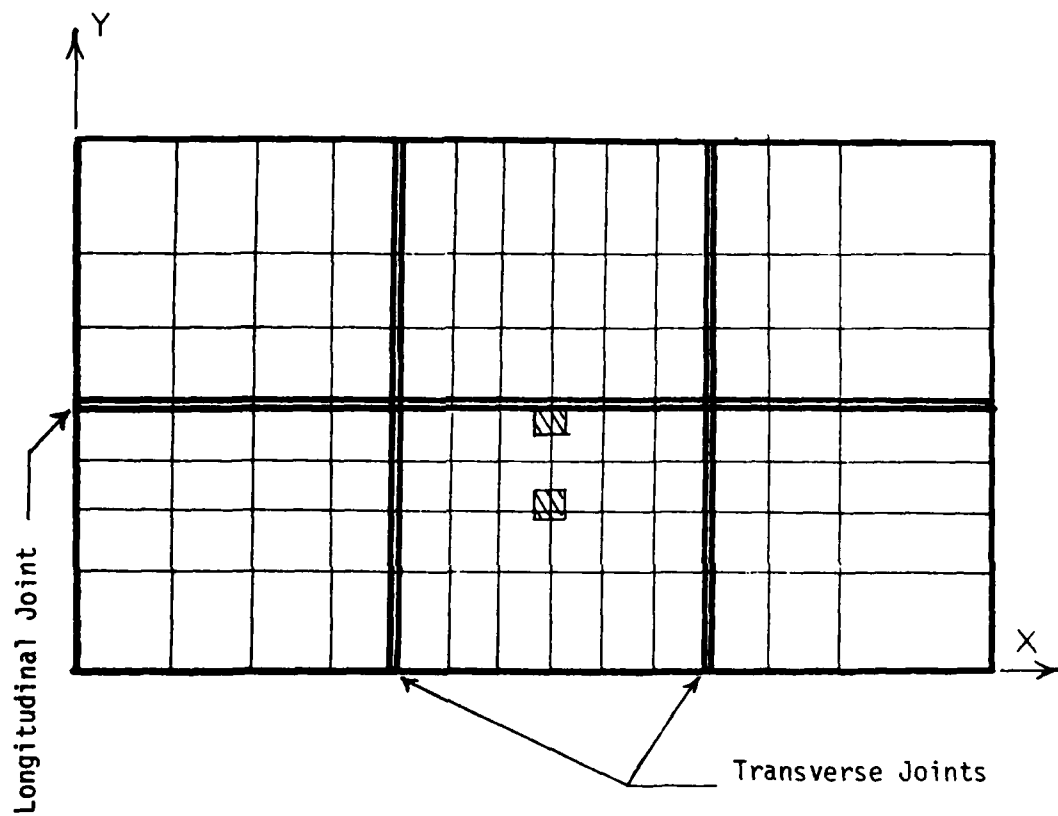


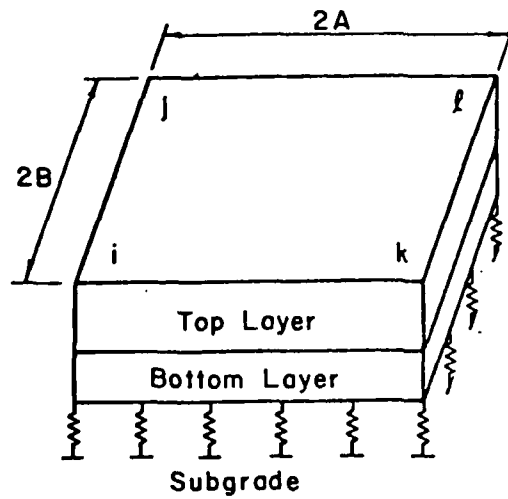
Figure 3-2. A Typical Finite-Element Mesh Used for Two-Dimensional Analysis

of a jointed concrete pavement are shown in Figure 3-1. It can be seen that because of the three-dimensional geometry and non-symmetric loading conditions, analysis of the jointed concrete pavement system should consider a three-dimensional approach. While it is possible to formulate a three-dimensional finite-element model that would represent the whole system, the amount of discretization and the computer costs required for solution of the problem would be high and impractical.

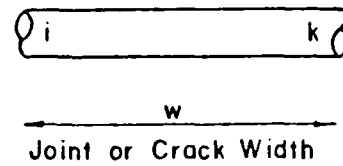
A two stage analysis of the jointed concrete pavement system might provide a more reasonable engineering approach. In this two stage analysis, a two-dimensional analysis is first performed, followed by a three-dimensional analysis of specific limited segments of the pavements. Results from the two-dimensional analysis are used as boundary conditions for the segments to be analyzed using the three-dimensional analysis.

#### Two-Dimensional Analysis

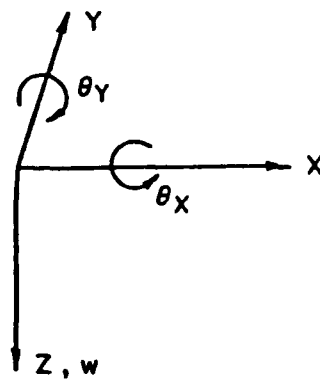
The two-dimensional analysis is based on the classical theory of medium-thick plate on Winkler foundation, and is capable of evaluating the structural response of the concrete pavement system with joints. Figure 3-2 shows a typical finite-element mesh used for this two-dimensional analysis. In this figure, six concrete slabs with a keyed longitudinal joint and two doveled transverse joints are shown. The six slabs are used because this is a general case with the loads applied on the middle slab, which is connected at each end to a neighboring slab by dowel bars or keyway. The use of more than six slabs can be included in the analysis but is not necessary because the additional slabs are sufficiently far from the applied loads as to have practically no effect on the stresses and deflections in the loaded slab. When the loads are applied near the joints, analysis of a system with only one adjacent slab is generally sufficient, and the slabs at the far end can be ignored.



a) Plate Element



b) Bar Element



c) Spring Element

Figure 3-3. Finite-Element Model of Pavement System

The rectangular plate elements with three degrees of freedom (one vertical deflection and two rotations) per node are used to represent the pavement slab, the stabilized base and overlay layer (Figure 3-3-a). For the case where two layers (slab and stabilized base or slab and overlay) are bonded, an equivalent layer based on the transformed section concept is used to determine the location of the neutral axis for the element. And in the case of unbonded layers, stiffness of each layer is used in formulation of the finite-element model. Dowels are represented as beam elements (Figure 3-3-b) with both shear and flexural stiffness, while spring elements which can transfer vertical forces only and as shown in Figure 3-3-c are used to model aggregate interlock and keyways. Assuming that the reactive pressure between subgrade and slab at any given point is proportional to the deflection at that point (Winkler foundation), the subgrade is represented by a set of spring elements supporting the slab elements (Figure 3-3-a). This representation of subgrade under the slab has been employed by several investigators (Refs. 2, 24, 30, 33) and has resulted in excellent results. Furthermore, this assumption results in a banded stiffness matrix for the pavement system and large computer storage requirements to solve the set of simultaneous equations are not required.

### Three-Dimensional Analysis

This approach involves use of the solid SAP finite-element program developed by Wilson (Ref. 45) at the Department of Civil Engineering, University of California, for three-dimensional analysis. Figure 3-4 shows a typical finite-element mesh used for three-dimensional analysis of a small section of the concrete slab near the joint and around a dowel bar.



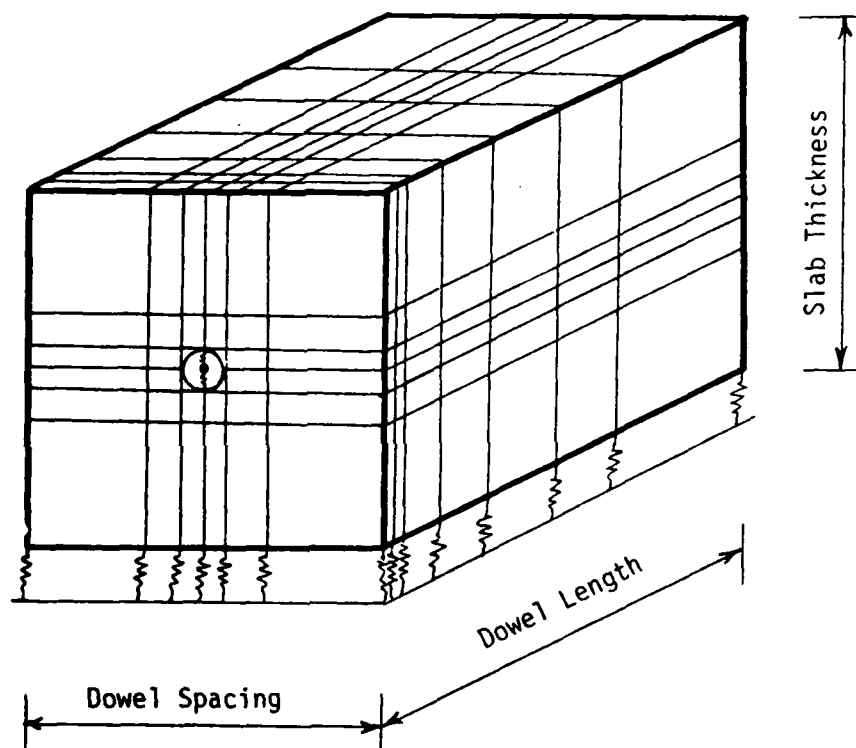


Figure 3-4. A Typical Finite-Element Mesh Used for Three-Dimensional Analysis

Three-dimensional, 8 node, isoparametric elements with three translational degrees of freedom per node, originally developed by Irons (Ref. 60), are employed to represent the slab segment under study. Subgrade, similar to that used with the two-dimensional model idealized as spring elements is also used in the three-dimensional analysis. Dowel bars are modeled by beam elements with both flexural and shear deformations, and spring elements, used to represent the interaction between dowel bars and the surrounding concrete. In the regions that dowel bar exerts pressure on concrete, very stiff springs are used to simulate the contact condition between dowel bar and concrete.

3.b.(2) Development of Stiffness Matrix for Rectangular Plate Element for Concrete Slab, Stabilized Base, and Overlay

The rectangular plate element shown in Figure 3-3-a represents the structural behavior of a pavement slab, a stabilized base, or an overlay. Displacement of a plate, based on the classical theory of medium-thick plates, is uniquely defined once the deflection  $W(x, y)$ , is known at all points. The complete formulation of this theory is presented in many standard references including Reference 20, and therefore will not be presented here. However, the basic assumptions used in the development of the theory are outlined as follows:

- (a) Lines normal to the middle surface in the undeformed plate remain straight, unstretched, and normal to the middle surface in the deformed plate.
- (b) Each lamina parallel to middle surface is in a state of plane stress.
- (c) No axial or in-plane shear stress results due to the loading.

The simplest rectangular element representation requires 12 degrees of freedom. They are three-displacement components at each node: a vertical deflection ( $W$ ) in the Z-direction, a rotation ( $\theta_x$ ) about the X-axis, and a rotation ( $\theta_y$ ) about the Y-axis. Corresponding to these displacement components there exists three force components at each node: a vertical force ( $P_W$ ), a couple about the X-axis ( $P_{\theta_x}$ ) and a couple about the Y-axis ( $P_{\theta_y}$ ), respectively.

A 12 term polynomial is chosen for expansion of  $W(x, y)$  as follows:

$$\begin{aligned} W(x, y) = & a_1 + a_2x + a_3y + a_4x^2 + a_5xy \\ & + a_6y^2 + a_7x^3 + a_8x^2y + a_9xy^2 \\ & + a_{10}y^3 + a_{11}x^3y + a_{12}xy^3 \end{aligned} \quad (3-3)$$

or

$$W = [N_\alpha] \{a\} \quad (3-4)$$

At any point within element,

$$\{\Delta\} = \begin{pmatrix} W \\ \theta_x \\ \theta_y \end{pmatrix} = \begin{pmatrix} W \\ -\frac{\partial W}{\partial y} \\ \frac{\partial W}{\partial x} \end{pmatrix} \quad (3-5)$$

By evaluating this expression at each of the four nodes,

$$\{\Delta\} = \begin{pmatrix} \Delta_i \\ \Delta_j \\ \Delta_k \\ \Delta_l \end{pmatrix} = [A] \{a\} \quad (3-6)$$

Inverting this 12 x 12 matrix,

$$\{a\} = [A^{-1}]\{\Delta\} \quad (3-7)$$

Then,

$$W = [N_{\alpha}] [A^{-1}] \{\Delta\} \quad (3-8)$$

or

$$W = [N] \{\Delta\} \quad (3-9)$$

Using the first assumption from the medium-thick plate theory namely, that the deformed state of the plate can be described in terms of its middle surface displacement, these displacements can be expressed as:

$$U(x, y) = -Z \frac{\partial W(x, y)}{\partial x} \quad (3-10)$$

$$V(x, y) = -Z \frac{\partial W(x, y)}{\partial y} \quad (3-11)$$

where:

$U$  = displacement of a point in  $X$ -direction

$V$  = displacement of the point in  $Y$ -direction

$Z$  = distance of the point from middle surface

Using the second assumption, the strains and stresses at a lamina located at distance  $Z$  from the middle surface can be expressed as:

$$\{\epsilon\} = \begin{pmatrix} \epsilon_x \\ \epsilon_y \\ \gamma_{xy} \end{pmatrix} = \begin{pmatrix} \frac{\partial U}{\partial x} \\ \frac{\partial V}{\partial y} \\ \frac{\partial U}{\partial y} + \frac{\partial V}{\partial x} \end{pmatrix} \quad (3-12)$$

or

$$\{\epsilon\} = Z \begin{bmatrix} -\frac{\partial^2 W}{\partial x^2} \\ -\frac{\partial^2 W}{\partial y^2} \\ 2\frac{\partial^2 W}{\partial x \partial y} \end{bmatrix} = Z\{\kappa\} \quad (3-13)$$

where  $\{\kappa\}$  is the curvature vector, and

$$\{\sigma\} = \begin{bmatrix} \sigma_x \\ \sigma_y \\ \tau_{xy} \end{bmatrix} = [C] \{\epsilon\} \quad (3-14)$$

where  $[C]$  is elasticity matrix. For an isotropic, linearly elastic materials, the elasticity matrix  $[C]$  can be written

$$[C] = \frac{E}{1-\mu^2} \begin{bmatrix} 1 & \mu & 0 \\ \mu & 1 & 0 \\ 0 & 0 & \frac{1-\mu}{2} \end{bmatrix} \quad (3-15)$$

where:

$E$  = modulus of elasticity

$\mu$  = Poisson's ratio

Thus, combining equations 3-13, 3-14 and 3-15, the stress vector can be written as:

$$\{\sigma\} = Z \frac{E}{1-\mu^2} \begin{bmatrix} 1 & \mu & 0 \\ \mu & 1 & 0 \\ 0 & 0 & \frac{1-\mu}{2} \end{bmatrix} \{\kappa\} \quad (3-16)$$

or, in shorthand notation:

$$\{\sigma\} = Z [C] \{\kappa\} \quad (3-17)$$

The bending moments in each layer can now be defined in terms of the stresses, as

$$\begin{matrix} M_x \\ \{M\}_i = M_y \\ M_{xy} \end{matrix} = \int_z Z_i \{\sigma\}_i dZ_i \quad (3-18)$$

i

where i is the number of layers = 1 or 2.

Other assumptions with respect to the condition of bond between concrete slab and overlay or concrete slab and stabilized base can be summarized as:

- (a) For the case of a bonded overlay or stabilized base, full strain compatability is assumed at the interface.
- (b) For the case of an unbonded overlay or stabilized base, existence of shear stresses at the interface is neglected.
- (c) Continuous contact is assumed between the concrete slab and unbonded overlay or unbonded stabilized base.

In the case of unbonded layers, the total bending moments can be determined from the equation:

$$\{M\} = \{M\}_{top} + \{M\}_{bottom} \quad (3-19)$$

or

$$\{M\} = \frac{h_t^3}{12} [C_{top}] + \frac{h_b^3}{12} [C_{bottom}] \quad \{K\}$$

where:

$h_t$  = thickness of the top layer

$h_b$  = thickness of the bottom layer

Equation 3-20 may also be expressed in shorthand notation as:

$$\{M\} = [D] \{\epsilon\} \quad (3-21)$$

where

$$[D] = \left( \begin{array}{c} \frac{Eh_t^3}{12(1-\mu^2)} \left( \begin{array}{ccc} 1 & \mu & 0 \\ \mu & 1 & 0 \\ 0 & 0 & \frac{1-\mu}{2} \end{array} \right)_{\text{top}} \\ + \frac{Eh_b^3}{12(1-\mu^2)} \left( \begin{array}{ccc} 1 & \mu & 0 \\ \mu & 1 & 0 \\ 0 & 0 & \frac{1-\mu}{2} \end{array} \right)_{\text{bottom}} \end{array} \right) \quad (3-22)$$

In the case where two layers are bonded together (slab and stabilized base or slab and overlay), an equivalent layer is calculated, based on the transformed section concept, to determine the location of the neutral axis for the element. The following equations give the location of neutral axis for bonded two-layer system using the first moment of the equivalent area of the transformed cross section.

$$\alpha = \frac{\frac{1}{2} (h_t + h_b) h_t}{h_t + \frac{E_b}{E_t} h_b} \quad (3-23)$$

$$\beta = \frac{1}{2} (h_t + h_b) - \alpha \quad (3-24)$$

where:

$\alpha$  = distance from the middle surface of the lower layer to the neutral axis

$\beta$  = distance from the middle surface of the upper layer to the neutral axis

Bending moments in this case can be determined from the following equation:

$$\{M\} = \int_{\beta - \frac{h_t}{2}}^{\beta + \frac{h_t}{2}} z_t^2 [C_{top}] dz_t + \int_{-\frac{h_b}{2} - \alpha}^{\frac{h_b}{2} - \alpha} z_b^2 [C_{bottom}] dz_b \quad \{\kappa\} \quad (3-25)$$

or

$$\{M\} = [D] \{\kappa\} \quad (3-26)$$

where

$$[D] = \begin{pmatrix} \frac{E(12\beta^2 h_b + h_t^3)}{12(1 - \mu^2)} & \begin{vmatrix} 1 & \mu & 0 \\ \mu & 1 & 0 \\ 0 & 0 & \frac{1-\mu}{2} \end{vmatrix}_{top} \\ + \left( \frac{E(12\alpha^2 h_t + h_b^3)}{12(1 - \mu^2)} \right. & \left. \begin{vmatrix} 1 & \mu & 0 \\ \mu & 1 & 0 \\ 0 & 0 & \frac{1-\mu}{2} \end{vmatrix}_{bottom} \right) \end{pmatrix} \quad (3-27)$$

Curvature vector  $\{\kappa\}$  may be expressed in terms of deflection as:

$$\{\kappa\} = \begin{pmatrix} \kappa_x \\ \kappa_y \\ \kappa_{xy} \end{pmatrix} = \begin{pmatrix} -\frac{\partial^2 W}{\partial x^2} \\ -\frac{\partial^2 W}{\partial y^2} \\ 2 \frac{\partial^2 W}{\partial x \partial y} \end{pmatrix} = [B] [A^{-1}] \{\Delta\} \quad (3-28)$$



Internal virtual work of pavement layers are given by the relationship:

$$\delta W_{int} = - \int \int_{Area} \{\delta \kappa\}^T [M] dx dy \quad (3-29)$$

But since:

$$\{\delta \kappa\} = [B] [A^{-1}] \{\delta \Delta\} \quad (3-30)$$

or

$$\{\delta \kappa\}^T = \{\delta \Delta\}^T [A^{-1}]^T [B]^T \quad (3-31)$$

$$\{M\} = [D] \{\kappa\} = ([D_{top}] + [D_{bottom}]) \{\kappa\}$$

or

$$\{M\} = ([D_{top}] [B] [A^{-1}] + [D_{bottom}] [B] [A^{-1}]) \{\Delta\} \quad (3-32)$$

Thus:

$$\begin{aligned} \delta W_{int} = & - \{\delta \Delta\}^T [A^{-1}]^T \left( \int \int_{Area} [B]^T [D_{top}] [B] dx dy \right. \\ & \left. + \int \int_{Area} [B]^T [D_{bottom}] [B] dx dy \right) [A^{-1}] \{\Delta\} \end{aligned} \quad (3-33)$$

or

$$\delta W_{int} = - \{\delta \Delta\}^T ([K_{top}] + [K_{bottom}]) \{\Delta\} \quad (3-34)$$

where

$[K_{top}]$  = stiffness matrix of the top layer, (12 x 12)

$[K_{bottom}]$  = stiffness matrix of the bottom layer, (12 x 12)

External virtual work consists of two parts, one part due to the loading and another part due to the reaction of the subgrade. Assuming that subgrade

behaves as Winkler foundation, the following equation can be used to evaluate this reaction.

$$q(x, y) = -k(x, y) W(x, y) \quad (3-35)$$

where  $k$  is the modulus of subgrade support.

$$\begin{aligned} \delta W_{\text{ext}} = & \int \int_{\text{Area}} p(x, y) \delta W \, dx \, dy \\ & + \int \int_{\text{Area}} q(x, y) \delta W \, dx \, dy \end{aligned} \quad (3-36)$$

where  $p(x, y)$  is the externally applied load. From Equation 3-8 we have:

$$\delta W = [N_{\alpha}] [A^{-1}] \{\delta \Delta\} = \{\delta \Delta\}^T [A^{-1}]^T [N_{\alpha}]^T \quad (3-37)$$

Thus,

$$\begin{aligned} \delta W_{\text{ext}} = & \{\delta \Delta\}^T [A^{-1}]^T \int \int_{\text{Area}} p(x, y) [N_{\alpha}]^T \, dx \, dy \\ & - \{\delta \Delta\}^T [A^{-1}]^T \int \int_{\text{Area}} k [N_{\alpha}]^T [N_{\alpha}] \, dx \, dy [A^{-1}] \{\Delta\} \end{aligned} \quad (3-38)$$

or

$$\delta W_{\text{ext}} = \{\delta \Delta\}^T \{P\} - \{\delta \Delta\}^T [K_{\text{SUB}}] \{\Delta\} \quad (3-39)$$

where:

$\{P\}$  = equivalent nodal loads (12 x 1)

$[K_{\text{SUB}}]$  = stiffness matrix of the subgrade (12 x 12)

Since:

$$\delta W_{\text{int}} + \delta W_{\text{ext}} = 0 \quad (3-40)$$

for each element we have,

$$([K_{\text{top}}] + [K_{\text{bottom}}] + [K_{\text{SUB}}]) \{\Delta\} = \{P\} \quad (3-41)$$

The stiffness matrix of a rectangular plate element, stiffness matrix of subgrade, and equivalent nodal load vector due to a uniform load over a rectangular area in the element are given in Appendix A.

#### Monotonic Energy Convergence

The conditions that deflection function  $W(x, y)$ , in Equation 3-3 must satisfy to guarantee monotonic energy convergence are:

- (a) Continuity of the displacement field within the elements.
- (b) Completeness of the displacement function; rigid body motions and constant curvature must be included in the displacement function.
- (c) Compatibility must exist between elements; elements must not overlap, separate, and there must be no sudden changes in slope across interelement boundaries.
- (d) The element should have no preferred directions.

A 12 degree-of-freedom element does not provide continuous normal slopes between elements (Refs. 46, 47). Thus, monotonic energy convergence is not guaranteed. Despite this, the element used apparently converges although not monotonically and in fact is superior to some conforming elements used by others, since the non-conformity tends to soften the inherently too stiff elements.

#### 3.b.(3) Stiffness Matrix for Beam Element for Dowel Bar

The beam element employed to represent a dowel bar at a joint is shown in Figure 3.3.b and has two degrees of freedom per node. Thus it has displacement components, namely a vertical deflection ( $W$ ) in the Z-direction, and a rotation ( $\theta_Y$ ) about the Y-axis. Corresponding to these two displacement components are two force components, namely a vertical force ( $P_W$ ) and a couple about the Y-axis ( $P_{\theta Y}$ ). The force-displacement relation for a dowel bar can be written in matrix form as:

$$\begin{array}{ccc}
 P_{wi} & & W_i \\
 P_{\theta Yi} & = [K_{dowel}] & \theta_{Yk} \\
 P_{wk} & & W_k \\
 P_{Yk} & & \theta_{Yk}
 \end{array} \quad (3-42)$$

where  $[K_{dowel}]$  is the stiffness matrix of the dowel bar, and is given by:

$$\begin{array}{cccc}
 D & 6\ell C & -D & 6\ell C \\
 6\ell C & (4 + \phi)\ell^2 C & -6\ell C & (2 - \phi)\ell^2 C \\
 -D & -6\ell C & D & -6\ell C \\
 6\ell C & (2 - \phi)\ell^2 C & -6\ell C & (4 + \phi)\ell^2 C
 \end{array} \quad (3-43)$$

where

$$C = \frac{EI}{\ell^3 (1 + \phi)}, \quad D = 1 / \left( \frac{1}{DCI} + \frac{1}{12C} \right)$$

$E$  = modulus of elasticity of the dowel bar

$I$  = moment of inertia of the dowel bar

$\ell$  = width of the joint opening

$$\phi = \frac{12EI}{GA_z \ell^2}$$

$G$  = shear modulus of the dowel bar

$A_z$  = beam cross-sectional area effective in shear, i.e.,

for a circular cross section  $A_z$  is equal to 0.9 times the actual cross section.

$DCI$  = spring stiffness representing the dowel-concrete interaction, use a large value if dowel-concrete interaction is neglected.

### 3.b.(4) Stiffness Matrix for Spring Element for Aggregate Interlock System and Keyway

Neglecting the moment transfer (if any) across a joint, where load transfer from one slab to an adjacent slab is achieved by means of aggregate interlock or keyway, the spring element shown in Figure 3-3-c with one degree of freedom per node is used. The displacement component at each node is a vertical deflection ( $W$ ) in the Z-direction, and the corresponding force component is a vertical force ( $P_W$ ). The force-displacement relation for a spring element can be written as:

$$\{P\} = [K_{Agg}] \{D\} \quad (3-44)$$

where  $[K_{Agg}]$  is the stiffness matrix of the spring element, and is given by

$$[K_{Agg}] = \begin{bmatrix} AG & -AG \\ -AG & AG \end{bmatrix} \quad (3-45)$$

where  $AG$  is the stiffness of the spring. For the case of the keyway, a very stiff spring is assumed in the analysis.

### 3.b.(5) Overall Stiffness Matrix

The overall structural stiffness matrix  $[K]_S$  is formulated by superimposing the effect of individual element stiffnesses using the topological or the element connecting properties of the pavement system. The overall stiffness matrix is used to solve the set of simultaneous equations having the form:

$$\{P\}_S = [K]_S \{\Delta\}_S \quad (3-46)$$

where

$\{P\}_S$  = externally applied loads for the whole system

$\{\Delta\}_S$  = nodal displacements for the whole system

The generalized stresses and deflections are then calculated.

### 3.b.(6) Computer Program

A computer program was written in FORTRAN IV for structural analysis of the jointed concrete pavements with load transfer system at the joints. A complete program listing and a User's Manual are being submitted as a separate report.

The input to the program is:

- (a) Geometry of the slab, including the type base or overlay, load transfer system, subgrade, and the slab dimensions.
- (b) Elastic properties of the concrete, stabilized base or overlay, load transfer system, and subgrade.
- (c) Loading.

The output given by the program is:

- (a) Stresses at any designated point in the slab, stabilized base or overlay.
- (b) Vertical stresses at any designated position on the subgrade.
- (c) Vertical deflection at any point in the pavement system.
- (d) Reactions on the dowel bars.
- (e) Shear stresses at the joint face for the aggregate interlock and keyed joint systems.

### 3.c Verification of the Finite-Element Model

To verify the accuracy of the computer program, it is necessary to compare the finite-element solutions with available theoretical solutions

and the results of experimental studies. Westergaard's equations (Ref. 2), Pickett and Ray's influence charts (Ref. 3), experimental studies at the AASHO Road Test (Ref. 4), and tests conducted by Teller and Sutherland (Ref. 5) are used for this purpose.

### 3.c.(1) Comparison with Westergaard's Solutions

Figure 3-5 shows the comparison between Westergaard's exact solutions (Equations 2-2 through 2-5) for an infinite slab with a single load of 50 kips (222 KN) placed on one edge far from any corner and in the interior of the slab far from any edges. The Westergaard solutions are indicated by the solid curves, and the finite-element solutions, by the small circles. Because the Westergaard solutions are based on a slab infinite in extent, a large slab of 25 ft (7.6 m) square was used in the finite-element analysis. The loaded area in Westergaard's solution was assumed to be a circle with diameter of 15 in. (38 cm) while a 15 in. (38 cm) square was used in the finite-element analysis. The modulus of elasticity and Poisson's ratio of the concrete slab were assumed to be  $5 \times 10^6$  psi (34.5 GPa) and 0.15, respectively for both analyses.

The comparison of the results from the analyses were made for a complete factorial of three slab thicknesses, 12, 14, and 16 in. (30.5, 40.6, and 50.8 cm), and three modulus of subgrade reactions 50, 200, and 500 pci (13.6, 54.2 and 135.5 N/cm<sup>3</sup>). Since the Westergaard analysis cannot take the subbase into account all slabs were assumed to be in direct and full contact with the subgrade.

The modulus of relative stiffness of the slab with respect to subgrade ( $\ell$ ), used in the Figure 3-5 is same as in the Equation 2-8.

### 3.c.(2) Comparison with Influence Charts

To check the accuracy of the model for multiple loading, influence

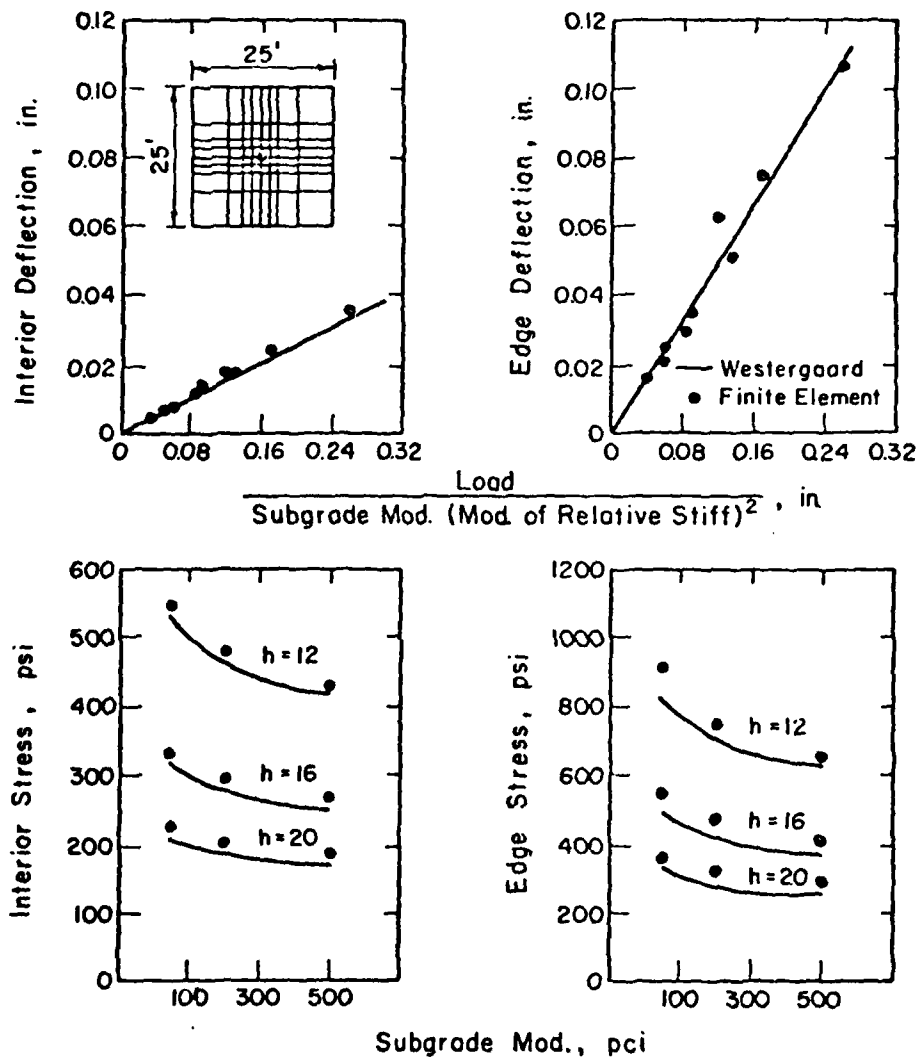


Figure 3-5. Comparison of Finite-Element Solutions with Westergaard's Equations



charts developed by Pickett and Ray (Ref. 3) were used. Figures 3-6 and 3-7 present influence charts for moments in a concrete slab for interior and edge loadings, respectively. Solution is accomplished by tracing the tire contact imprints on the charts, counting the number of blocks within the imprint areas and solving the equations given below:

$$M = \frac{p\ell^2 N}{10,000} \quad (3-47)$$

$$\sigma = \frac{6M}{h^2} \quad (3-48)$$

where:

M = moment

$\sigma$  = stress

p = tire pressure

$\ell$  = modulus of relative stiffnes

N = number of blocks

h = thickness of the concrete slab

Figure 3-8 shows the comparison of the results from the finite-element solutions with those obtained from the influence charts for the main gear of a DC-10-10 aircraft (Ref. 49) with a load of 220 kips (978 KN), placed at the edge and in the interior of the slab. Because the influence chart solutions are based on infinite slab, a large slab of 25 ft (7.6 m) was used in the finite-element analysis.

### 3.c.(3) Comparison with AASHO Road Test Results

Further verification of the finite-element model can be made by comparison with experimental results. The results of the strain measurements from AASHO Road Tests (Ref. 4) provide excellent data for making such comparisons. Tests were conducted on the main traffic loops where

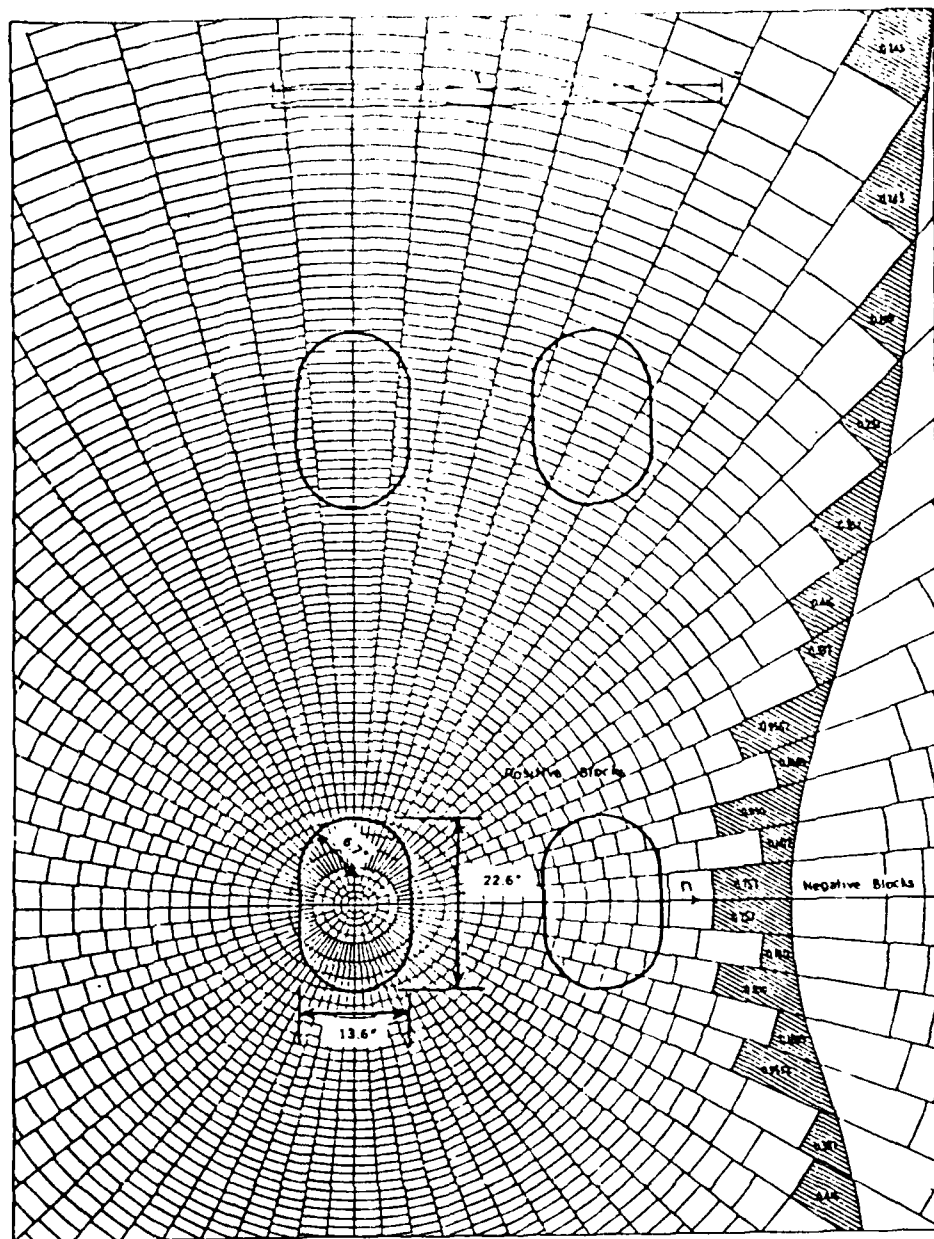


Figure 3-6. Influence Chart for the Moment in a Concrete Pavement Due to Interior Loading (Ref. 3)

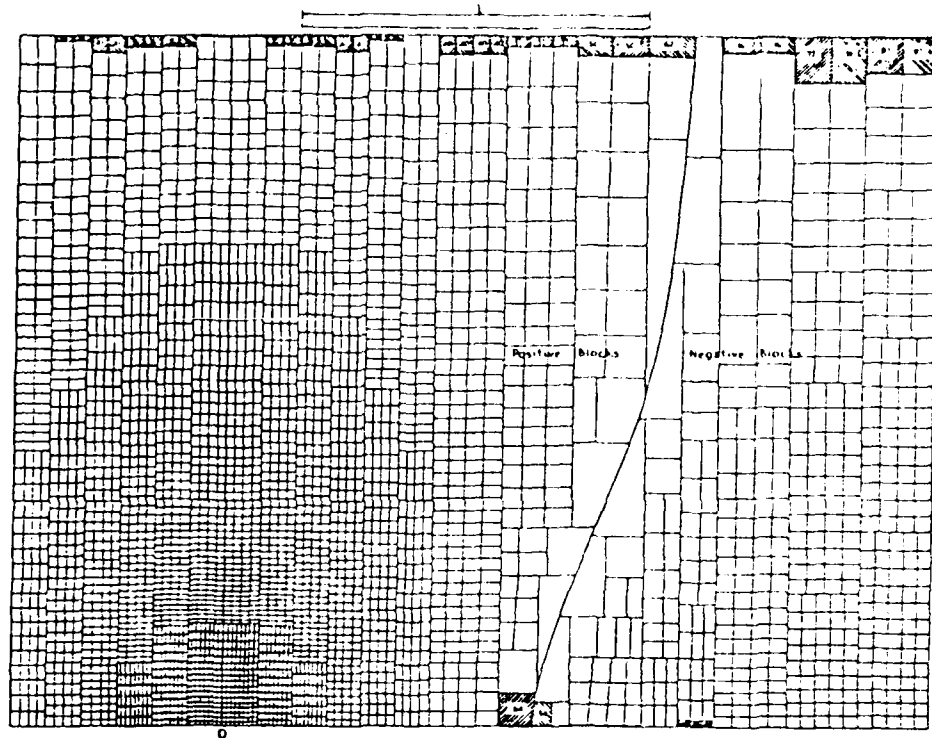


Figure 3-7. Influence Chart for the Moment in a Concrete Pavement Due to Edge Loading (Ref. 3)

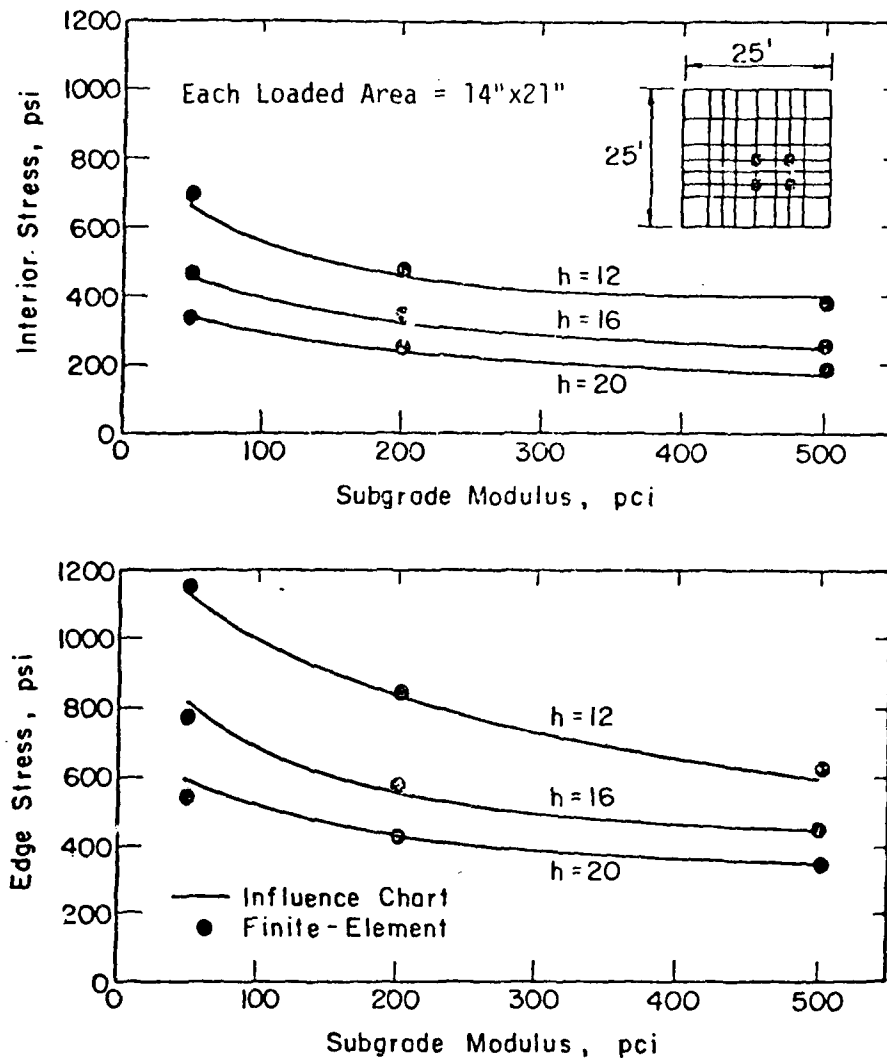


Figure 3-8. Comparison of Finite-Element Solutions with those Computed by Pickett's Influence Charts

the strain at the slab edge due to moving traffic 17 to 22 in. (43 to 56 cm) from the edge, was measured. The length of slabs were 15 ft (4.6 m) non-reinforced sections and 40 ft (12.2 m) reinforced slabs and slab widths were 12 ft (3.7 m). Each slab was of uniform thickness, but the thickness of the slabs tested ranged from 5 to 12.5 in. (12.7 to 31.8 cm). The measured dynamic modulus of elasticity and Poisson's ratio of concrete were assumed to be  $6.25 \times 10^6$  psi (43 GPa) and 0.28, respectively. The Road Test reports the modulus of subgrade reactions (k-values) on the subbase obtained by the plate bearing tests varied from approximately 85 to 200 pci (23 to 54 N/cm<sup>3</sup>) over all of the loops throughout the two year test period. An average of 150 pci (41 N/cm<sup>3</sup>) was used for k-value in the finite-element analysis.

Based on the statistical analysis study of the data from the tests, the following equation was developed (Ref. 4) for determination of edge stresses.

$$\bar{\sigma}_a = \frac{139.2 L_1}{10^{0.0031T} H^{1.278}} \quad (3-49)$$

where:

$\bar{\sigma}_a$  = edge stress, psi

$L_1$  = single axle load, kips

H = slab thickness, in.

T = standard temperature differential, °F

Figure 3-9 shows the comparison of the finite-element solutions with experimental results.

### 3.c.(4) Comparison with Public Roads Test Results

To check the accuracy of the finite-element computer program for prediction of stresses and deflections at concrete pavement joints with

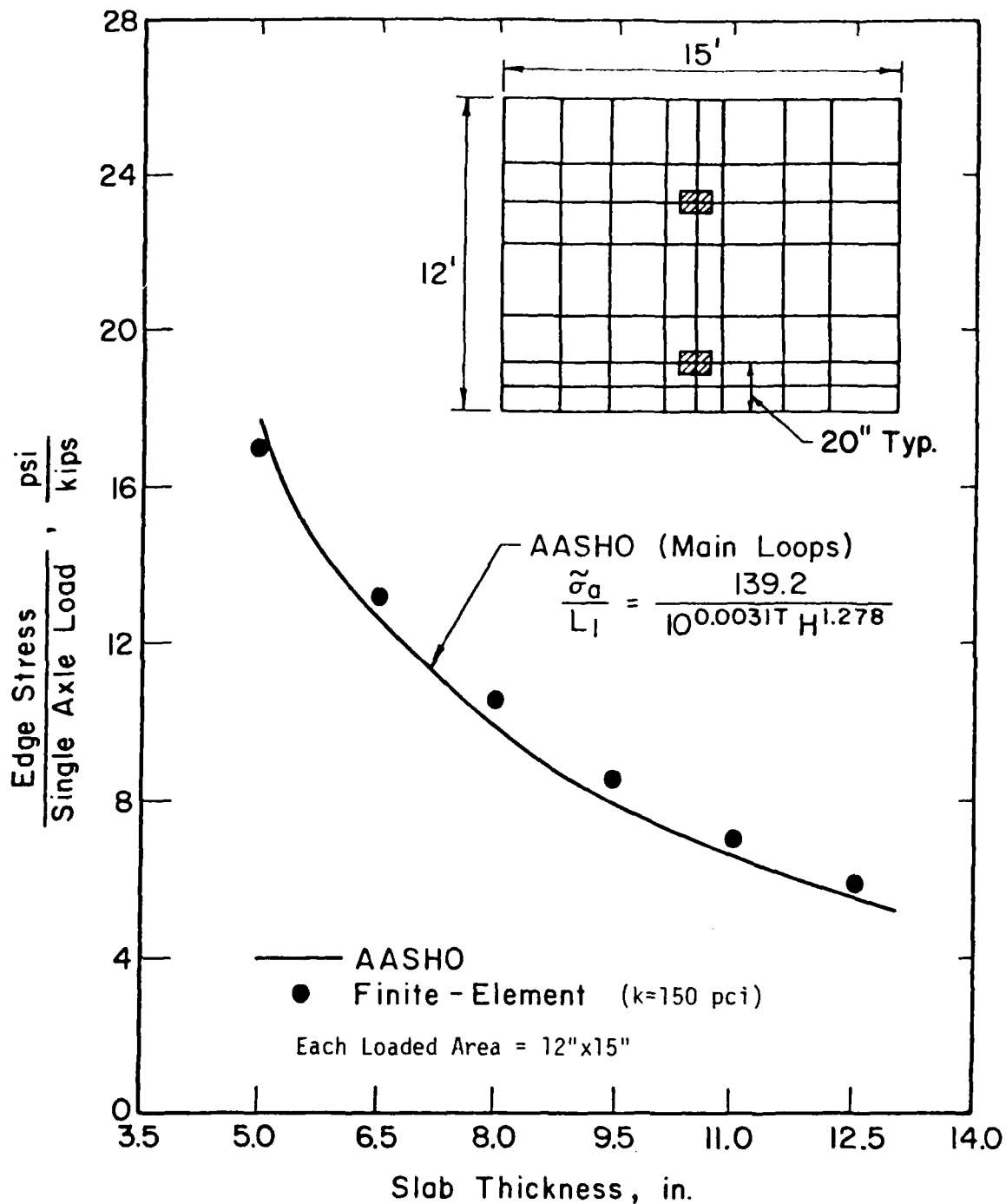


Figure 3-9. Comparison of Edge Stresses Computed with Finite-Element Program and those Measured at the AASHO Road Test

various load transfer system, the results of the strain and deflection measurements from the Bureau of Public Roads Test conducted by Teller and Sutherland (Ref. 5) can be used. Tests were conducted on 10 full-size concrete slabs, where each slab was 40 ft (12.2 m) long and 20 ft (6.1 m) wide. Four slabs had a uniform cross section, while the other six were of thickened edge designs in which slab thicknesses ranged from 6 to 9 in. (15.2 to 22.9 cm). Each slab was divided by a longitudinal and a transverse joint of a particular design. Different joint designs included in the investigation were butt joints with different dowel spacings, joints with a plane of weakness with and without dowels, corrugated joints, and keyed joints with triangular or trapezoidal tongues. The measured average modulus of elasticity of concrete and modulus of subgrade reaction were found to be  $5.5 \times 10^6$  psi (37.9 GPa) and 200 pci ( $54 \text{ N/cm}^3$ ) respectively. Figures 3-10 and 3-11 show a comparison of the results from the finite-element solutions with experimental results. The loaded area used in all analysis was 8 in. (20.3 cm) square.

These comparisons show that the finite-element solutions check very closely with both theoretical (Figures 3-5, 3-8) and experimental (Figures 3-9, 3-10, 3-11) results, thus verifying the accuracy of the two-dimensional finite-element computer program.

### 3.d Summary

Due to the three-dimensional nature of the structural analysis of jointed concrete pavement and pavement joint system, a two stage analysis has been suggested. In first stage a two-dimensional analysis of the jointed concrete pavement with various load transfer systems at the joints is performed. And then in the second stage, a three-dimensional analysis of a small section of the concrete pavement system near and at the joint is

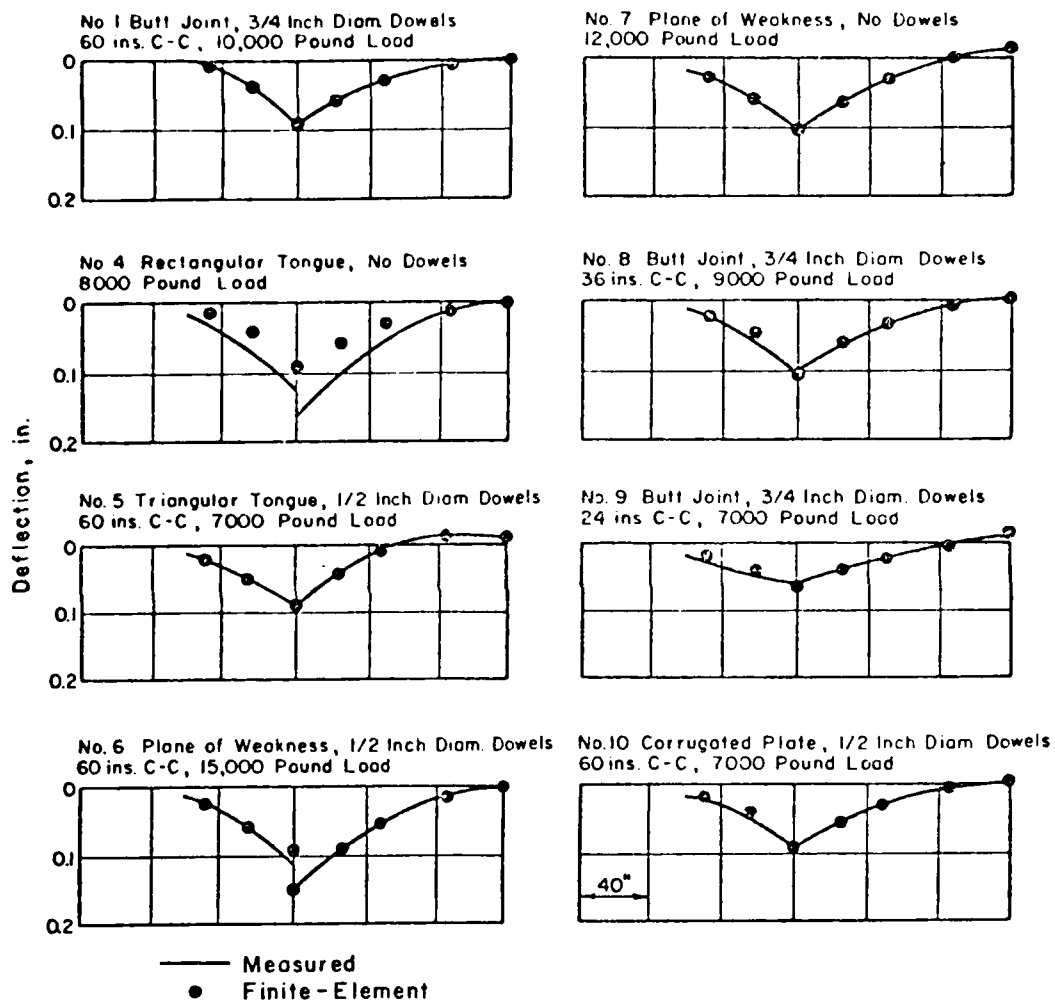


Figure 3-10. Comparison of Slab Deflections Computed with Finite-Element Program and those Measured at the Public Roads Test



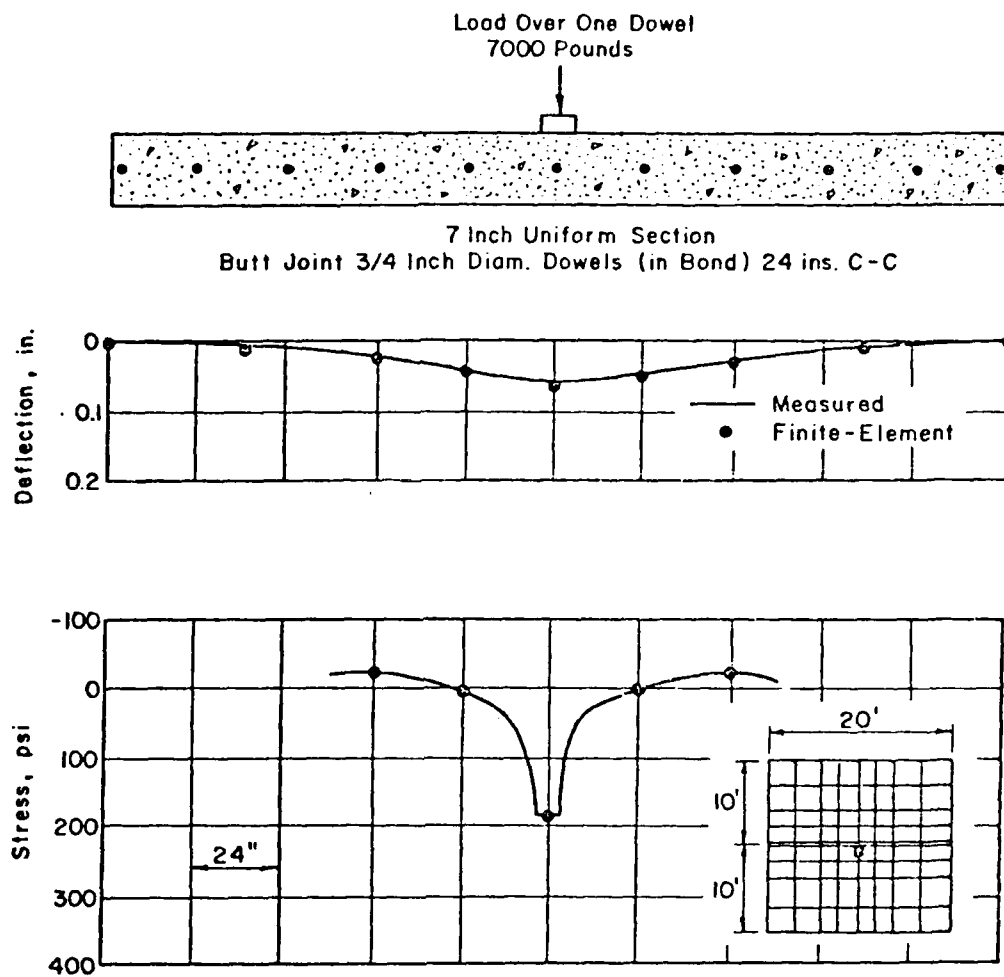


Figure 3-11. Comparison of Joint Deflections and Stresses Computed with Finite-Element Program and those Measured at the Public Roads Test

made. The input to the three-dimensional analysis is obtained from the results of the two-dimensional analysis in terms of the proper boundary conditions.

For the two-dimensional analysis stage, a finite-element model based on the classical theory of medium-thick plate on Winkler foundation was developed for analysis of jointed concrete pavement system. Various types of load transfer systems such as dowel bars, aggregate interlock, keyways, or a combination of them could be considered at the pavement joints. The model is also capable of handling the effect of a stabilized base or an overlay (either with perfect bond or no bond), on the structural response of the pavement system. Further, the model was verified by comparison with the available theoretical solutions and the results from experimental studies.

CHAPTER 4  
APPLICATION OF THE METHOD TO ANALYSIS  
OF JOINTED CONCRETE PAVEMENTS AND  
PAVEMENT JOINTS

4.a General

The method of analysis for jointed concrete pavements and pavement joints developed in Chapter 3 is a powerful method for predicting the structural response of concrete pavement systems. To illustrate the application of the methodology, the results of studies on several pavement systems are presented in this chapter.

Current design procedures are based on assumptions of continuous slabs, infinite in extent, calculating the stresses and deflections for the continuous slab and then superimposing the selected joint system on the designed slab. By use of the two-dimensional finite-element model developed in Chapter 3, it is possible to analyze jointed concrete pavements with a prescribed finite size and with various load transfer system at the joints in a realistic manner. Since a primary purpose of the load transfer system at the joints is to reduce the high stresses and deflections at the slab edges, the effectiveness of various load transfer systems are to be evaluated by determining reduction of stress and deflections.

Slabs with stabilized bases or slabs with thickened edges are also used in jointed concrete pavements to reduce the edge stresses and deflections. The effectiveness of these designs can also be evaluated using the model as described later in this chapter.

4.b Doweled Joints

In the finite-element analysis of doweled joints, actual properties

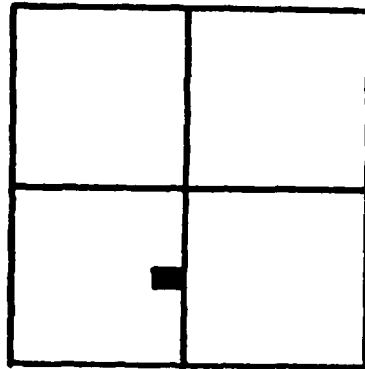
and dimensions for the concrete slabs and dowel bars were used. Load transferred by each dowel as well as the stresses and deflections of the concrete slabs were computed for a complete factorial of seven factors:

- (1) Dowel diameter: 1, 1 1/4, and 2 in. (25.4, 31.8, and 50.8 mm).
- (2) Dowel spacing: 10, 15, and 30 in. (25.4, 38.1, and 76.2 cm).
- (3) Dowel length: 8, 14, and 24 in. (20.3, 35.6, and 6.01 cm).
- (4) Slab thickness: 12, 16, and 20 in. (30.5, 40.7, and 50.9 cm).
- (5) Modulus of foundation support: 50, 200, and 500 pci (13.6, 54.2, and 135.5 N/cm<sup>3</sup>).
- (6) Joint width opening: 0.01, 0.10, and 0.25 in. (0.025, 2.54, and 6.35 mm).
- (7) Load position: edge, protected corner, and unprotected corner.

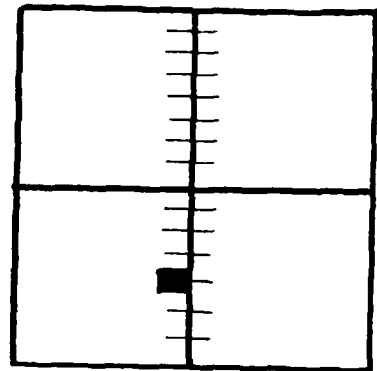
This factorial represents the analysis of 2187 separate pavement systems. All dowels were assumed to be round steel bars having modulus of elasticity and Poisson's ratio of  $29 \times 10^6$  psi (199.81 GPa) and 0.29, respectively. The modulus of elasticity and Poisson's ratio of concrete slab were  $5 \times 10^6$  psi (34.45 GPa) and 0.15, respectively.

Figure 4-1 shows various loading cases, and Table 4-1 summarizes a typical result of the effect of load positions on the critical slab stresses and deflections, and on the maximum dowel shear forces. It can be seen that dowel bars have very important effects on reducing maximum slab stresses and deflections. Furthermore, in the case of a doweled joint, maximum slab stress occurs under edge loading; while the maximum slab deflection and maximum dowel shear force occur when loaded at an unprotected corner load.

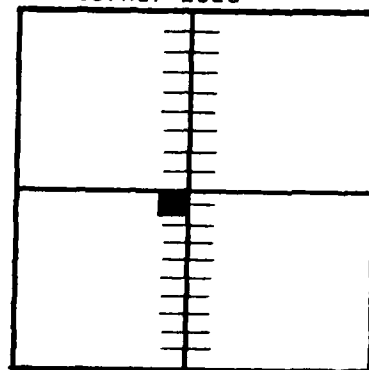
a) Free Edge Load



b) Doweled Edge Load



c) Doweled Unprotected Corner Load



d) Doweled Protected Corner Load

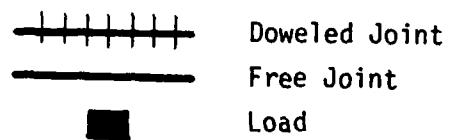
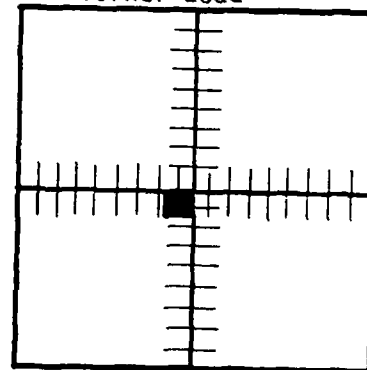


Figure 4-1. Various Loading Cases

Table 4-1. A Typical Result\* of Maximum Slab Stress and Deflection and Maximum Dowel Shear Force Due to Various Load Position

Load Position	Slab Stress		Slab Deflection		Dowel Shear	
	Psi	(MPa)	in	(mm)	Kips	(KN)
Free Edge	485	(3.34)	0.034	(0.86)		
Doweled Edge	257	(1.77)	0.017	(0.43)	6.86	(30.5)
Unprotected Corner	-157	(1.08)	0.043	(1.09)	12.26	(54.5)
Protected Corner	- 72	(0.50)	0.021	(0.53)	8.75	(38.9)

\* Results obtained in a 16 in. (40.7 cm) concrete slab on a subgrade with a k-value of 200 Pci (54.2 N/cm<sup>3</sup>) under a 50 Kips (222 KN) load. Dowels were 1-1/4 in. (31.8 mm) in diameter and spaced 15 in. (38.1 cm) center to center.

Figure 4-2 shows a typical comparison between the finite-element solutions and those by conventional analysis of dowel reactions under edge and unprotected corner loadings. The conventional analysis of dowel shear force distribution along the joint is based on Friberg's (Ref. 42) analysis. In his study, Friberg observed that, according to the theoretical analysis presented by Westergaard (Ref. 2), maximum negative moment at a free slab edge under an edge loading occurs at a distance  $1.8\ell$  from the point of applied load, where  $\ell$  is the radius of relative stiffness as defined in Equation 2-8. Thus, it was assumed that the dowel bar immediately under the applied load carried full capacity and those on either side carried a load decreasing to zero at a distance of  $1.8\ell$  from the central dowel. Because of a lack of data from viable analytical tools, it was assumed that the distribution of transferred load was linear. Figure 4-2 illustrates, however, that the distribution of dowel shear forces among dowel bars is not linear. Only the dowels within a distance  $\ell$  from the central load are effective in transferring the major part of the load from the loaded slab to the adjacent slab, and dowels farther away from the load are not effective. This agrees with the experimental studies conducted by Sutherland (Ref. 41) and Teller and Cashell (Ref. 35). It also shows that the shear force on the dowel immediately beneath the load is greater than indicated by the conventional analysis.

An approximation of the non-linear distribution of dowel shear force for design purposes may be made by assuming that the dowel bar immediately under the applied load carries full capacity and the dowels on either side carry a load decreasing to zero at a distance of  $\ell$  from this dowel. Figure 4-3 shows the effect of dowel spacing and load position on the maximum dowel shear force. Based on a complete factorial of slab thickness, subgrade

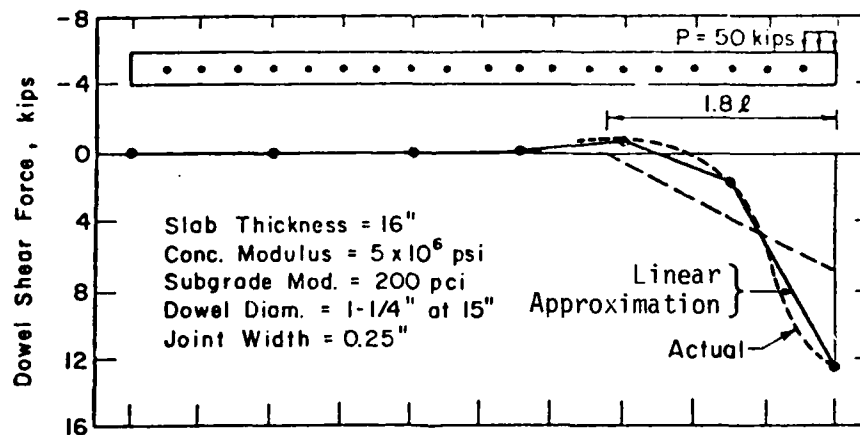
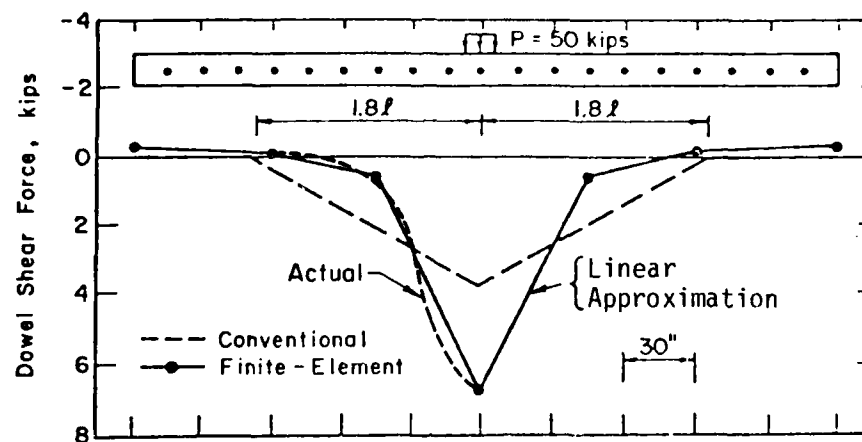


Figure 4-2. Comparison of Dowel Shear Forces Computed with Finite-Element Program with Conventional Analysis



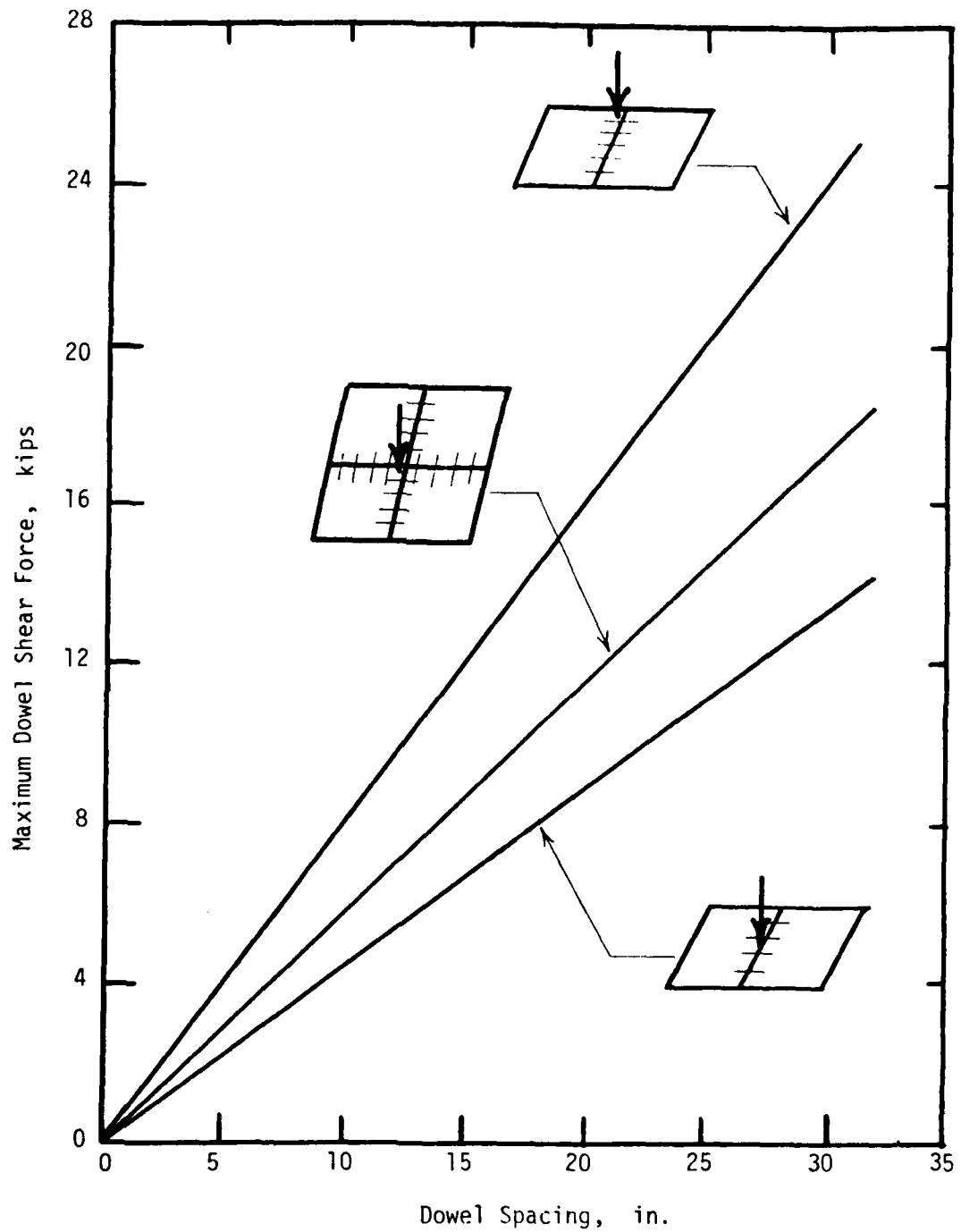


Figure 4-3. Effect of Dowel Spacing and Load Position on the Maximum Dowel Shear Force

10-A078 836

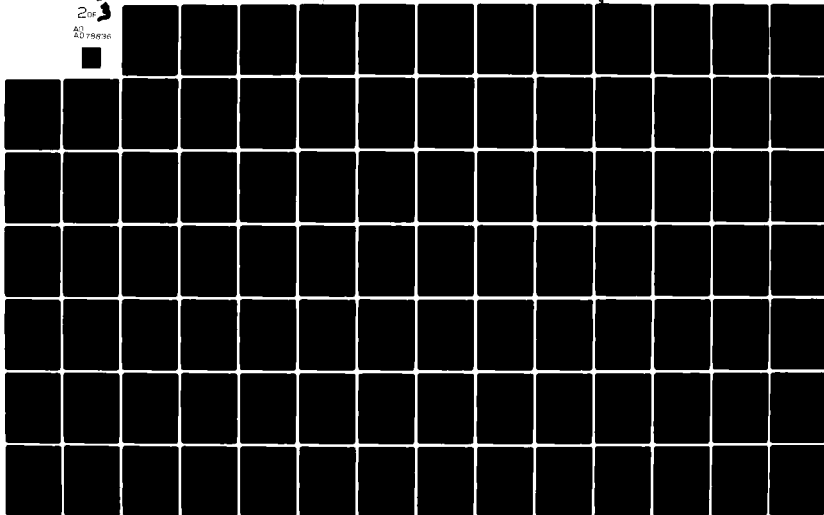
ILLINOIS UNIV AT URBANA-CHAMPAIGN DEPT OF CIVIL ENGIN--ETC F/G 13/2  
LONGITUDINAL JOINT SYSTEMS IN SLIP-FORMED RIGID PAVEMENTS. VOLU--ETC(U)  
NOV 79 A M TABATABAIE ; E J BARENBERG DOT-FA-11-8474

UNCLASSIFIED

FAA-RD-79-4-2

NL

2 of 3  
AD 784736



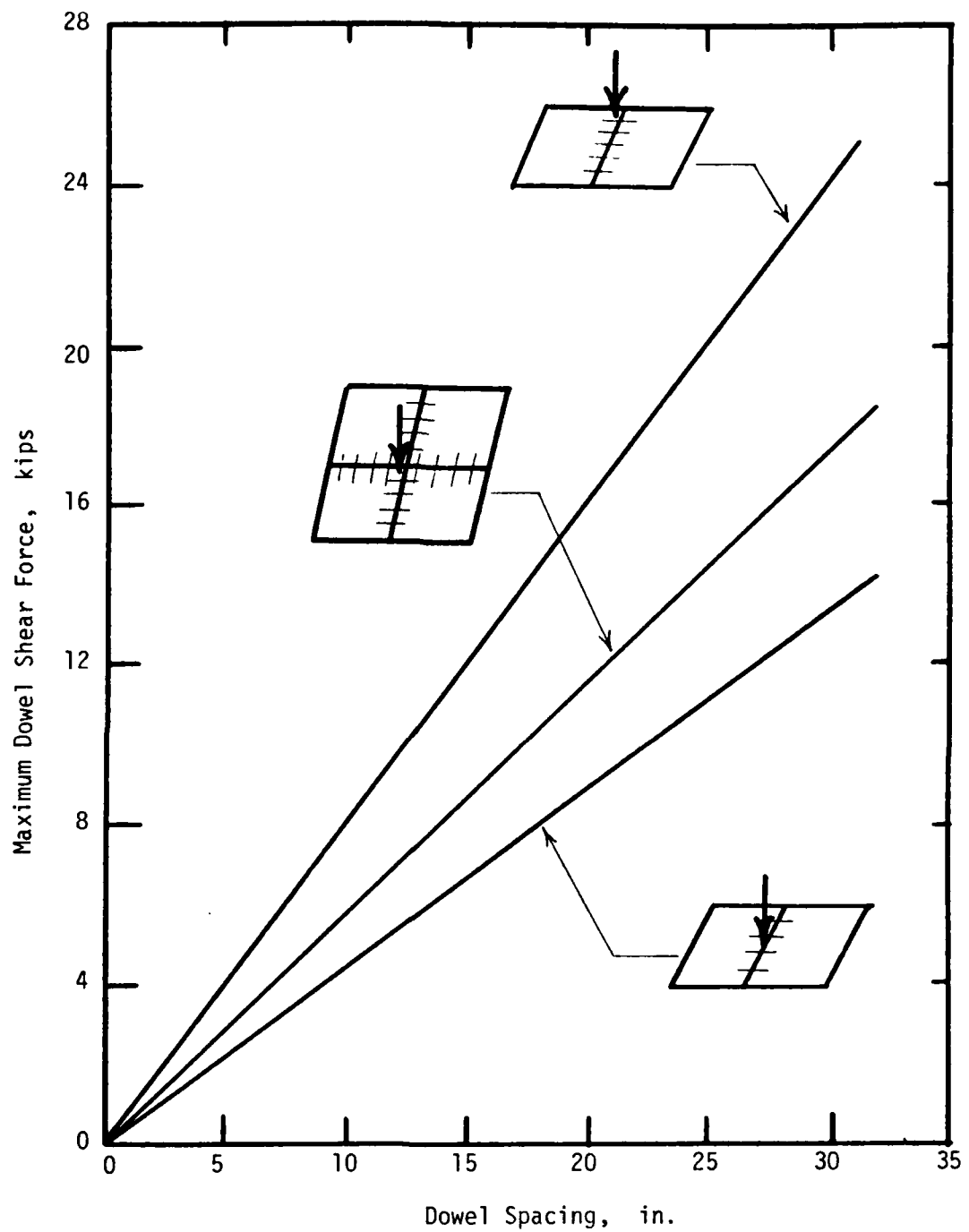


Figure 4-3. Effect of Dowel Spacing and Load Position on the Maximum Dowel Shear Force

k-value, dowel diameter, dowel spacing, joint width opening, and load position, the following relationship was developed for estimating the maximum dowel shear force (load transferred by dowel).

$$F_{\max} = \alpha SP \quad (4-1)$$

where:

$F_{\max}$  = maximum dowel shear force, kips

$S$  = dowel spacing, in.

$P$  = applied wheel load, kips

$\alpha$  = 0.0091, for edge load

$\alpha$  = 0.0116, for protected corner load

$\alpha$  = 0.0163, for unprotected corner load

These results will be used as part of the input to three-dimensional analysis of doweled joints.

Figures 4-4 and 4-5 show the effect of doweled joints on maximum tensile edge stresses and deflections in concrete slab, for a load of 50 kips (222 KN) applied at the edge directly over a dowel. It can be seen from these figures that dowel bars are capable of reducing the maximum tensile edge stresses in a concrete slab to stresses near or below those stresses obtained from interior loadings (assuming that there is no dowel looseness). This may seem somewhat surprising at first but upon reflection will be seen as logical. The ratio stresses under a given load at an interior point and near a free edge is approximately 0.55. If a very efficient load transfer system is used, say one approaching 100 percent efficiency, then the ratio of stresses between the stress at the edge with load transfer to a free edge is .50. This is less than the .55 ratio between the stress due to the interior load and that near a free edge. However, corresponding maximum edge deflections

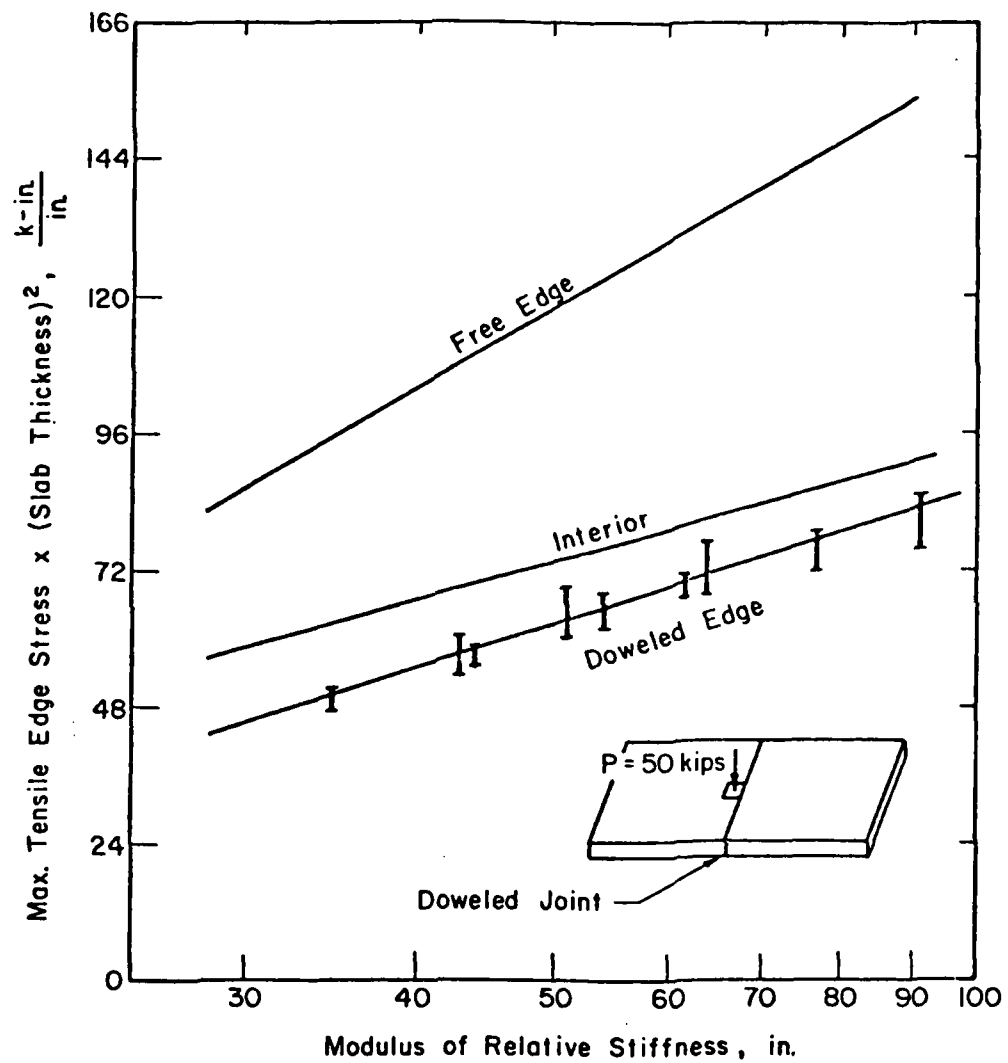


Figure 4-4. Effect of Dowel Bars in Reducing Maximum Tensile Edge Stresses

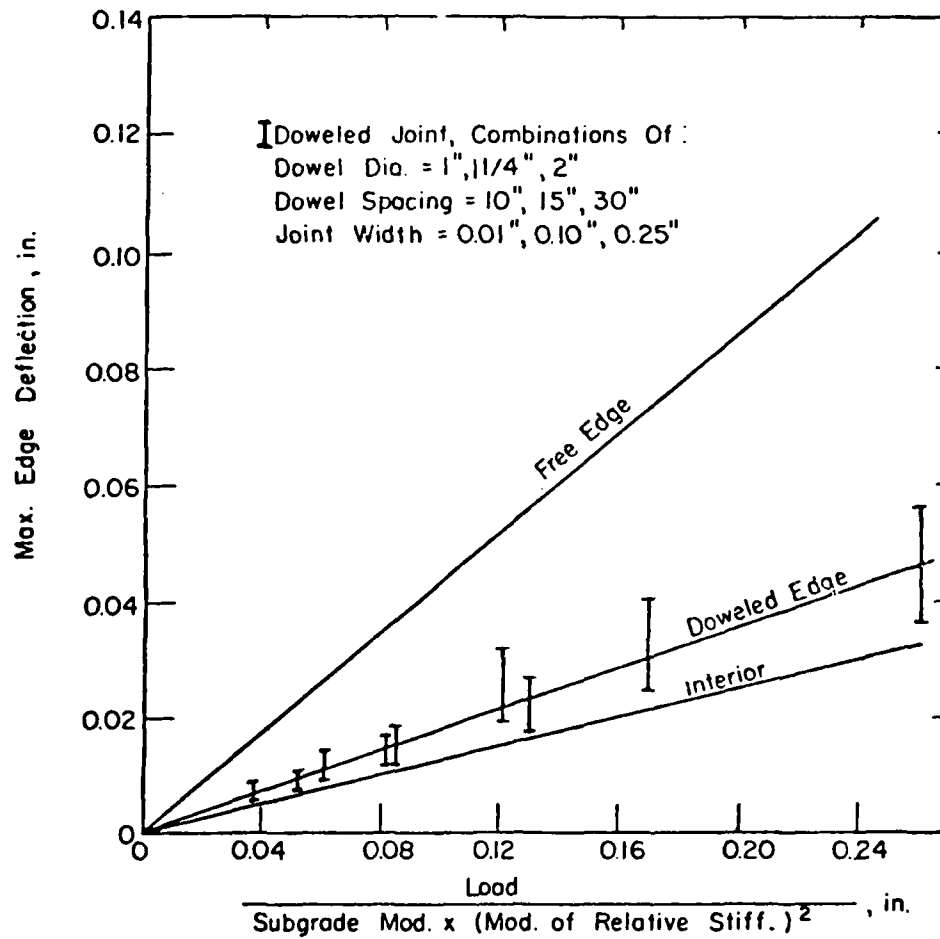


Figure 4-5. Effect of Dowel Bars in Reducing Maximum Edge Deflections

can be reduced only by an average of about 50 percent. Based on the complete factorial analysis, following relationships were developed for estimating the maximum tensile edge stress and maximum edge deflection in concrete slab due to an edge load.

$$\sigma_D = \frac{P}{h^2} (1.595 \log \ell - 1.451) \quad (4-2)$$

$$\Delta_D = \beta \frac{P}{k \ell^2} \quad (4-3)$$

where:

P = applied wheel load, kips

$\sigma_D$  = maximum tensile edge stress, psi

$\Delta_D$  = maximum edge deflection, in.

K = modulus of subgrade reaction, pci

h = slab thickness, in.

$\ell$  = modulus of relative stiffness, in.<sup>-1</sup>

$$\beta = \frac{(0.04 \frac{P}{k \ell^2} + 0.02) D^{1/4}}{(0.97 + 2.48W - 6.33W^2) S^{1/8} h^{1/2}}$$

W = width of joint opening, in.

D = dowel diameter, in.

S = dowel spacing, in.

The effect of multiple loads on maximum tensile edge stress and deflection in the concrete slab and on the maximum dowel shear force are shown in Figures 4-6 through 4-8. These figures can be used for determining the effect of multiple loadings on the critical slab stresses and deflections.

Stresses in dowel bars are in the form of shear, bending, and bearing stresses. These stresses can be determined analytically to determine factors which affect load-transfer characteristics of dowel bars and concomitant

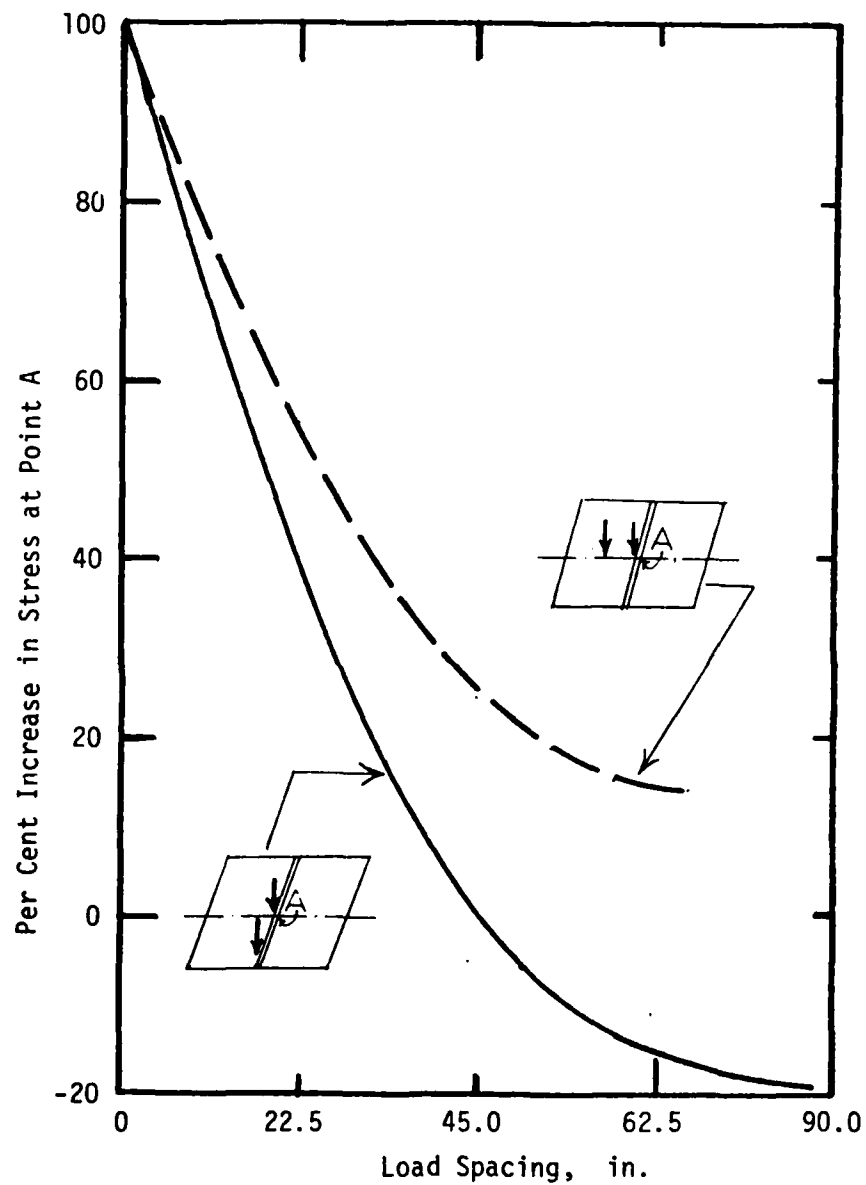


Figure 4-6. Effect of Multiple Loads on Maximum Tensile Edge Stresses



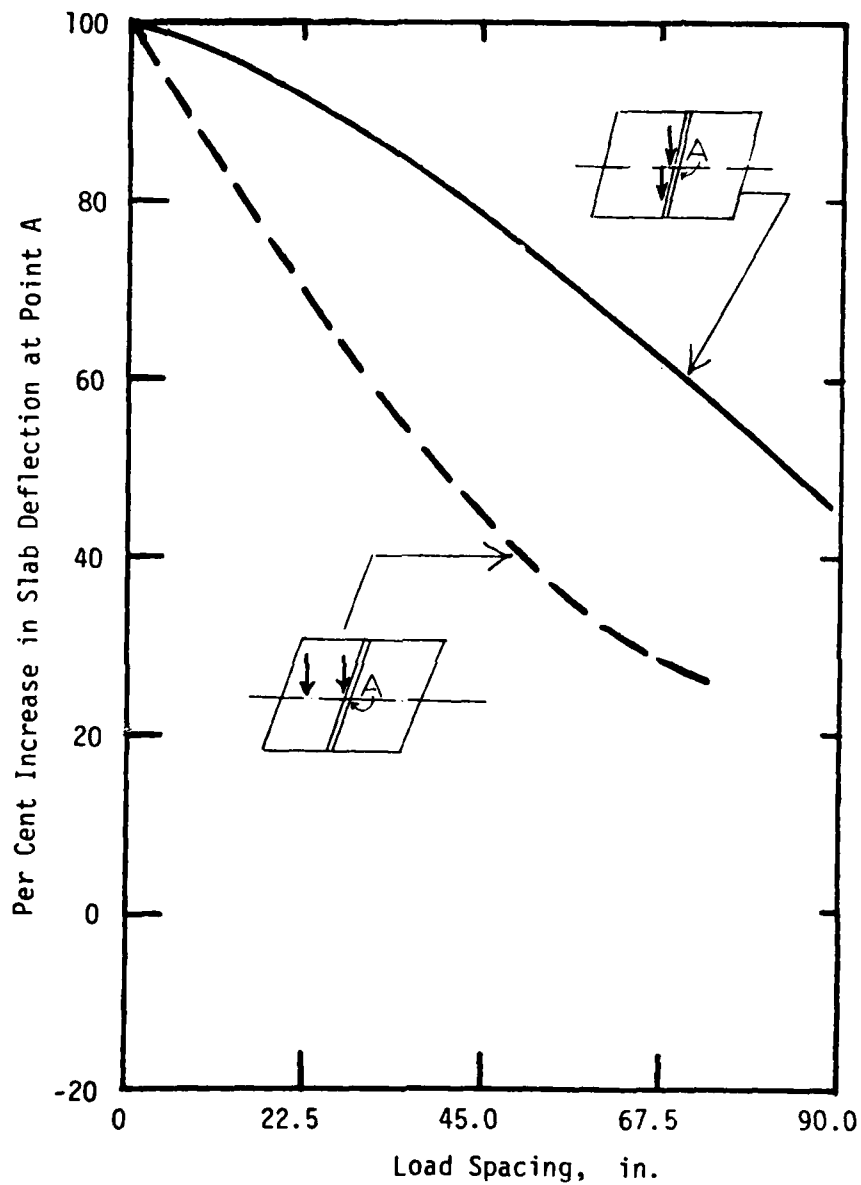


Figure 4-7. Effect of Multiple Loads on Maximum Edge Deflections

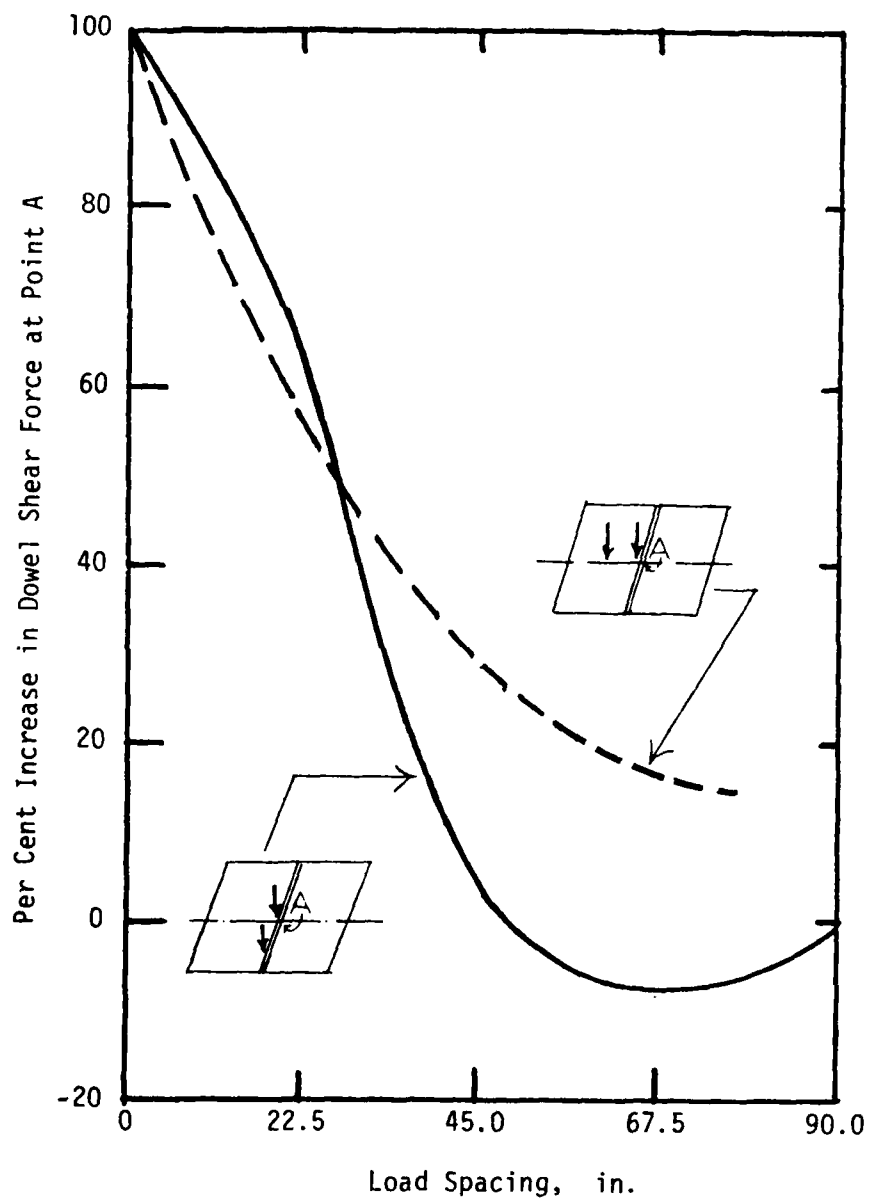


Figure 4-8. Effect of Multiple Loads on Maximum Dowel Shear Forces

performance of the joints. As was discussed in Section 2.a.(4), current analyses of dowel bars are based upon the principles first presented by Timoshenko (Ref. 37), where a dowel bar encased in concrete was modeled as a semi-infinite beam on a Winkler foundation. In reality, however, the interaction between a loaded dowel and surrounding concrete is in a three-dimensional state of stress, and three-dimensional analysis should be used to evaluate the system.

The three-dimensional analysis of the concrete surrounding a dowel bar was made using a finite-element program developed by Wilson (Ref. 45). Results of the two-dimensional finite-element study were incorporated in this model in terms of proper boundary conditions for three-dimensional analysis of bearing stress on concrete as well as stresses and deflections of dowel bars. A typical comparison of three-dimensional finite-element solutions with conventional dowel analysis based on beam on Winkler foundation is shown in Figures 4-9 and 4-10. As can be seen from the results presented in these figures, the finite-element solutions resulted in similar values for dowel deflections and concrete bearing stresses when similar assumptions were used for representing the dowel bar-concrete interaction. However, the finite-element solutions, using the actual elastic properties of the dowel bars and the concrete, resulted in values for dowel deflections and concrete bearing stresses different from those obtained using conventional analysis using a K value of 1,500,000 pci ( $406,500 \text{ N/cm}^3$ ) for modulus of dowel reaction which is the normally accepted value for this property.

The effect of some of the factors affecting dowel deflections and concrete bearing stress are illustrated in Figures 4-11 and 4-12. It was found that the dowel diameter and concrete modulus of elasticity have

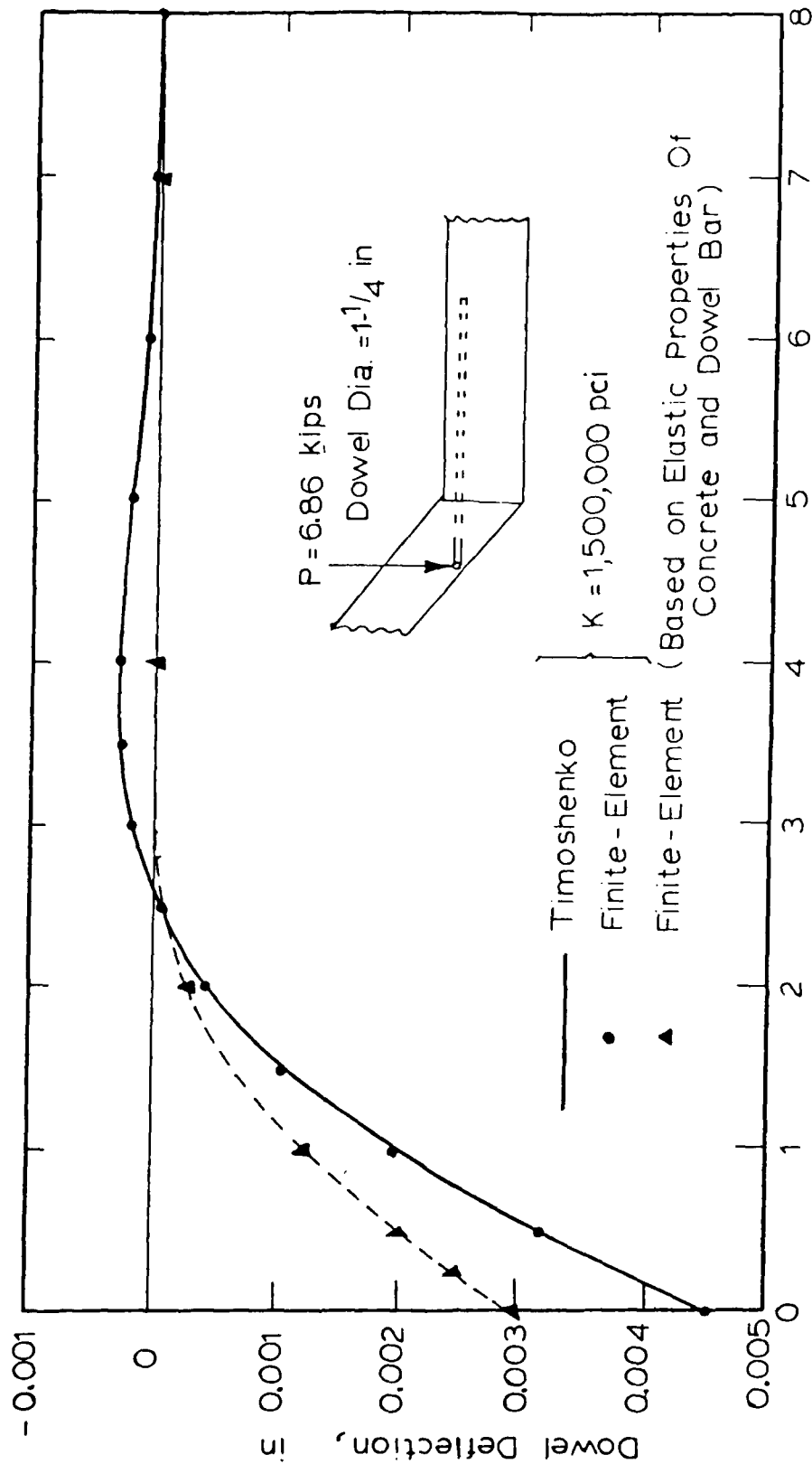


Figure 4-9. Comparison of the Finite-Element Solutions with Timoshenko's Solution for Dowel Deflections

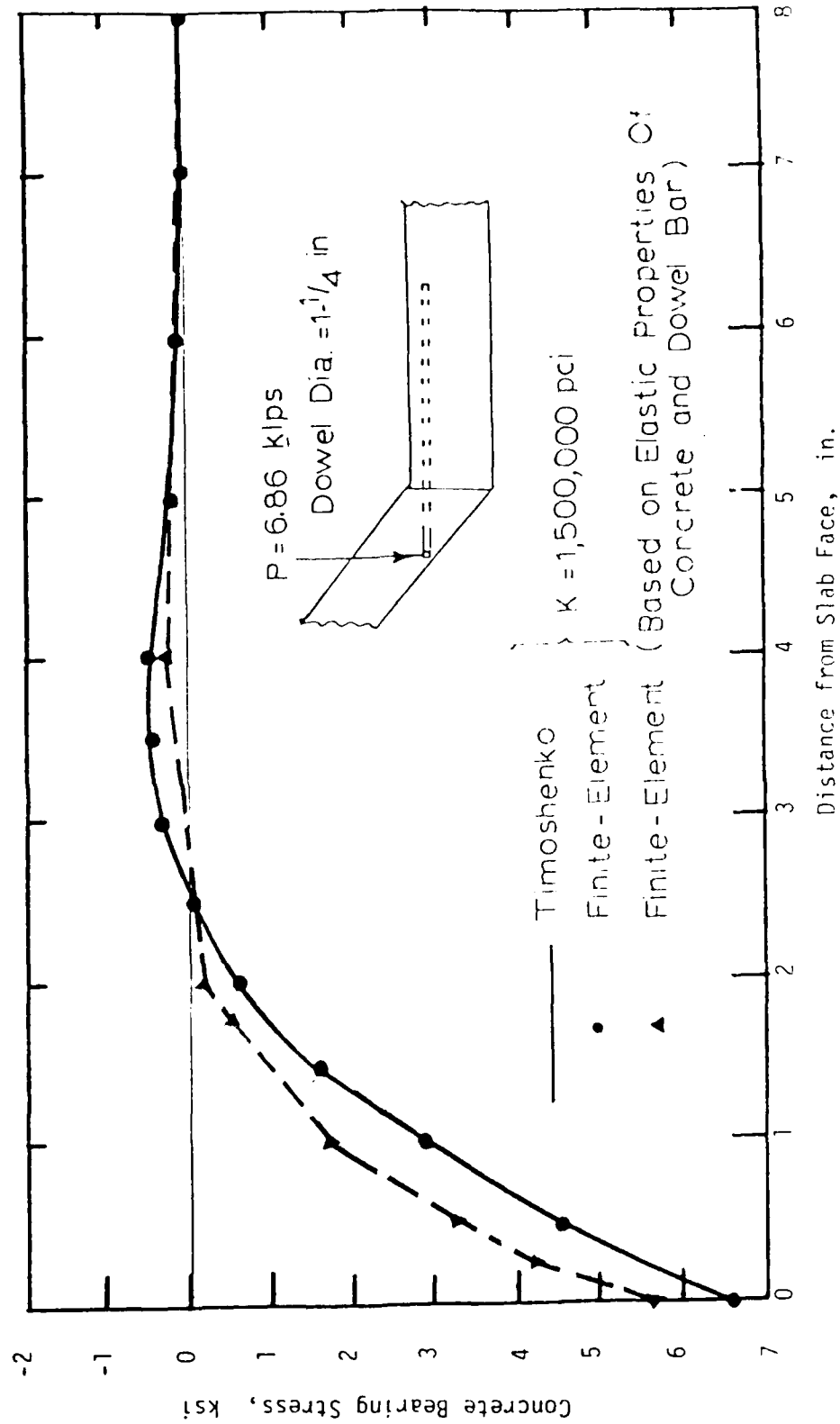


Figure 4-10. Comparison of the Finite-Element Solutions with Timoshenko's Solution for Concrete Bearing Stresses

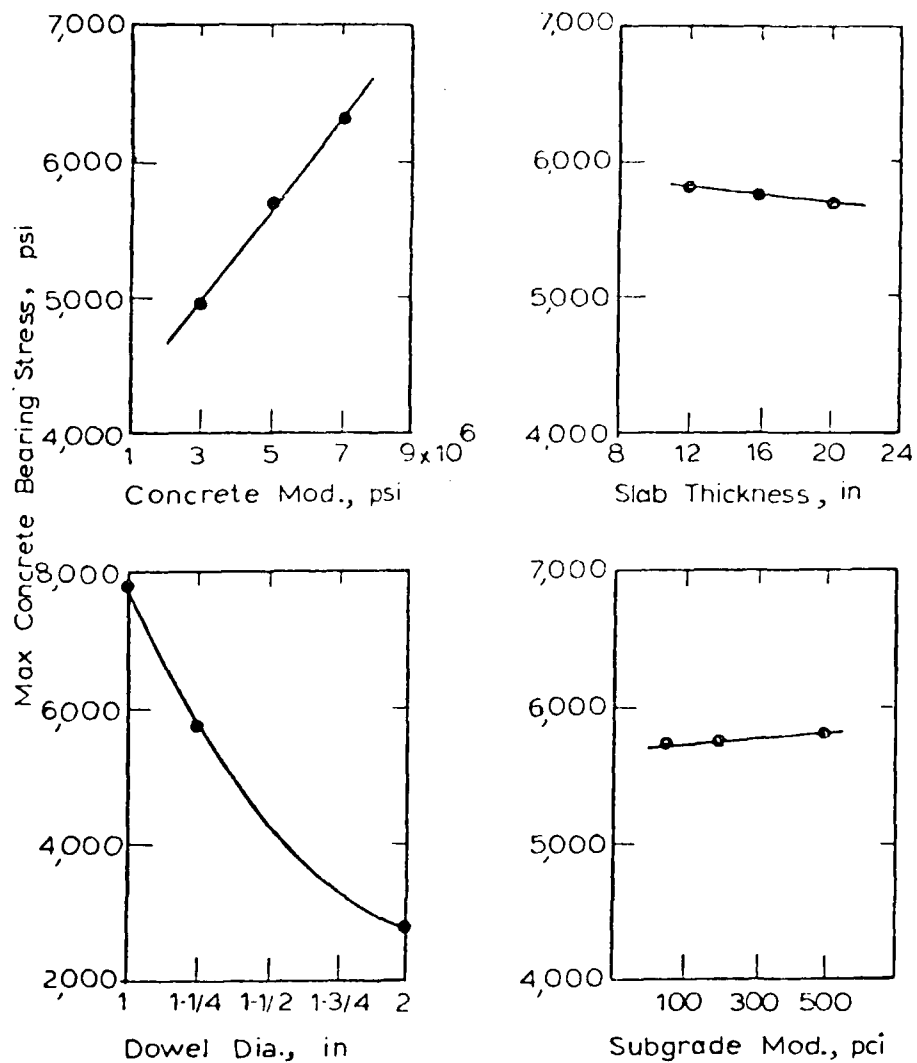


Figure 4-11. Effect of Concrete Modulus, Slab Thickness, Dowel Diameter and Subgrade Modulus on Maximum Concrete Bearing Stress

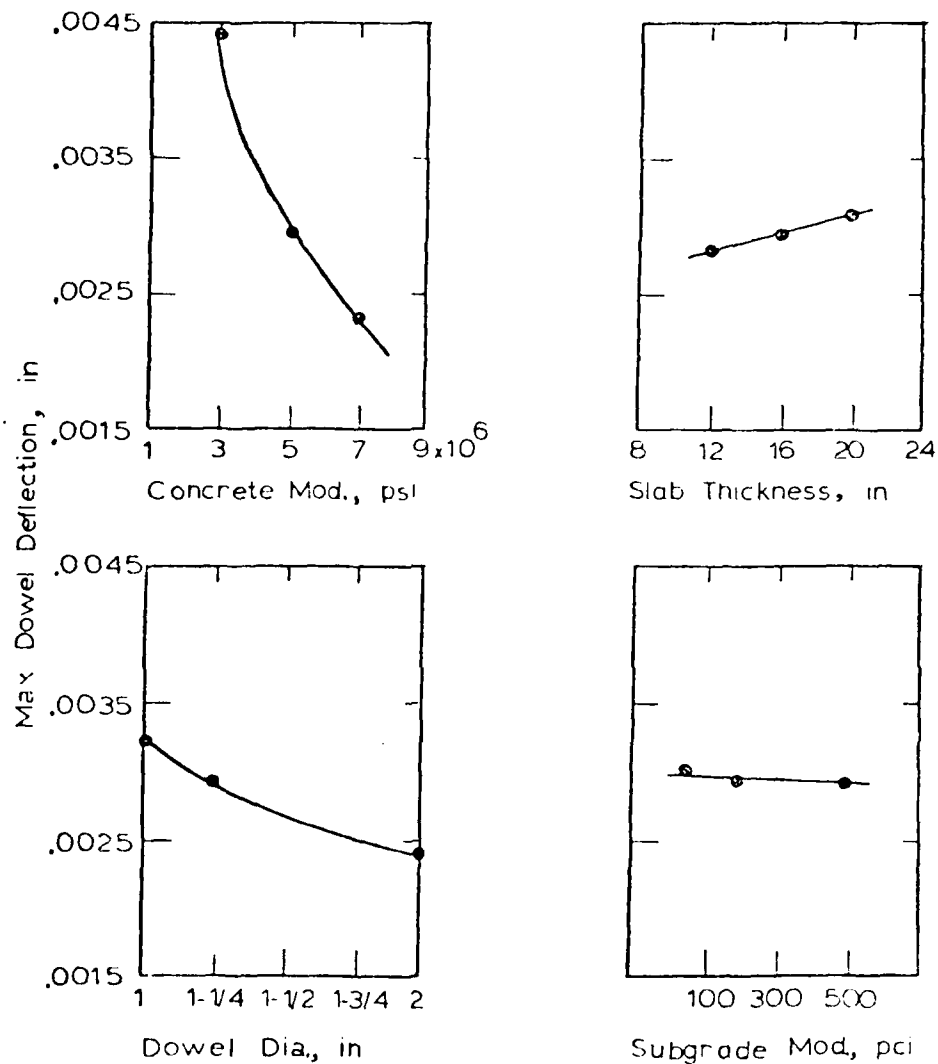


Figure 4-12. Effect of Concrete Modulus, Slab Thickness, Dowel Diameter and Subgrade Modulus on Maximum Dowel Deflection

a very significant effect on the maximum dowel deflection and concrete bearing stresses. Similar conclusions were also reached: by Friberg (Ref. 38), Marcus (Ref. 44), and Teller and Cashell (Ref. 35), based on various laboratory studies of dowel bars. The following relationships, based on the results of two- and three-dimensional analysis, were developed for estimating the maximum dowel shear and bending stresses, and bearing stress on concrete.

$$\tau_{\max} = \alpha \frac{SP}{D^2} \quad (4-4)$$

$$SR_{\max} = \alpha \frac{(1890 - 0.087E)(1.425 - 0.296)}{D^3} \quad (4-5)$$

$$\sigma_{\max} = \alpha \frac{(800 + 0.068E)}{D^{4/3}} (1 + 0.355W)SP \quad (4-6)$$

where:

SP = maximum transferred load by dowel

$\tau_{\max}$  = maximum dowel shear stress, psi

$SR_{\max}$  = maximum dowel bending stress, psi

$\sigma_{\max}$  = maximum bearing stress on concrete, psi

D = dowel diameter, in.

S = dowel spacing, in.

E = concrete modulus of elasticity, ksi

W = width of joint opening, in.

$\alpha$  = 0.0091, for edge load

$\alpha$  = 0.0116, for protected corner load

$\alpha$  = 0.0163, for unprotected corner load

The concrete bearing stress given in Equation 4-6 is usually the controlling factor for dowel design. This equation is represented graphically in Figures 4-13 and 4-14 which can be used directly for the design of doweled joints.



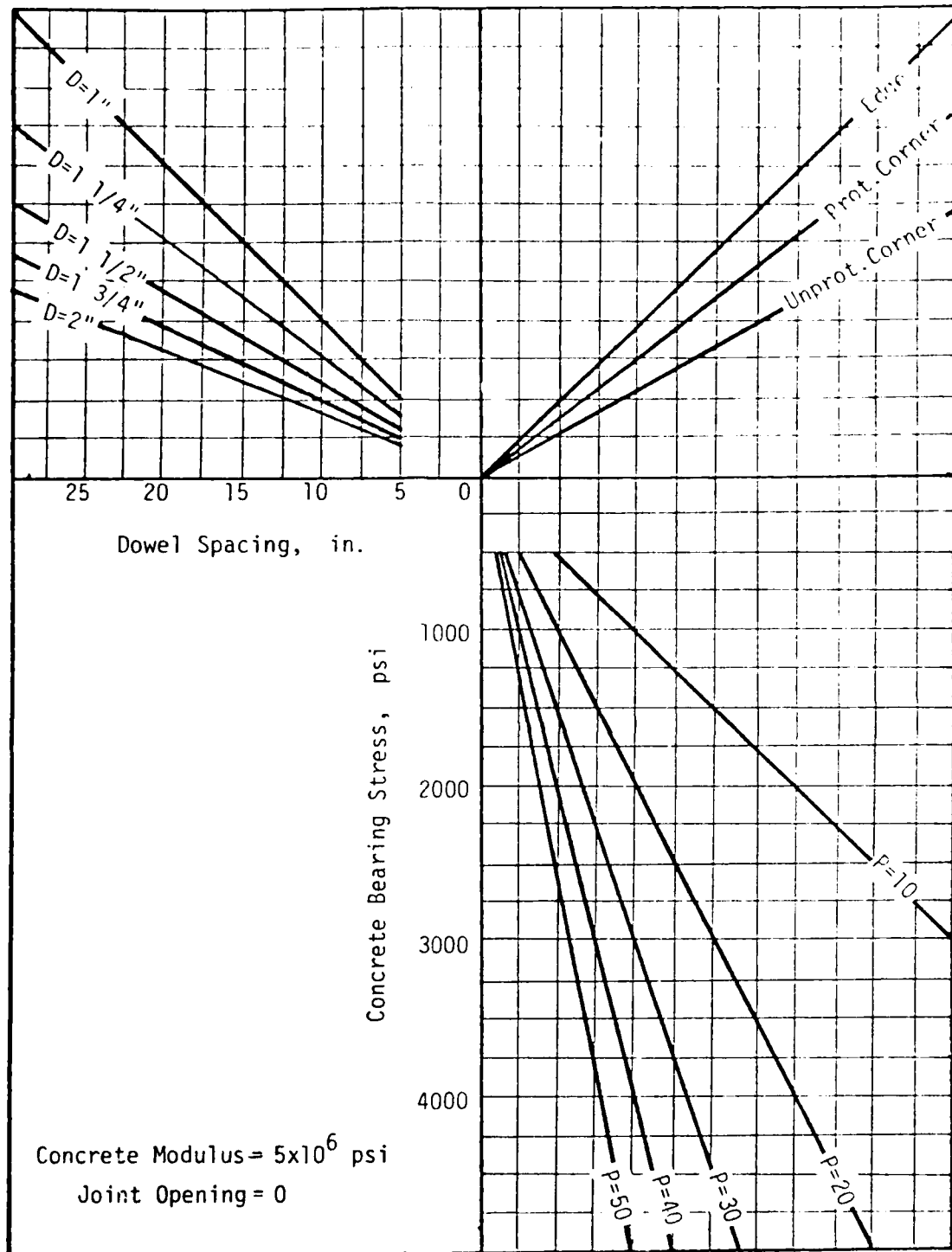


Figure 4-13. Design Chart for Dowel Bars, for various Load Positions

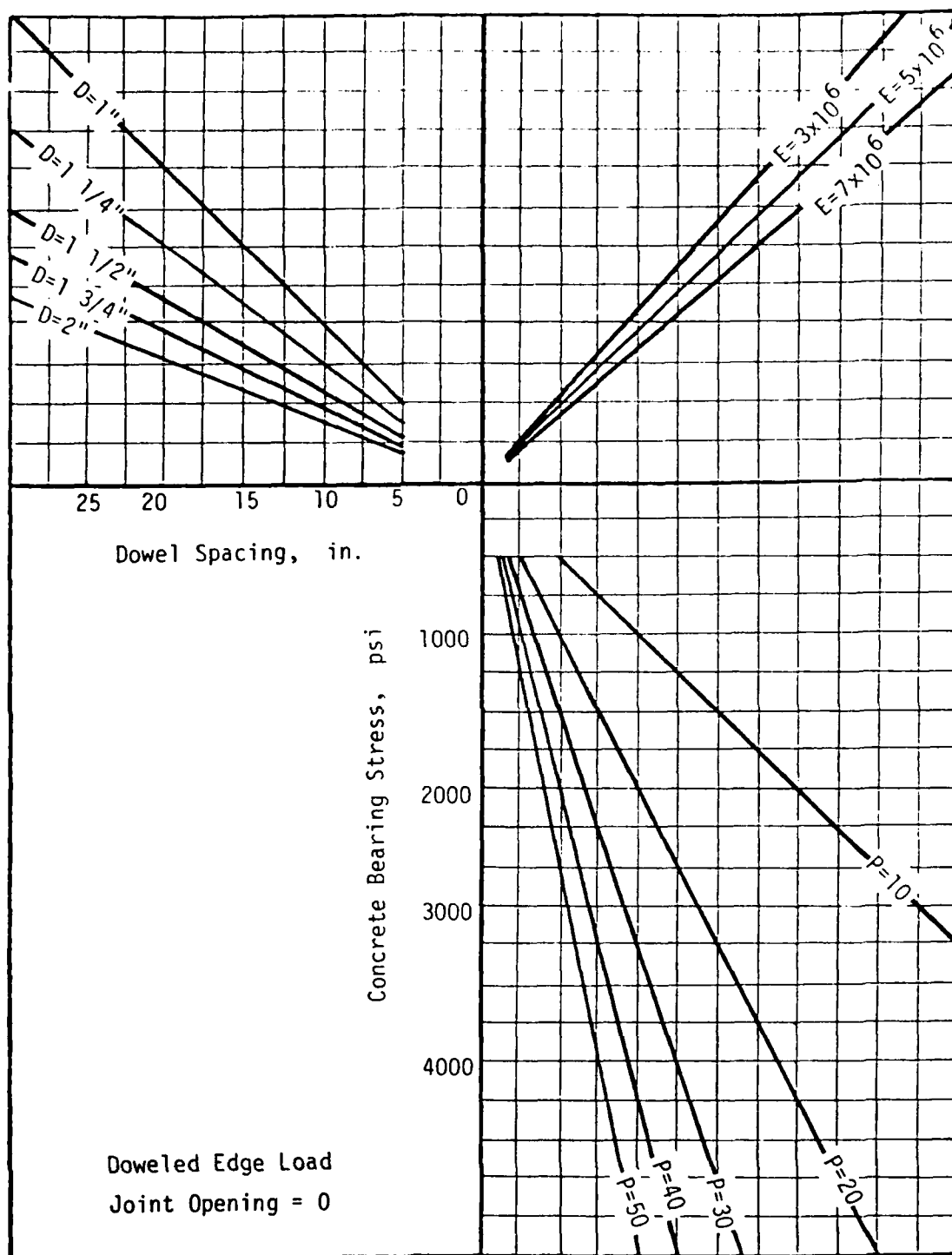


Figure 4-14. Design Chart for Dowel Bars for Various Concrete Modulus

Dowel bars are designed by limiting the bearing stress on concrete to values recommended by the American Concrete Institute (Ref. 43) as given in Equation 2-24. This equation was developed based from laboratory test results conducted by Marcus (Ref. 44) and others, where dowels were subjected to static loads, and may not be applicable to doweled joints subjected to many repeated load applications. Figures 2-15 through 2-17 illustrate the effect of load magnitude, number of load applications, diameter and length of dowel bars, and width of joint opening on the dowel looseness caused by repetitive loadings. Since load transfer effectiveness by doweled joints progressively reduces as the dowel looseness increases (Figure 2-14), it is essential that dowel looseness be kept at an absolute minimum. To do this concrete bearing stress should be kept low by using dowels of adequate diameter, length, and spacings.

Table 4-2 summarizes values for dowel looseness as found by Teller and Cashell (Ref. 35) for various dowel bars, after 600,000 cycles of a 10 kip (44.45 kN) load. Figure 4-15 shows a high correlation between bearing stress on concrete as determined by Equation 4-6 and dowel looseness as reported in Reference 35. It can be seen from Figure 4-15 that by limiting maximum bearing stress on concrete, dowel looseness can be minimized. Although more data from experimental studies is needed to establish a limiting criteria for maximum bearing stress on concrete, Figure 4-15 might suggest a value of 0.3 times concrete strength for this purpose. This value corresponds to 0.001 in. (.03 mm) for dowel looseness after 600,000 load applications which is probably a tolerable value.

Control of doweled joint faulting from repeated load may be another benefit gained by limiting concrete bearing stress. Although it has been found that doweled joints exhibit much less faulting than undoweled joints (Refs. 9, 10, 50), there are reported cases where doweled pavement joints

Table 4-2. Dowel Looseness\* Resulting from  
600,000 Cycles of a 10 Kips  
(44 KN) load (Ref. 35)

Dowel Diameter		Dowel Looseness	
in	(mm)	in	(mm)
5/8	(16)	0.0046	(0.117)
3/4	(19)	0.0026	(0.066)
7/8	(22)	0.0024	(0.061)
1	(25)	0.0020	(0.051)
1-1/8	(29)	0.0019	(0.048)
1-1/4	(32)	0.0021	(0.053)

\* Compressive strength of concrete was measured to be 5,610 Psi (38.65 MPa).

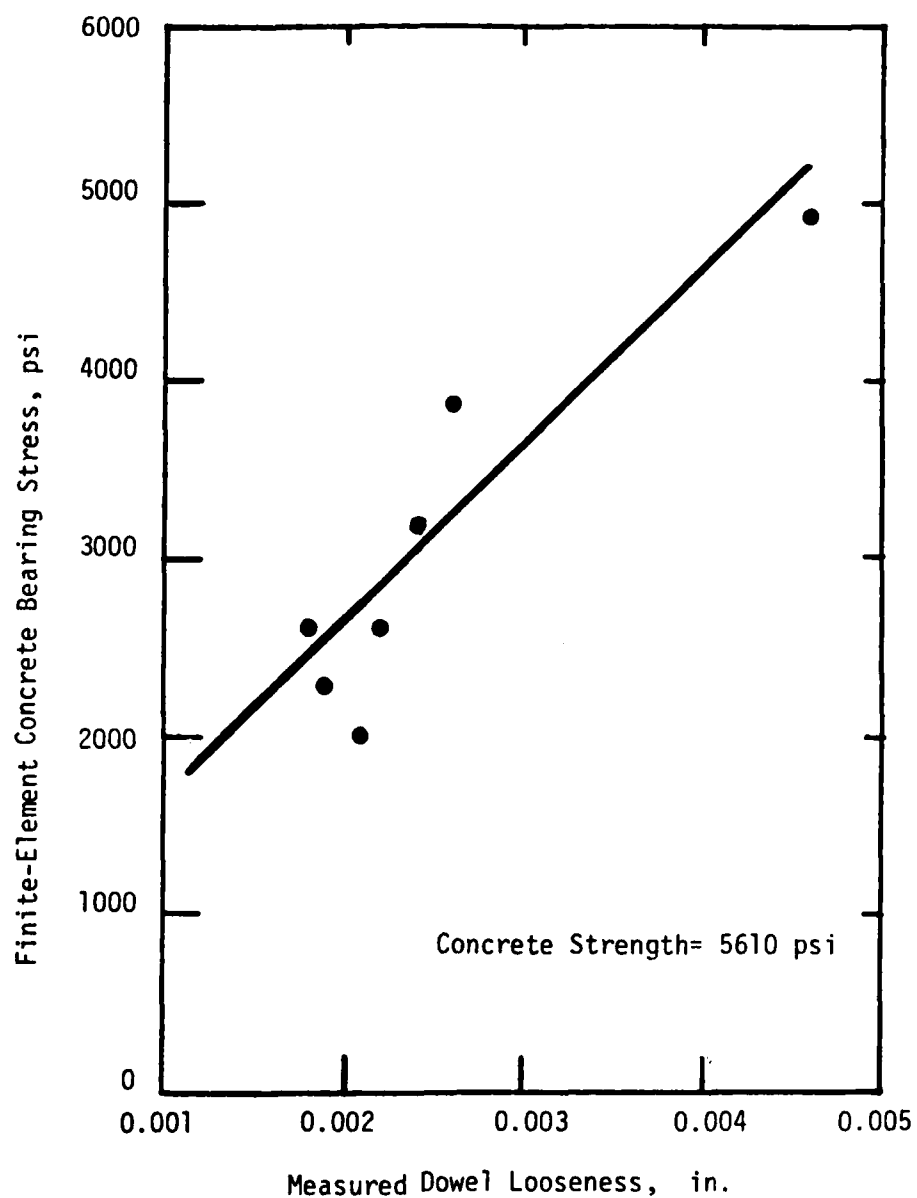


Figure 4-15. Relation between Concrete Bearing Stress and Dowel Looseness, after 600,000 Load Applications

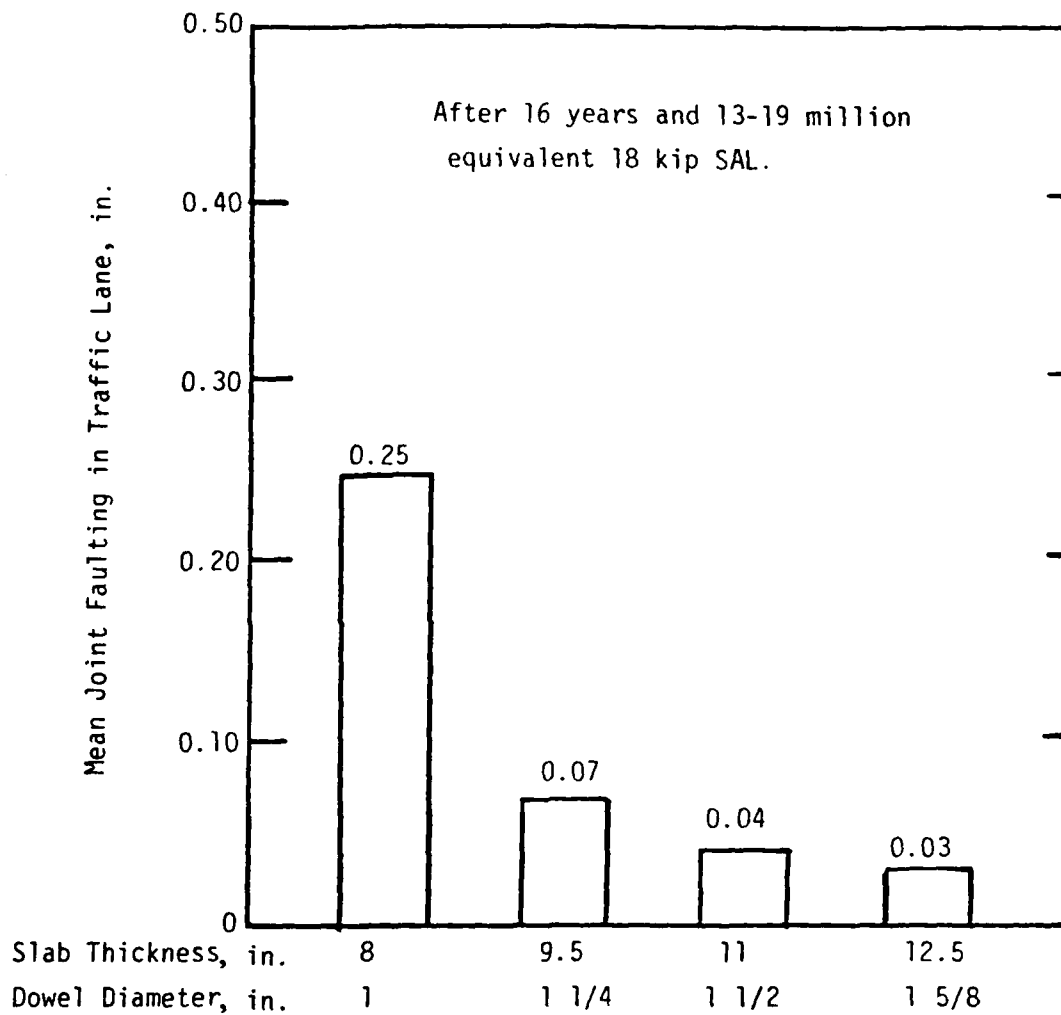


Figure 4-16. Joint Faulting on Plain Jointed Concrete Pavements at the AASHO Road Test site (Ref. 58)

that have developed serious faulting. The AASHO Road Test sections (Ref. 4) of plain jointed concrete pavement left in service for more than 14 years are good examples. The mean joint faulting for various sections summarized by Darter and Barenberg (Ref. 59) are shown in Figure 4-16. These sections have been subjected to 13-19 million equivalent 18 kip (80 KN) single axle loads, and there has been some pumping of the subbase. The sections with 8 in. (20.3 cm) thick slabs with a dowel diameter of 1 in. (25.4 mm) spaced 12 in. (30.5 cm) center to center showed very serious faulting, but faulting decreased with increased slab thickness and dowel diameter. Figure 4-17 shows a high correlation between the calculated bearing stress on concrete, as determined by Equation 4-6 and slab faulting. Data in this figure also suggest a value of 0.3 times concrete strength as a realistic maximum bearing stress on concrete when doweled joints are subjected to a high number of load repetitions, such as in highway pavements. For airfield pavements, where the number of load repetition is usually lower, the use of other criteria may be justified.

#### 4.c Joints with Aggregate Interlock

In the finite-element model, the aggregate interlock was modeled as a series of vertical springs adjoining two adjacent slabs at the joint. The stiffness of these springs (Agg) can be related to the joint efficiency (Eff), which is a physical property of the joint system and can be measured in the field.

The joint efficiency in this study is defined as the ability of the load transfer system to transfer part of the load from loaded slab to the adjacent slab, and is determined as:

$$EFF = \frac{\Delta_U}{\Delta_L} \times 100 \quad (4-7)$$

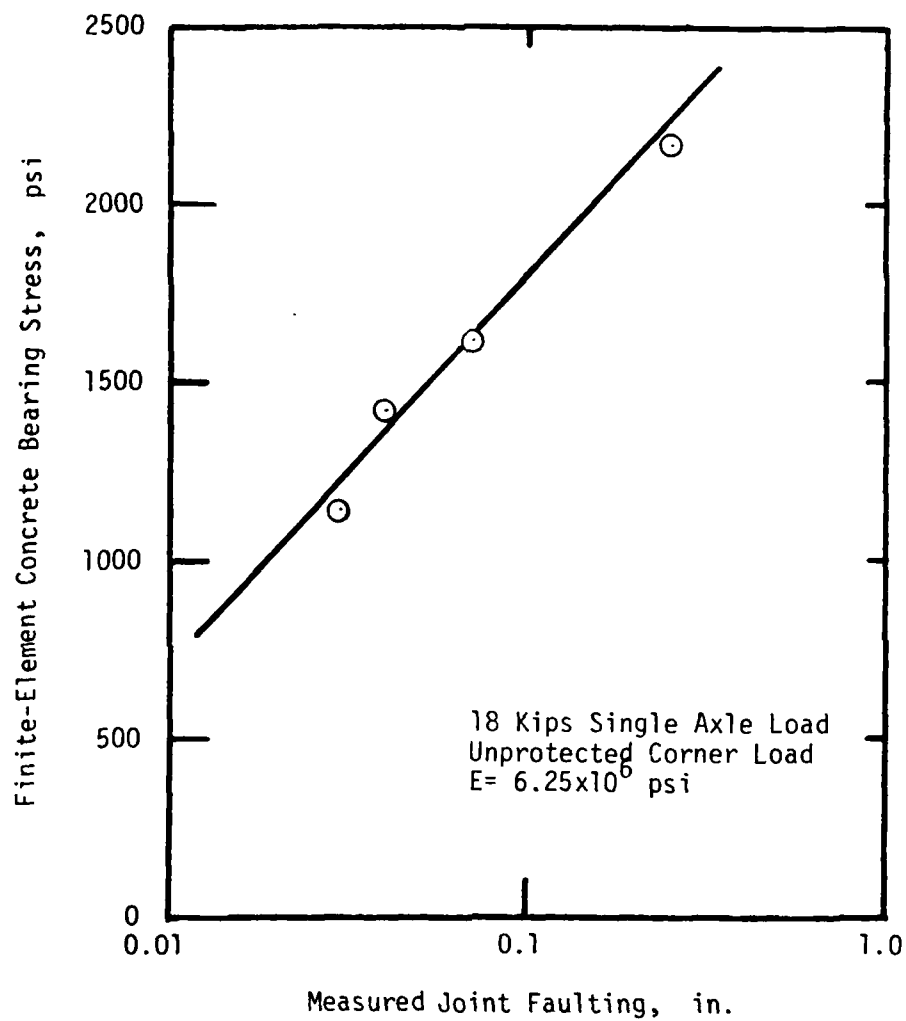


Figure 4-17. Relation between Concrete Bearing Stress and Joint Faulting



where:

$\Delta_U$  = deflection of the unloaded slab

$\Delta_L$  = deflection of the loaded slab

Note that if there is no load transfer system at the joint, then  $EFF = 0\%$ , and if two slabs deflect same amount (a perfect load transfer system), the  $Eff = 100\%$ .

The relation between spring stiffness (Agg) and joint efficiency (Eff) as a function of slab and subgrade properties is shown in Figure 4-18.

Figures 4-19 and 4-20 show the effect of different degrees of aggregate interlock in reducing the maximum tensile edge stress and edge deflection in a 12 in. (30.5 cm) thick concrete slab. Figure 4-19 illustrates that a good degree of aggregate interlock ( $Agg > 10^6$ ) is necessary to reduce the maximum tensile edge stresses to levels of interior stresses. Since efficiency of joints with aggregate interlock is reduced as width of joint opening is increased, the joints must be very tightly closed, to achieve a high degree of joint efficiency with aggregate interlock.

The advantage of using a stabilized base under concrete slabs, where load is transferred by aggregate interlock, has been emphasized by different investigators (Refs. 16, 52). Figure 4-21 shows the combined effect of a stabilized base and aggregate interlock in reducing the maximum tensile edge stresses in the concrete slab. As the results in Figure 4-21 illustrate, a combination of a 4 in. (10.2 cm) cement stabilized base with some degree of aggregate interlock ( $Agg = 5 \times 10^3$ ) is comparable to a high degree of aggregate interlock alone ( $Agg > 10^6$ ), in reducing the maximum tensile edge stresses in a 12 in. (30.5 cm) slab.

Slab thickness has a great effect on the long-term load transfer ability of joints with aggregate interlock systems. In a study conducted

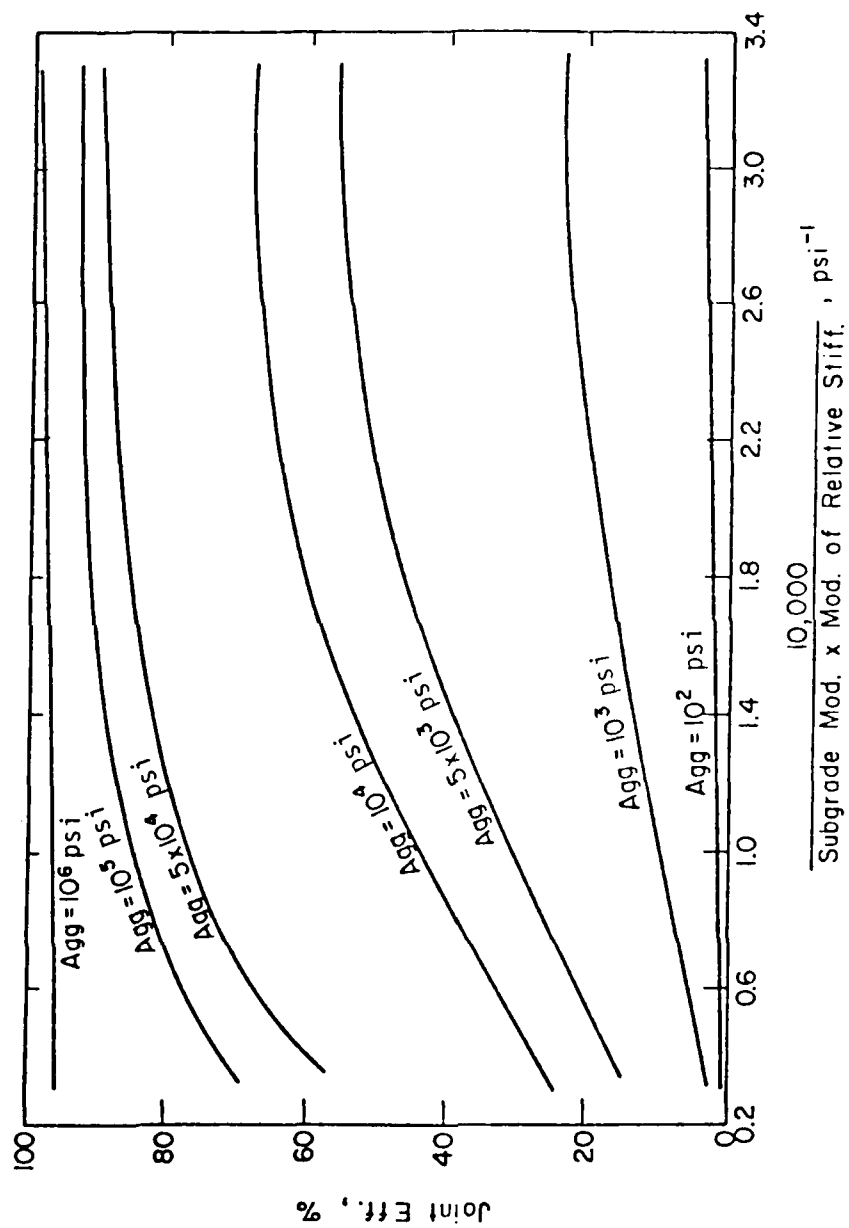


Figure 4-18. Relation between Joint Efficiency (Eff) and Spring Stiffness (Agg)

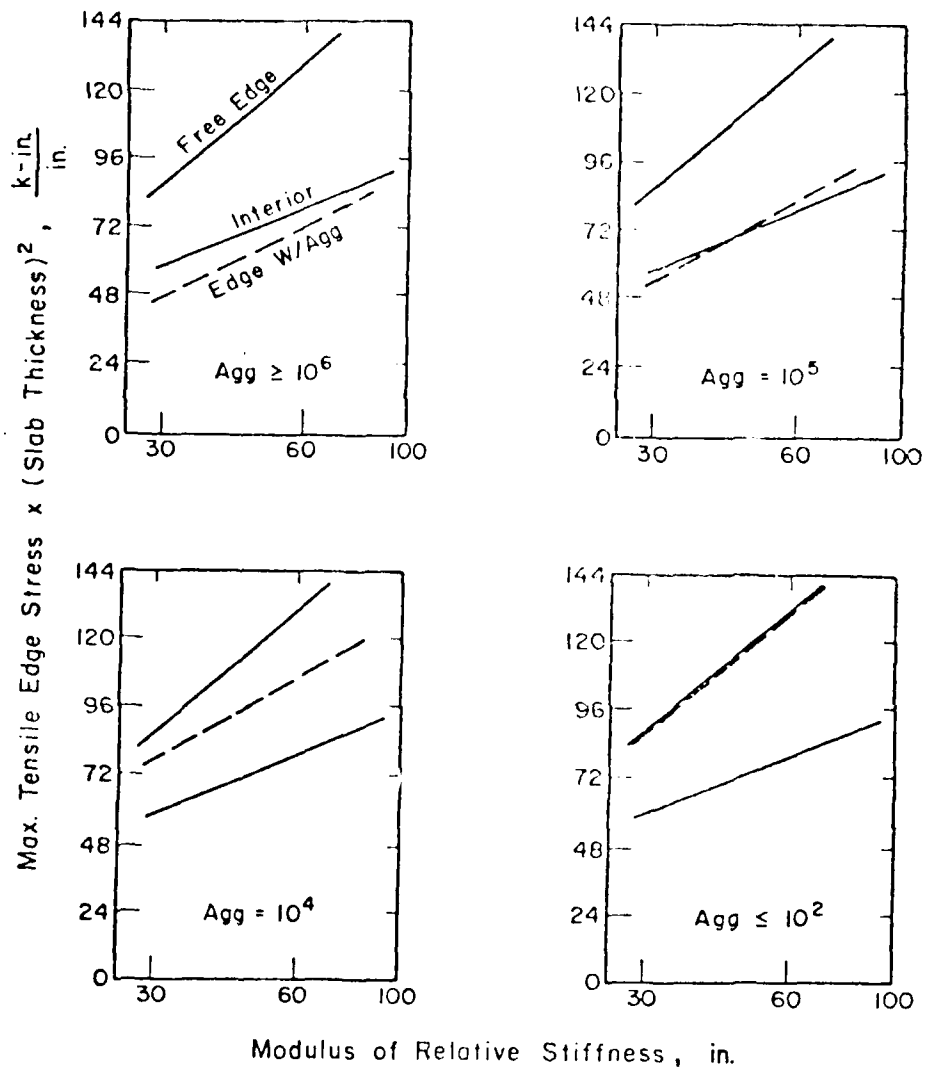


Figure 4-19. Effect of Aggregate Interlock in Reducing Maximum Tensile Edge Stresses

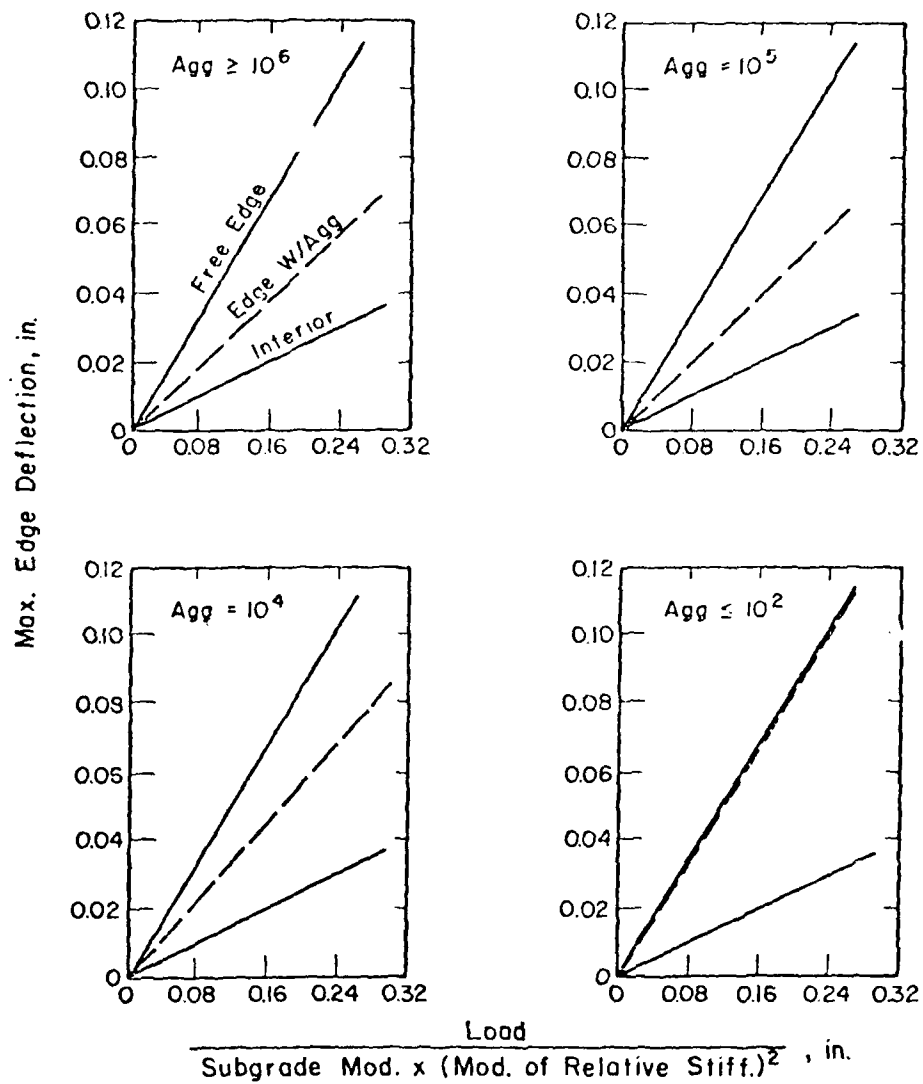


Figure 4-20. Effect of Aggregate Interlock in Reducing Maximum Edge Deflections

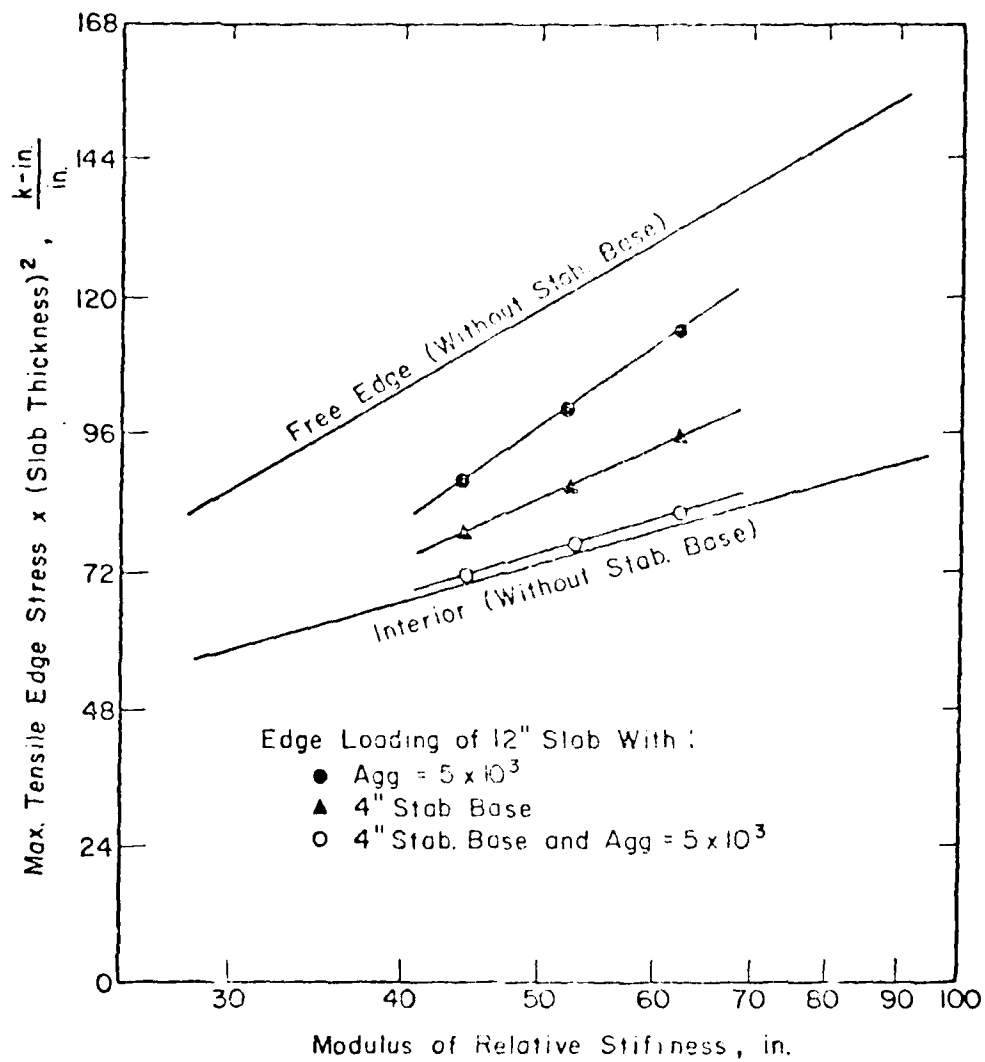


Figure 4-21. Combined Effect of Bonded Stabilized Base and Aggregate Interlock in Reducing Maximum Tensile Edge Stresses

by Colley and Humphrey (Ref. 53), it was found that under repetitive load and at a specified joint opening, the loss of the joint effectiveness was higher in the 7 in. (17.8 cm) slab than in the 9 in. (22.9 cm) slab. This is believed to be due to the level of shear stresses at the joint interface, since a slab with the greater thickness offers a larger interlocking area and a lower overall deflection under a given load than a slab with lesser thickness. The results of the finite-element study for the effect of the slab thickness on the maximum shear stresses at the joint interface is shown in Figure 4-22. Results in Figure 4-22 show that for a given degree of aggregate interlock, thicker slabs result in lower maximum shear stresses at the joint interface, so with many repeated loads the thicker slabs will retain their aggregate interlock for more load applications than will the thinner slabs. While the factors and trends affecting the long-term joint performance of slabs with aggregate interlock are clear, the specific criteria for design must still be developed.

#### 4.d Keyed Joints

In the finite-element method, keyways were modeled as very stiff vertical springs adjoining two adjacent slab edges at the joint. Figures 4-23 and 4-24 show the effect of a keyway system in reducing maximum tensile edge stresses and deflections in concrete slabs. Although keyed joints might seem to be effective in reducing the stresses at the slab edges, localized failures due to stress concentration at the sharp fillets of the keys and keyways are likely to occur. The most serious type of keyway failure occurs when the upper keyway portion shears through to the pavement surface.

The problem of stress concentration at the pavement joints can be analyzed using a finite-element model developed by Nasseir, Takahashi,

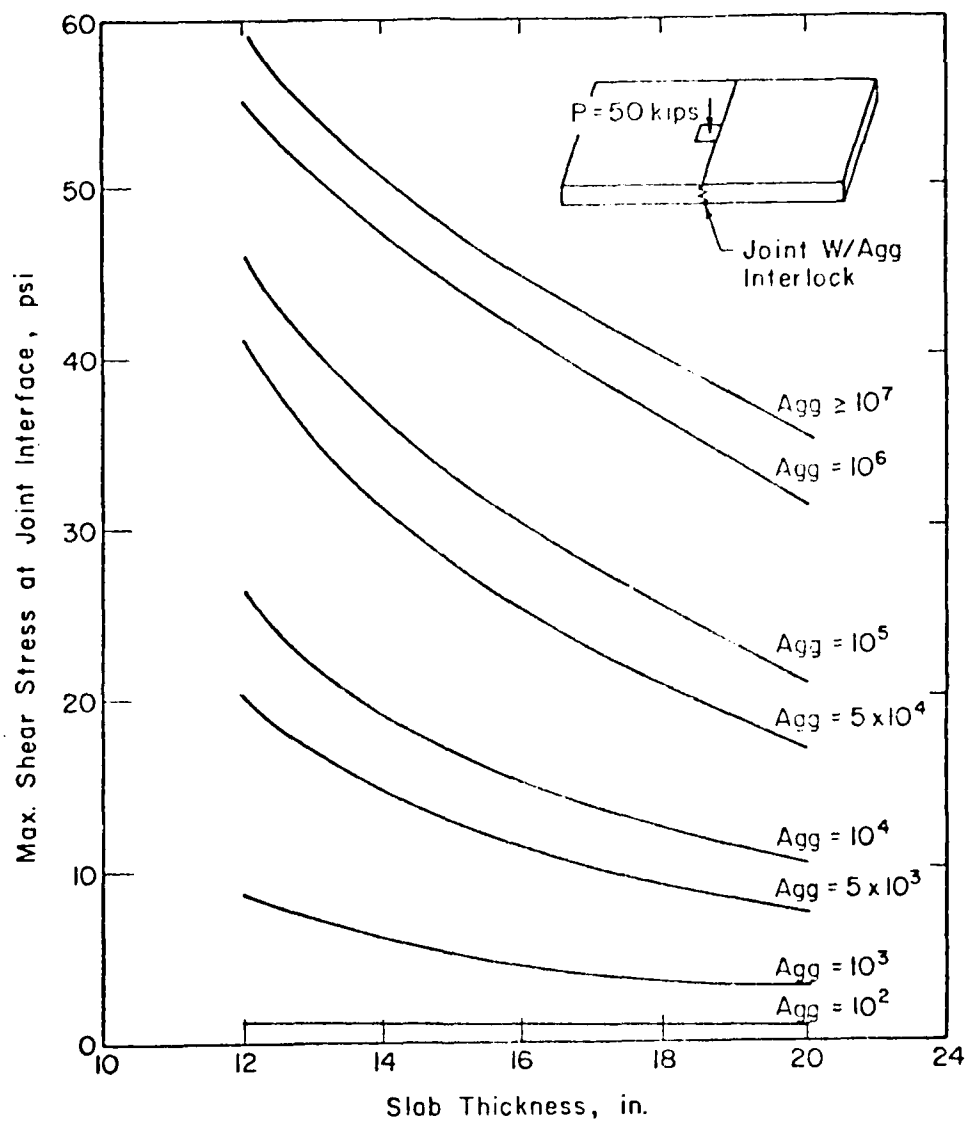


Figure 4-22. Effect of Slab Thickness on Maximum Shear Stresses at Joint Interface

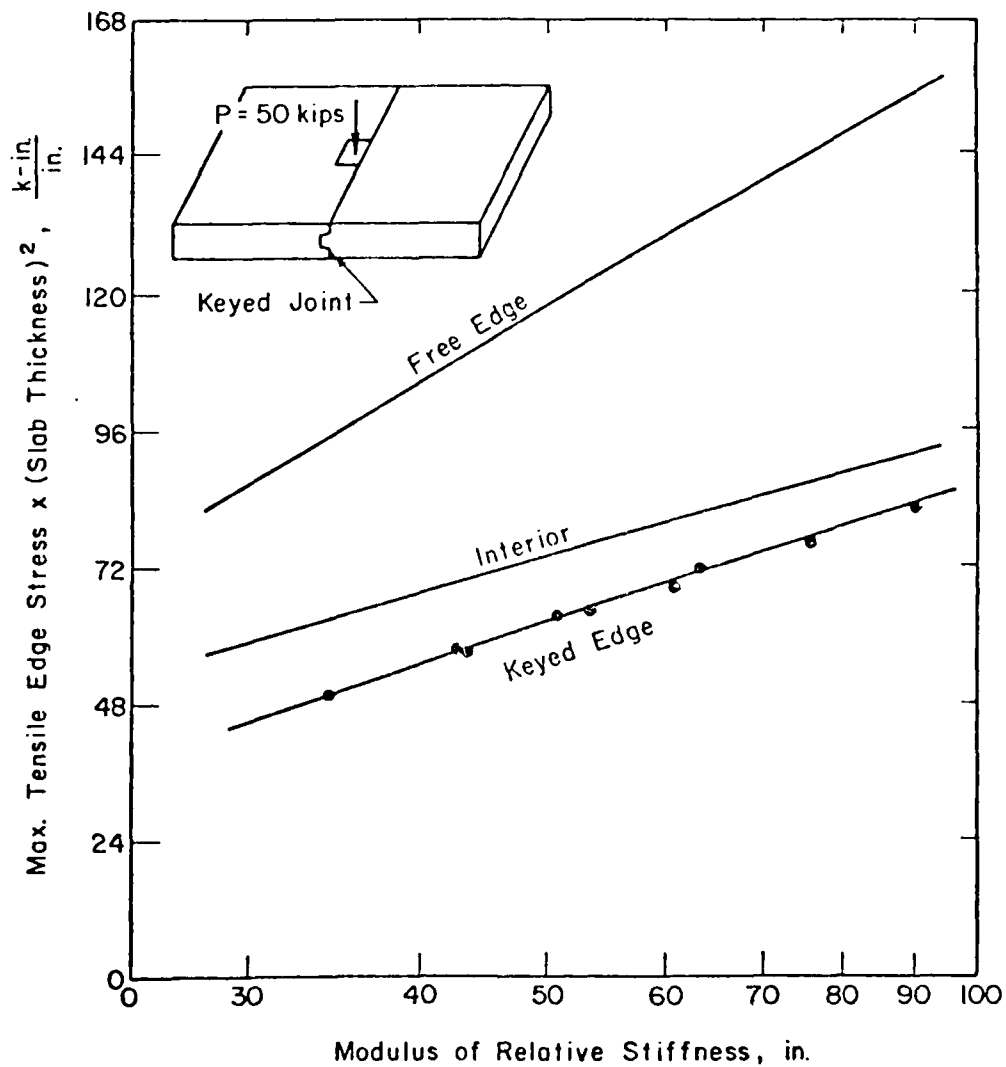


Figure 4-23. Effect of Keyway in Reducing Maximum Tensile Edge Stresses



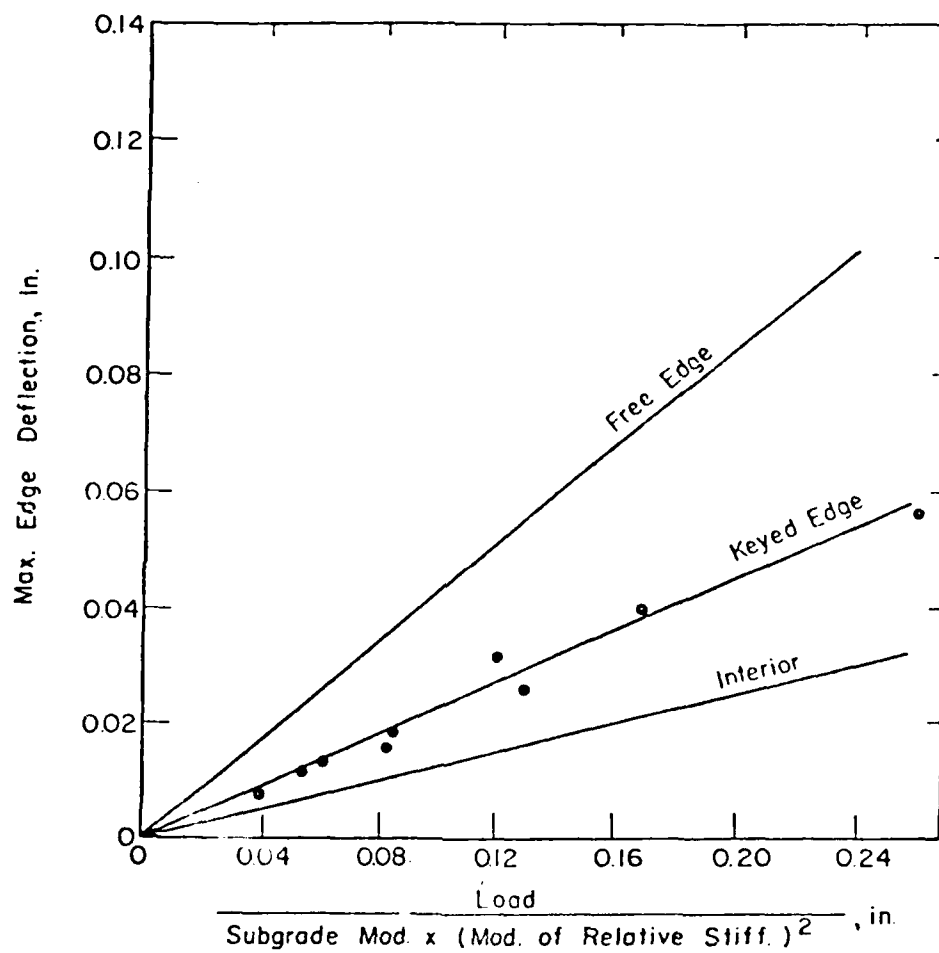


Figure 4-24. Effect of Keyway in Reducing Maximum Edge Deflections

and Crawford (Ref. 54). The model is a modified version of the axisymmetric/ plane stress finite-element computer program, developed by Wilson (Ref. 55), and is capable of simulating the response of multicomponent structures exhibiting slippage and/or separation at boundaries of contact between components. The model has been verified in Reference 54, by comparing the finite-element solutions with the results of photoelastic experiments on small models of a hatch cover and a keyed joint.

To study the effect of several parameters such as key design, slab thickness, subgrade support, stabilized base, tie bars, and load position on the problem of stress concentration at keyed joints, several concrete beams containing keyed joints were analyzed. Figure 4-25 shows a typical finite-element configuration used in these analyses. Different key designs such as a standard trapezoidal key recommended by the U. S. Army, Corps of Engineers (Ref. 15), a key with double height (large key), a key with double depth (deep key), a round key, a round smooth key without sharp fillets, and a Z-key were considered in the study. Figures 4-26 through 4-32 show the effect of design parameters such as key shape, slab thickness, and base type on the tensile stress contours in the key and keyway systems. These figures and Tables 4-3 through 4-5 show that key shape has very significant effects on the stress concentration at the keyway, and that stabilized bases and thicker slabs are beneficial and result in lower tensile stresses in the keyway system. Similar conclusions were reached by various investigators (Refs. 15, 16, 17, 18), based on both laboratory studies and field investigations.

The results from this analytical study and performance of keyed joints in service indicate that keyed joints are a serious structural weakness in the concrete pavements, and serious keyway failures such as shearing of the upper portion of the keyway, or the key itself may occur. This is due to

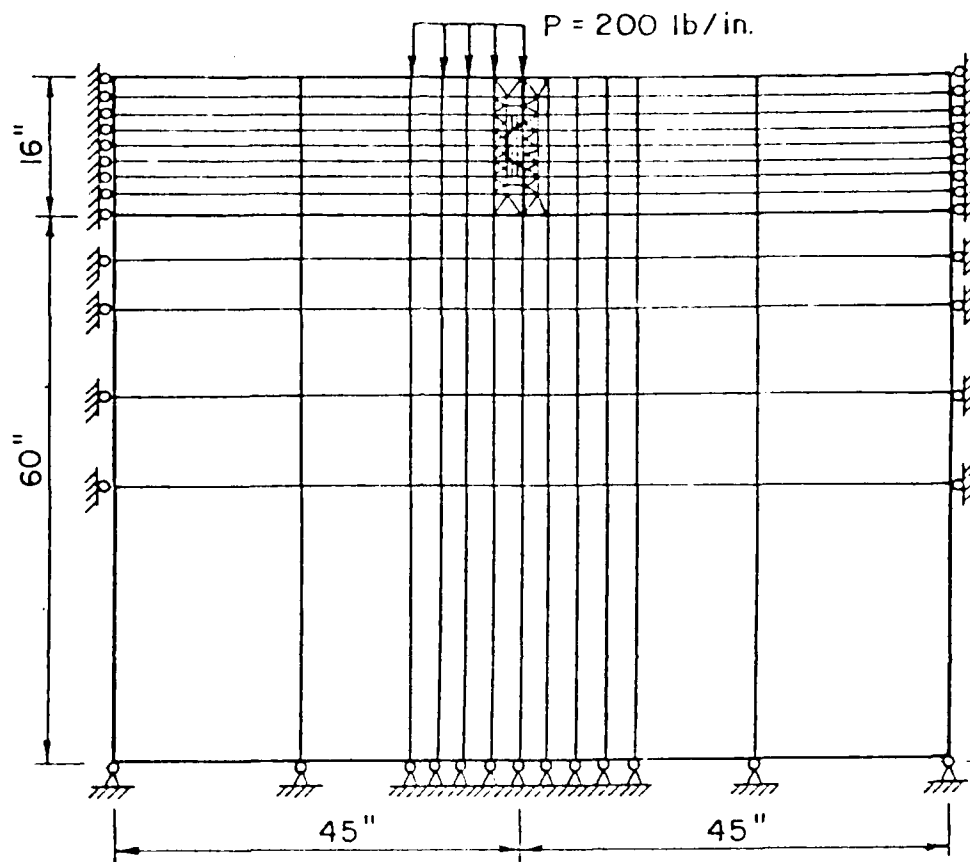


Figure 4-25. A Typical Finite-Element Mesh Used for Analysis of Keyed Joints

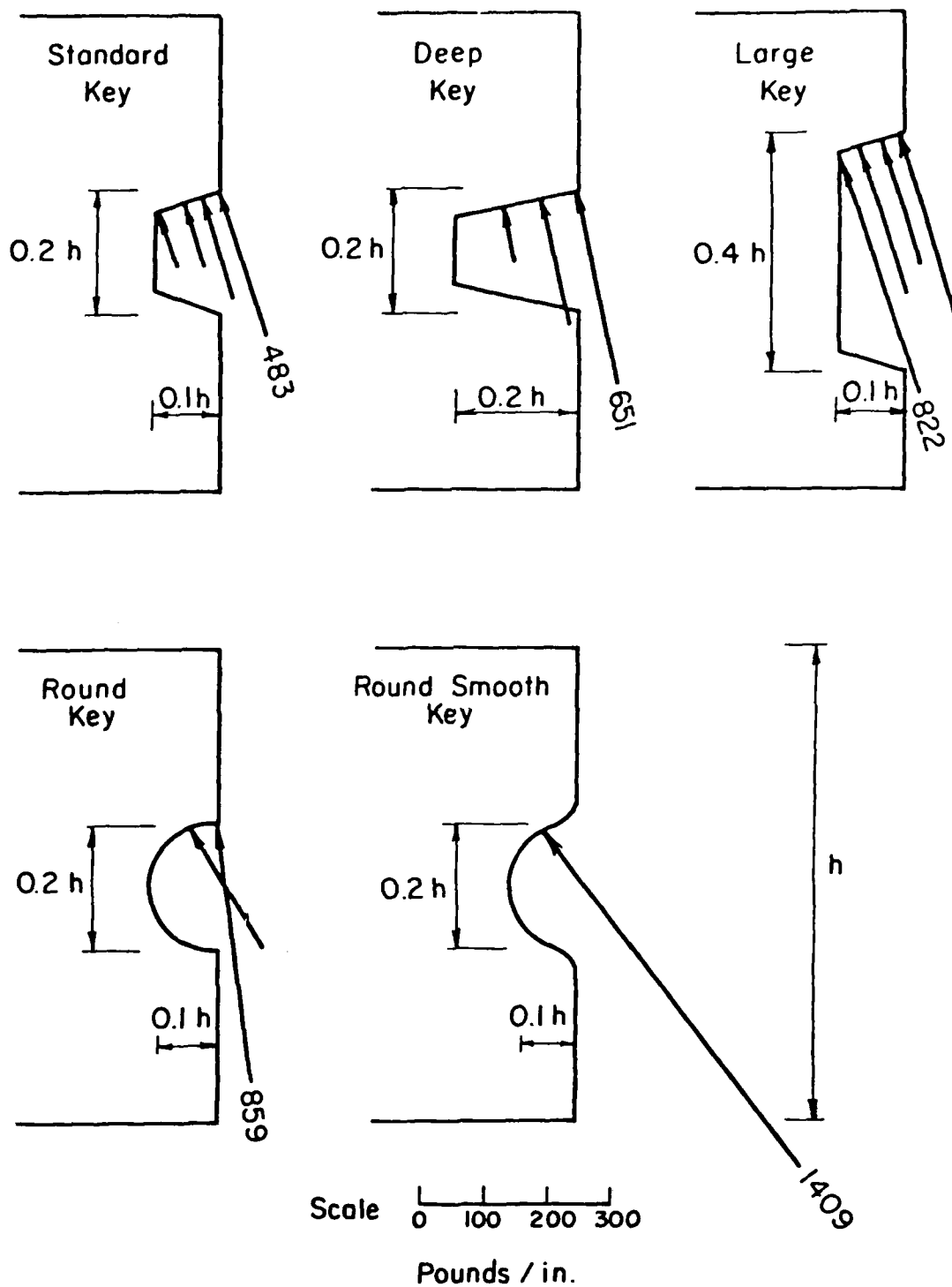


Figure 4-26. Distribution of Nodal Forces Normal to the Contact Boundaries for Different Key Designs

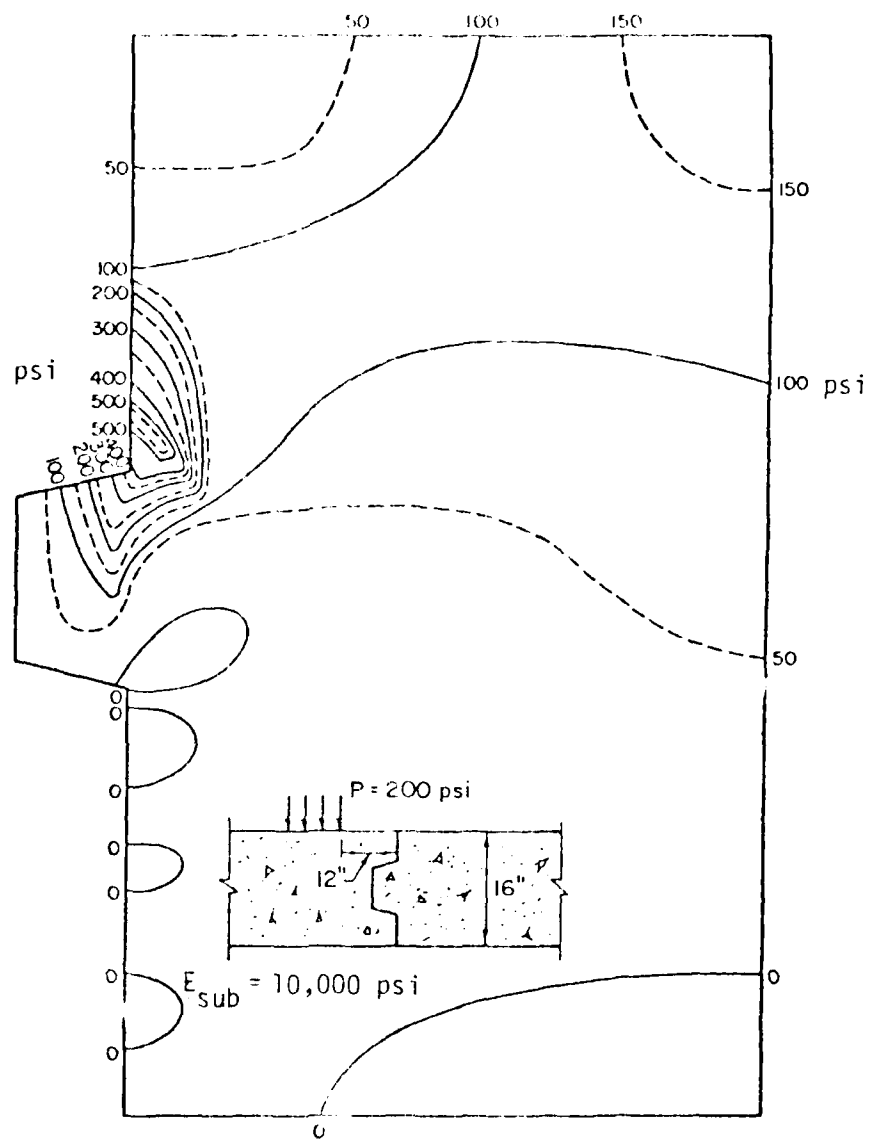


Figure 4-27. Tensile Stress Contours for a Standard Key in a 16 in. (40.6 cm) Slab, Male Side

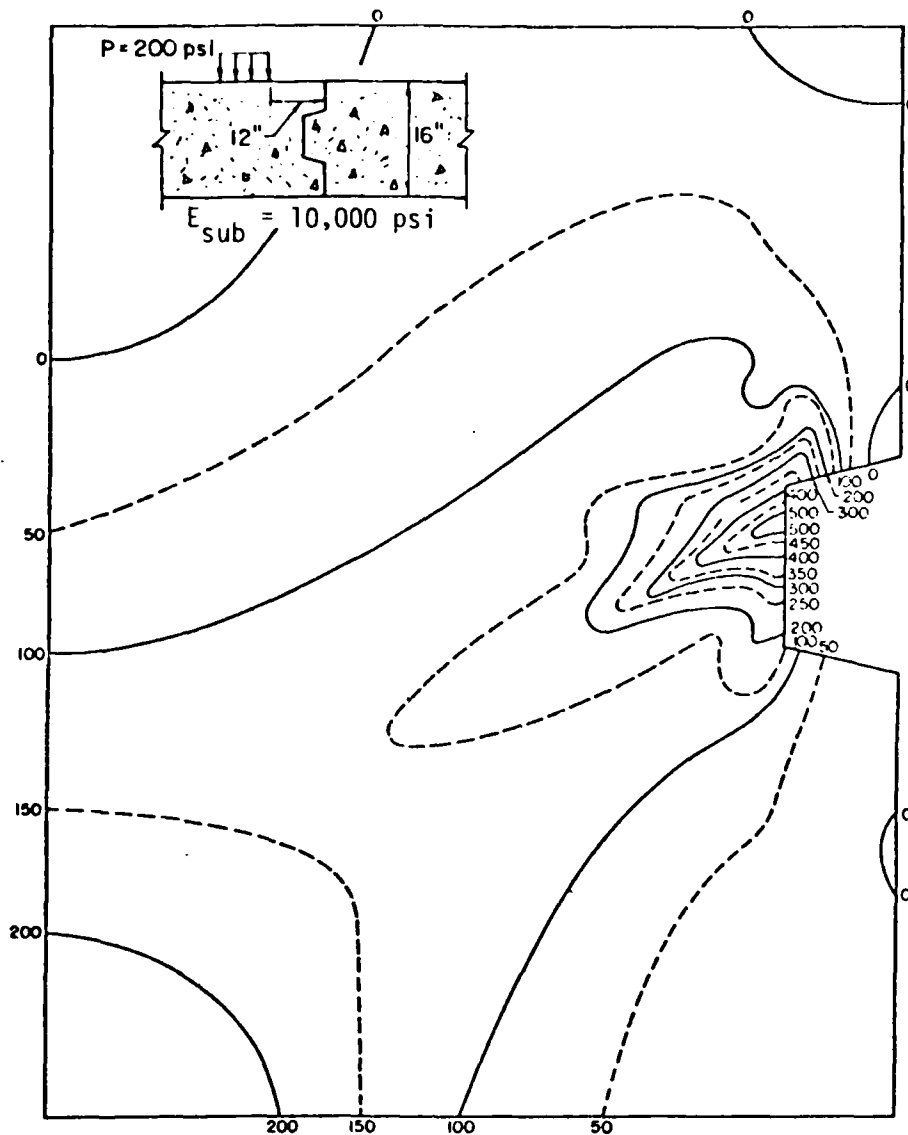


Figure 4-28. Tensile Stress Contours for a Standard Key in a 16 in. (40.6 cm) Slab, Female Side

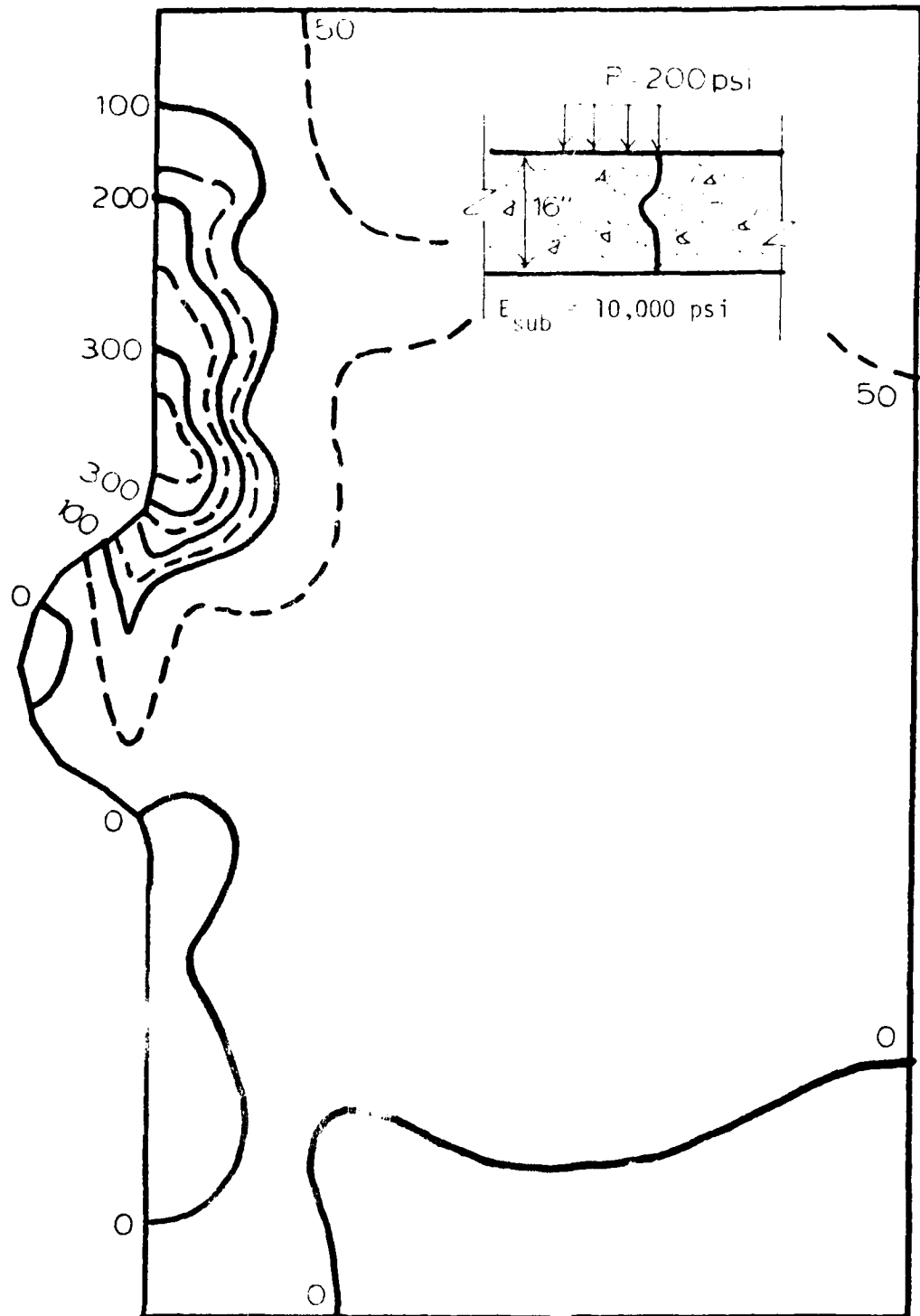


Figure 4-29. Tensile Stress Contours for a Round Smooth Key in a 16 in. (40.6 cm) Slab, Male Side

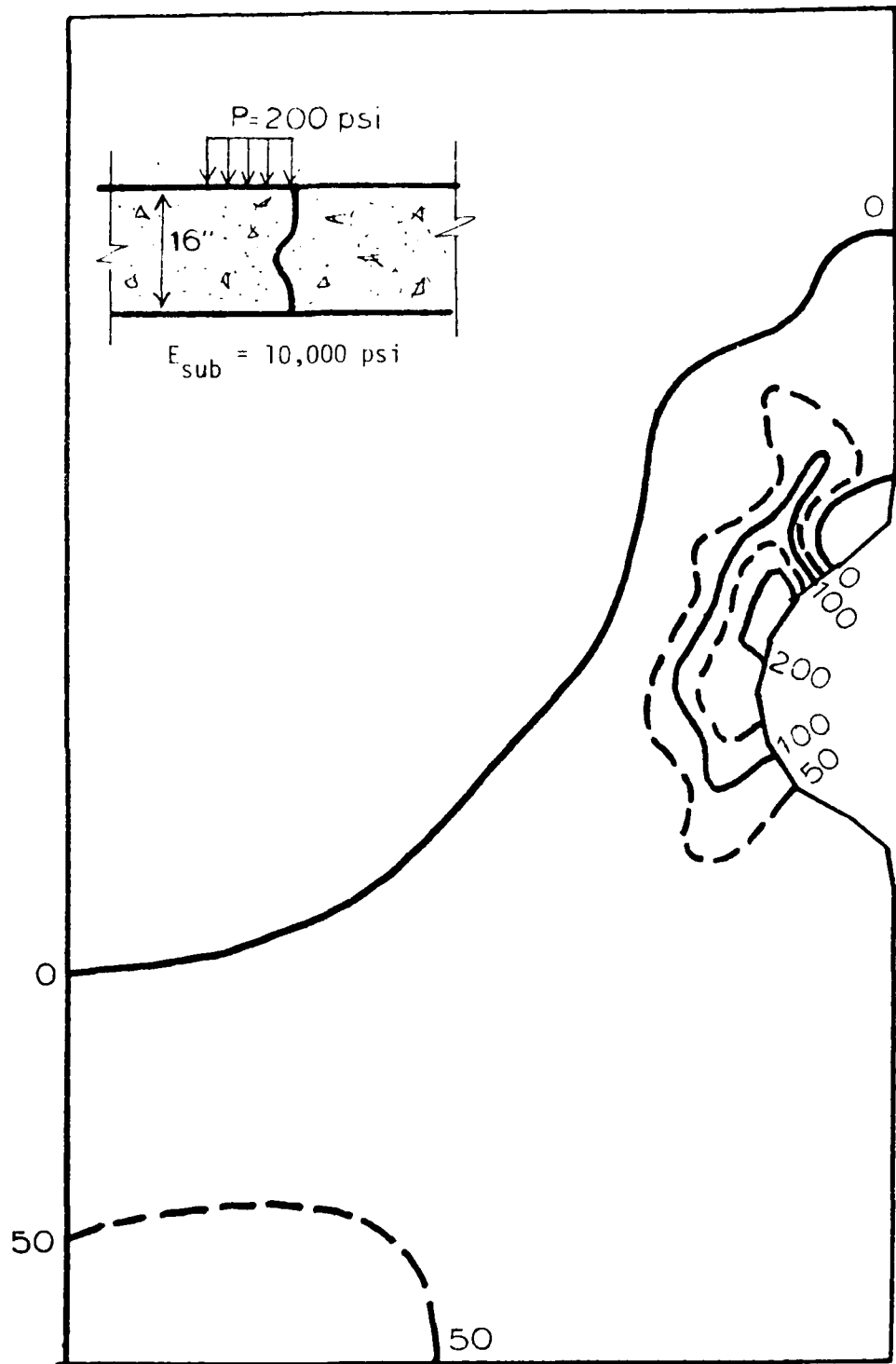


Figure 4-30. Tensile Stress Contours for a Round Smooth Key in a 16 in. (40.6 cm) Slab, Female Side



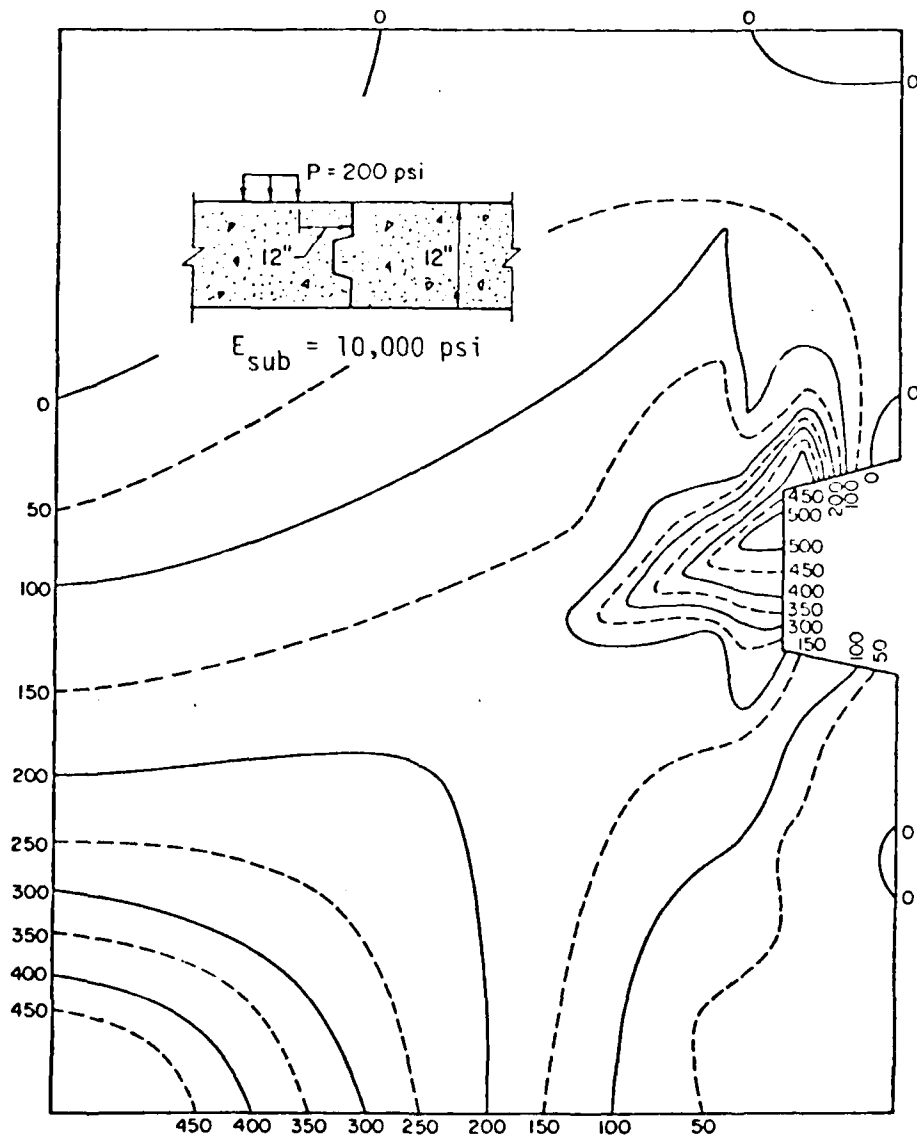


Figure 4-31. Tensile Stress Contours for a Standard Key in a 12 in. (30.5 cm) Slab

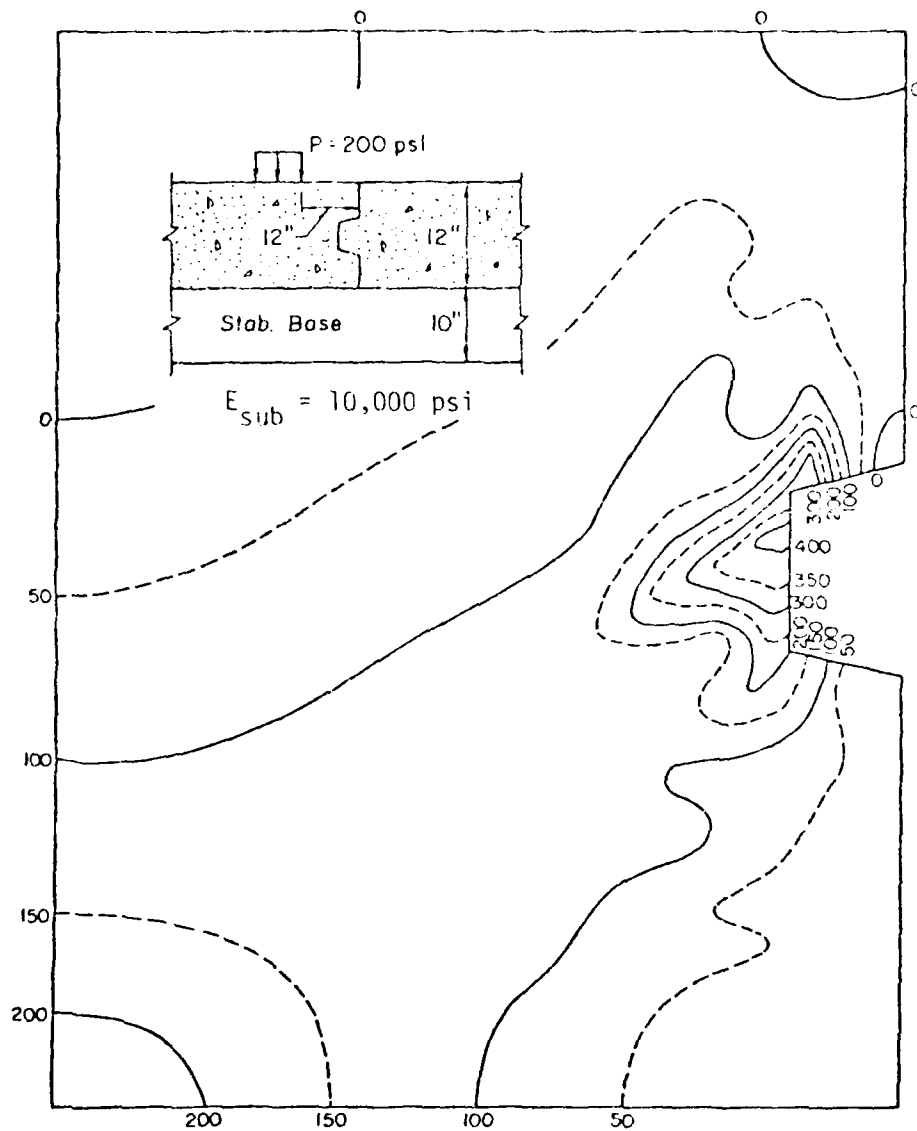


Figure 4-32. Tensile Stress Contours for a Standard Key in a 12 in. (30.5 cm) Slab on a 10 in. (25.4 cm) Cement Stabilized Base

Table 4-3. Effect of Key Design on Maximum Tensile Stress in the Slab\*

Key Design	Keyway		Key	
	Psi	(MPa)	Psi	(MPa)
Standard Key	312	(2.15)	586	(4.04)
Large Key	1023	(7.05)	1229	(8.47)
Deep Key	259	(1.78)	589	(4.06)
Round Key	451	(3.11)	501	(3.45)
Round Smooth Key	201	(1.38)	344	(2.37)
Z-Key	721	(4.97)	274	(1.89)

\* Slab thickness was 16 in. (40.6 cm).

Table 4-4. Effect of Slab Thickness on  
Maximum Tensile Stress in the  
Slab\*

Slab Thickness		Keyway		Key	
in	(cm)	Psi	(MPa)	Psi	(MPa)
12	(30.5)	524	(3.61)	546	(3.76)
16	(40.6)	501	(3.45)	518	(3.57)
20	(50.8)	439	(3.02)	480	(3.31)

\*Standard key joint, and load was applied 12 in. (30.5 cm)  
from the joint.

Table 4-5. Effect of Cement Stabilized Base on  
Maximum Tensile Stress in the Slab\*

Stabilized Base Thickness		Keyway		Key	
in	(cm)	Psi	(MPa)	Psi	(MPa)
0	( 0 )	524	(3.61)	546	(3.76)
5	(12.7)	467	(3.22)	456	(3.14)
10	(25.4)	412	(2.84)	372	(2.56)

\*Slab thickness was 12 in. (30.5 cm), and load was applied 12 in. (30.5 cm) from the joint.

the effect of localized stresses which may be more than twice the intensity of conventional edge stresses. For example, the maximum edge stress in a 16 in. (40.6 cm) slab on a subgrade with modulus of 200 pci ( $54.2 \text{ N/cm}^3$ ) under a 50 kips (222 kN) load is about 250 psi (1.7 MPa), while tensile stress at the keyway root is about 500 psi (3.8 MPa). Therefore, keyed joints are not recommended for concrete pavements with heavy load or for relatively thin slabs, especially over weak foundations.

#### 4.e Butt Joints on Stabilized Bases

Base courses are used under concrete slabs for various reasons including:

- (1) To control pumping,
- (2) For a construction platform,
- (3) To control frost action,
- (4) To control subgrade shrinkage and swelling,
- (5) To assist drainage.

Stabilization of the base or subgrade also results in additional benefits such as increased slab support, prevention of consolidation of the subgrade and base, minimizing intrusion of hard granular particles into pavement joints through minimizing pumping, and finally, providing improved load transfer at pavement joints by minimizing edge deflections and stresses in the concrete slabs.

The effect of a cement stabilized base on joint effectiveness and performance has been studied by Colley and Humphrey (Ref. 53), Childs (Ref. 52), and Ball and Childs (Ref. 16). Types of stabilized bases other than cement treated, such as lean concrete and bituminous, have been used in Europe. Lokken (Ref. 56) summarizes the performance of these bases under concrete slabs. These studies provide evidence of improved joint effectiveness and joint performance when treated bases were used.

In concrete pavement design procedures, the effect of stabilized bases is usually taken into consideration by using an equivalent k-value which is a function of subgrade k-value and thickness of the base (Refs. 57, 58). However, in the finite-element method developed in this study, a stabilized base was treated as a second pavement layer acting in conjunction with the concrete slab. Elastic properties of the stabilized base as well as the condition of bond between concrete slab and stabilized base (perfect bond or no bond), are significant parameters and are input to the finite-element program. This makes it possible to determine the stresses and deflections in the concrete slab as well as the stresses in the stabilized base directly from the program.

Figures 4-33 and 4-34 show the effect of 4, 6, and 10 in. (10.2, 15.2, and 25.4 cm) bonded cement stabilized bases with a modulus of elasticity of  $1 \times 10^6$  psi (6.89 GPa) and a Poisson's ratio of 0.25 in reducing the maximum edge tensile stresses and deflections in the concrete slabs with thicknesses of 12, 16, and 20 in. (30.5, 40.6, and 50.8 cm). Figure 4-33 illustrates that to reduce the edge stresses in a pavement with a stabilized base to values comparable to interior stresses in a pavement with no stabilized base, the thickness of cement stabilized base should be at least equal to one-half the concrete slab thickness. These results will change with different subbase properties and with interface condition between the slab and subbase. Specific criteria for design and procedures for determining the optimum design conditions are not available at this time.

#### 4.f Thickened Edge Slab with Butt Joints

The effects of increasing the thickness of slab edges on maximum tensile edge stresses and deflections of the concrete slabs are shown in Figure 4-35 and 4-36. Three slab thicknesses included in the study

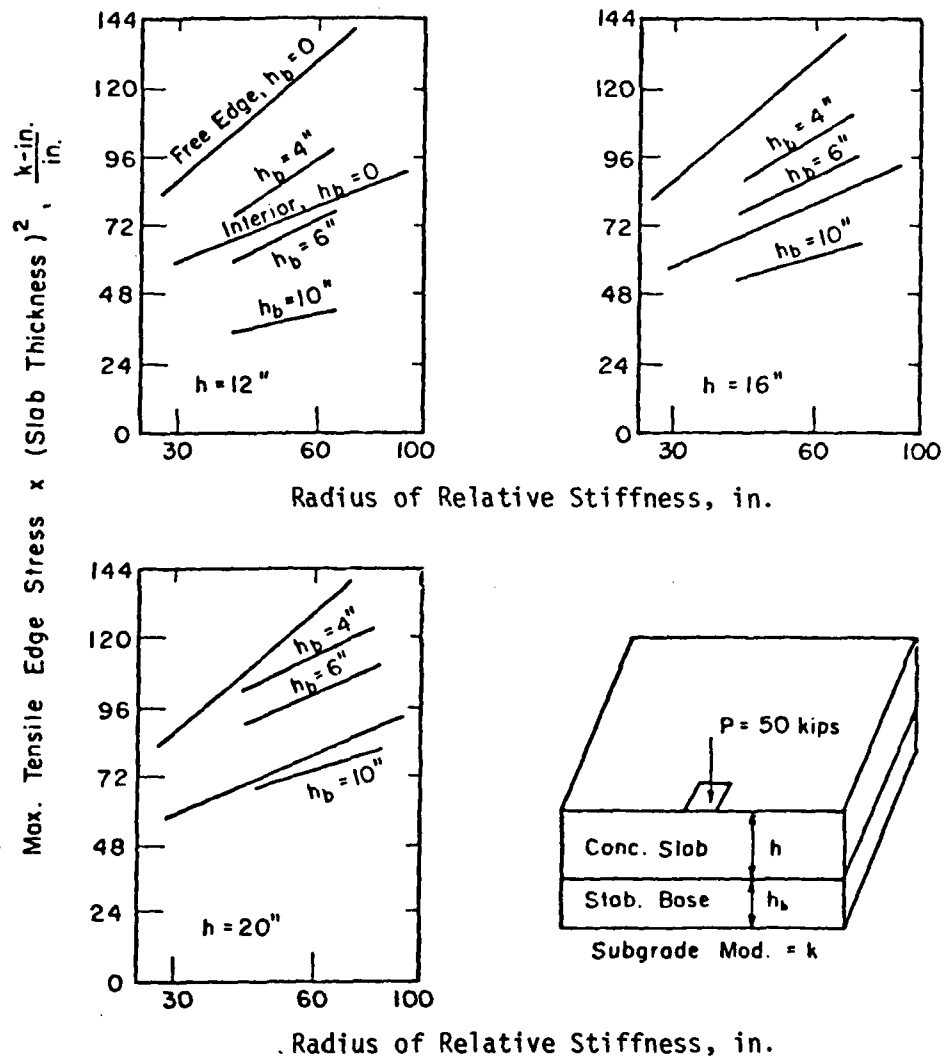


Figure 4-33. Effect of Bonded Stabilized Base in Reducing Maximum Tensile Edge Stresses



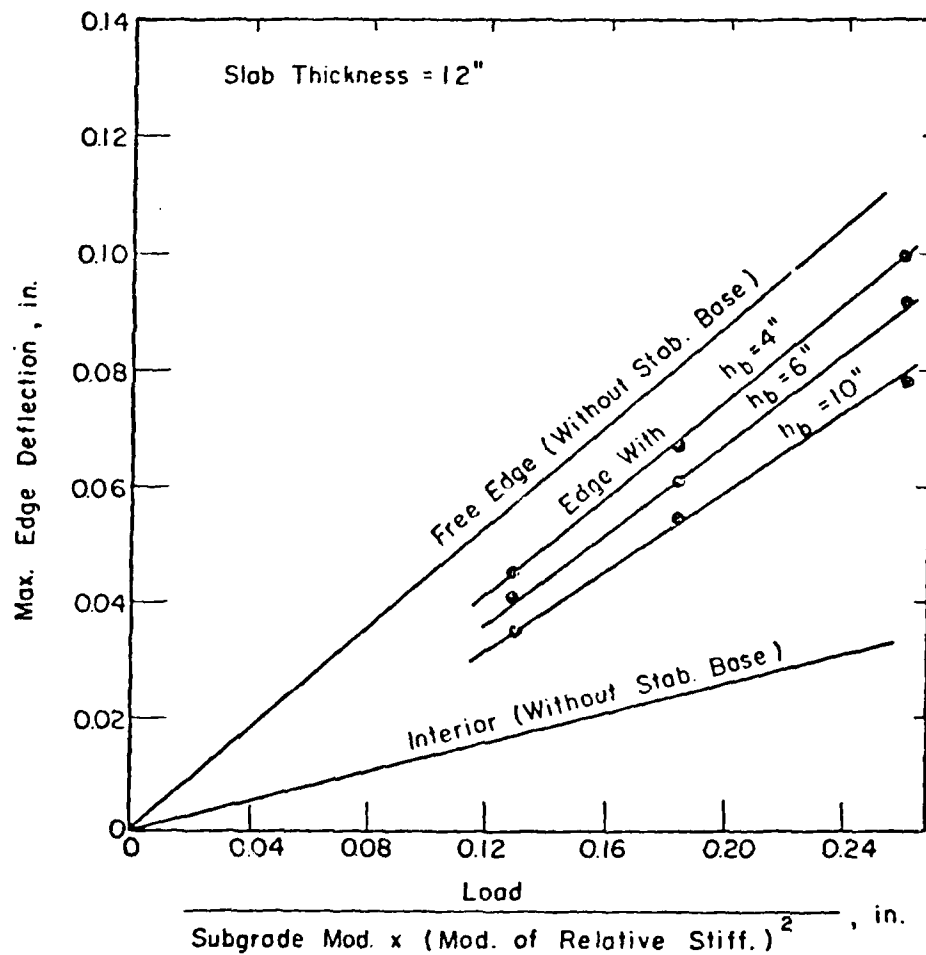


Figure 4-34. Effect of Bonded Stabilized Base in Reducing Maximum Edge Deflections

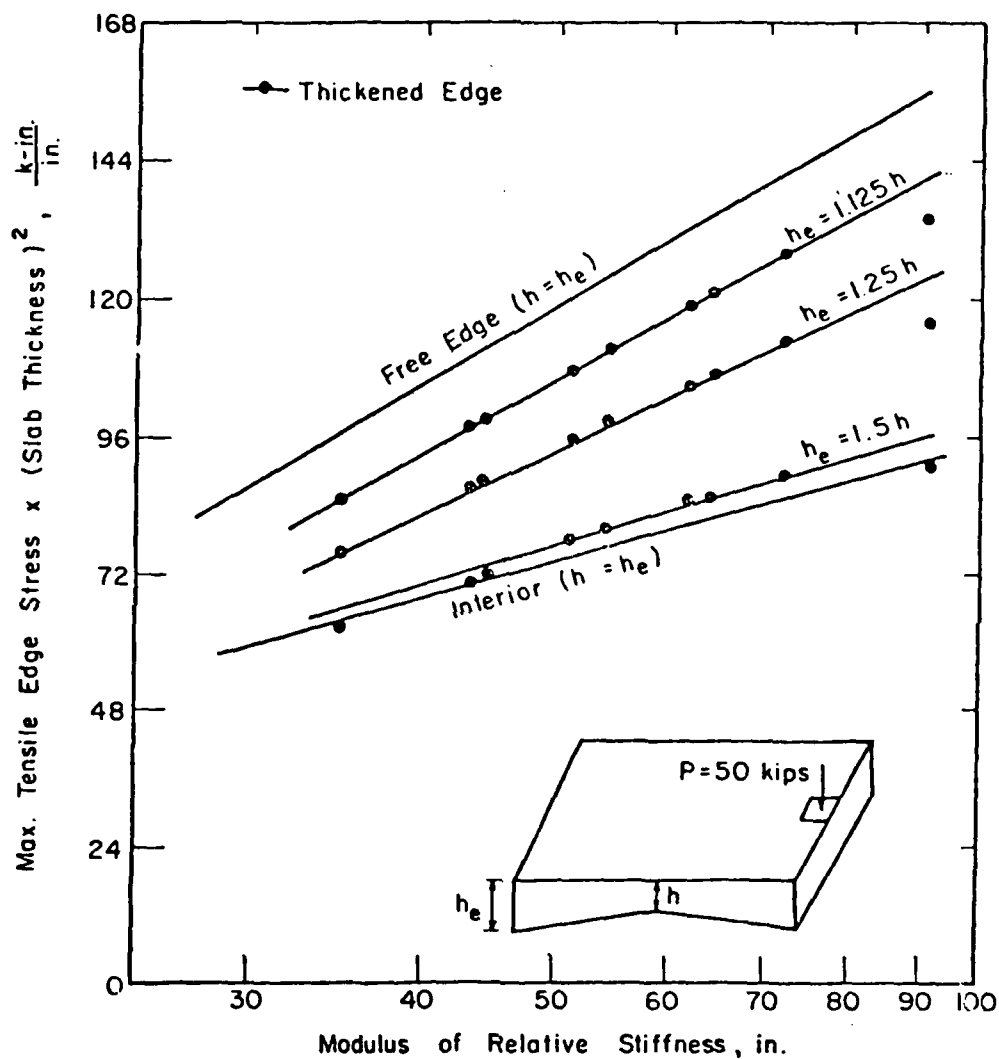


Figure 4-35. Effect of Thickened Edge Slab in Reducing Maximum Tensile Edge Stresses

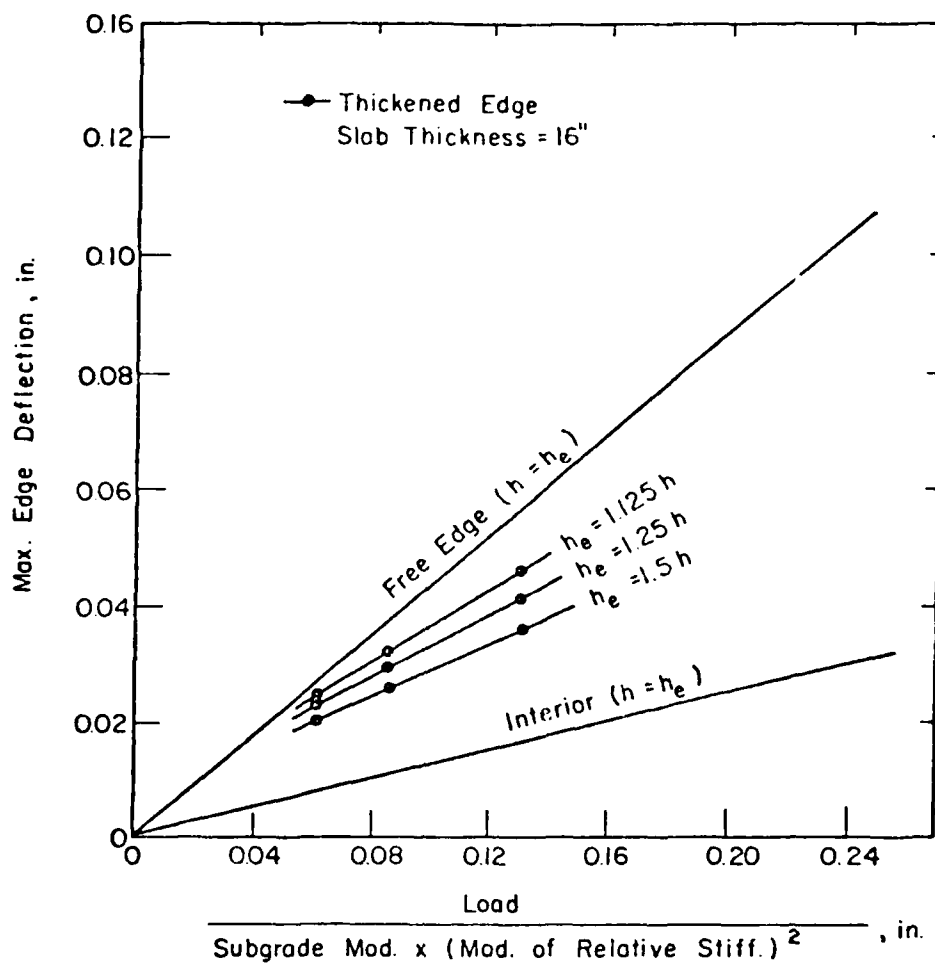


Figure 4-36. Effect of Thickened Edge Slab in Reducing Maximum Edge Deflections

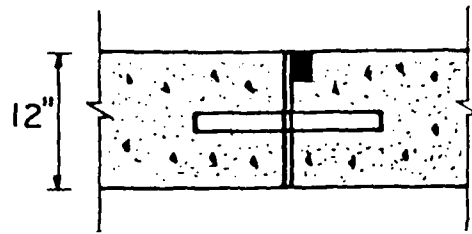
were 12, 16, and 20 in. (30.5, 49.6, and 50.8 cm) on subgrades with k-value of 50, 200, and 500 pci (13.6, 54.2, and 135.5 N/cm<sup>3</sup>). The slab thickness at the edges were increased by increments of 1/8, 1/4, and 1/2 based on the thickness at the interior of the slabs. Figure 4-35 illustrates that increasing slab thickness at the edge by about 50% of the interior thickness of the slab results in a design which reduces maximum tensile edge stress to the levels of interior stress.

Results from a series of tests by Teller and Sutherland (Ref. 5), on ten full size slabs tested under static loads suggest that for a balanced section (a section in which maximum stress under free edge load to be equal to stress under interior load), the thickness of the edge should be about 1.6 times the interior slab thickness. This agrees in general, with conclusions reached from the finite element analyses of the thickened edge pavements.

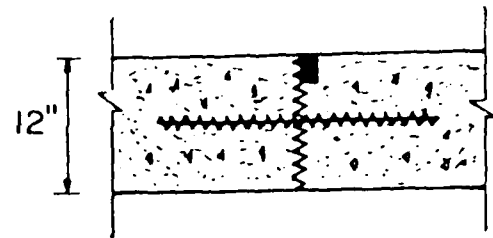
#### 4.g Example Problem

The results of the two-dimensional finite-element study may be used for evaluating the capabilities of different pavement joint designs. For example, first those joint designs with the same effect on the stresses or deflections in the concrete slab can be considered. Then a relative cost and performance analysis of the different designs can be made to select the final joint design.

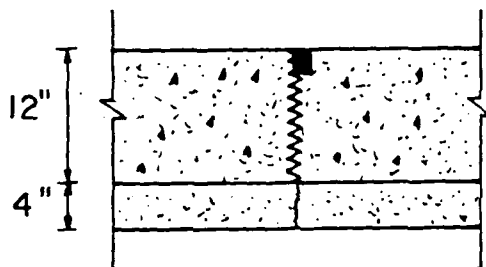
Consider the desirability of limiting maximum tensile stress in a 12 in. (30.5 cm) thick airfield slab under a single load of 30 kips (133 kN) resting on a subgrade with k-value of 200 pci (54 N/cm<sup>3</sup>) to a level equal to the interior stress in the slab under interior load (290 psi, or 2.0 MPa). Figure 4-37 shows six possible equivalent pavement joint systems for this purpose. They are:



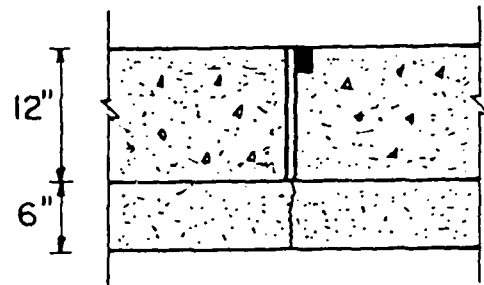
(a) Doweled Joint



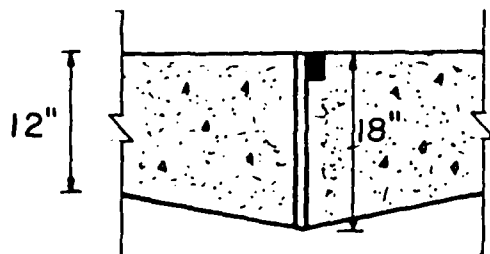
(b) Tied Joint With  
Aggregate Interlock



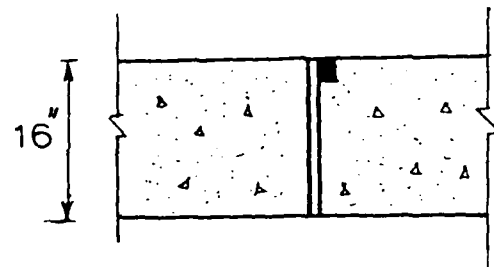
(c) Joint With Aggregate  
Interlock On Stab. Base



(d) Butt Joint On  
Stab. Base



(e) Thickened Edge Joint



(f) Butt Joint

Figure 4-37. Possible Joint Designs for the Example Problem

- (1) A 12 in. (30.5 cm) slab with dowel bars of 1 1/2 in. (38 mm) in diameter, 24 in. (61 cm) long, and spaced at intervals of 12 in. (30.5 cm) center to center.
- (2) A 12 in. (30.5 cm) slab with tied aggregate interlock joint, where no separation is allowed at the joint ( $\text{Agg} > 10^6$ ).
- (3) A 12 in. (30.5 cm) slab on a 4 in. (10.2 cm) cement stabilized base with some aggregate interlock ( $\text{Agg} = 5 \times 10^3$ ).
- (4) A 12 in. (30.5 cm) slab with butt joints on a 6 in. (15.2 cm) cement stabilized base.
- (5) A 12 in. (30.5 cm) slab with thickened edge joints, where edge thickness is equal to 18 in. (45.7 cm).
- (6) A 16 in. (40.6 cm) slab with butt joint and no load transfer system at the joint.

All of these designs are capable of limiting maximum tensile slab stress at the joint to about 290 psi (2.0 MPa). Selection of the final design should be based on other factors such as total cost of the systems and performance considerations. Performance evaluation of alternate systems are in need of further evaluation before specific recommendations can be made.

Tied keyed joints were not recommended since failures associated with stress concentration at the key and keyway may result in localized failures which are difficult to repair.

In addition to the joint and slab systems described above, a joint system developed at the Laboratoire Central Des Ponts et Chaussees in France was also analyzed. This system as shown in Figure 4-38 is patented in France and was developed primarily as a means of upgrading the load transfer efficiency of existing pavement joints.

A recent report by Mr. Ray (Ref. 62) in the form of private communication makes the following points with respect to this jointing system.

The proposed system consists in reestablishing the load transfer by preventing the relative vertical movements of the crack lips by straddling over the crack one or several metallic elements of suitable form (see diagram, Figure 4-38). These elements are introduced into a drilled hole centered in the plane of the crack. They are secured to the two adjacent slabs by gluing or by friction.

#### 1. Glued Metal Key

The key which we showed in Purdue had the following characteristics:

outer diameter: 70 mm

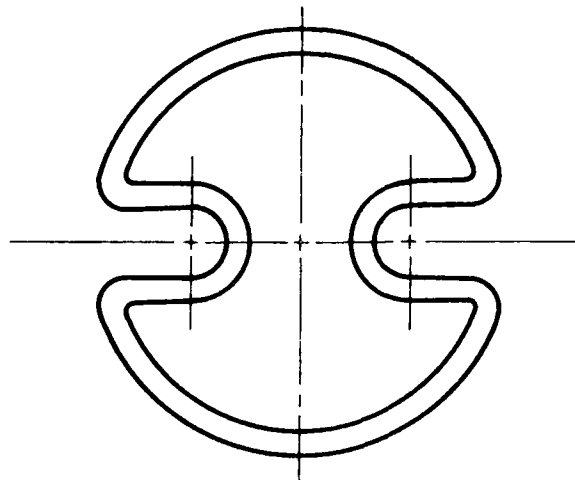
thickness: 4 mm

length: 240 mm

It was made of cold-drawn ordinary mild steel (elastic limit of about 25 h bars). It was noted that this key has excessive stiffness in spite of the folds enabling its deformation with the expansion and constriction of the slabs. The elastic limit of the system was reached for a force of 15 to 20 t and a deformation of 0.5 to 0.8 mm.

About 100 keys of this type were installed in December 1976 on a travelled pavement. The result of this first experiment is the following:

- (a) The immediate effectiveness of the device is good (see accompanying figure, Figure 4-39) and is dependent on how well the gluing is performed. Cold weather, premature opening to traffic or the presence of water in the pavement will lead to failure.
- (b) As the thickness of the keys is too large, the elastic deformation is smaller than the average movement of the joints. They were thus compressed beyond the elastic limit during the summer of 1977. At the end of that year, with



Cross Section  
of Key

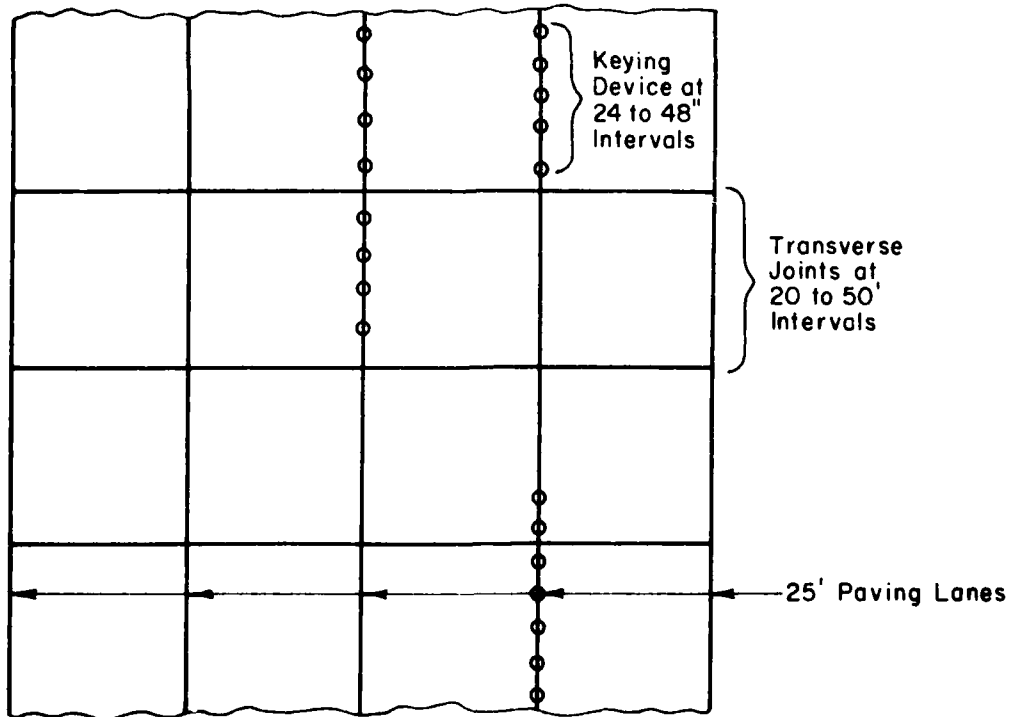


Figure 4-38. Possible Layout of Joints with French Keying Device.



# RECORDING OF SLAB DEFORMATION COTTER EFFECT

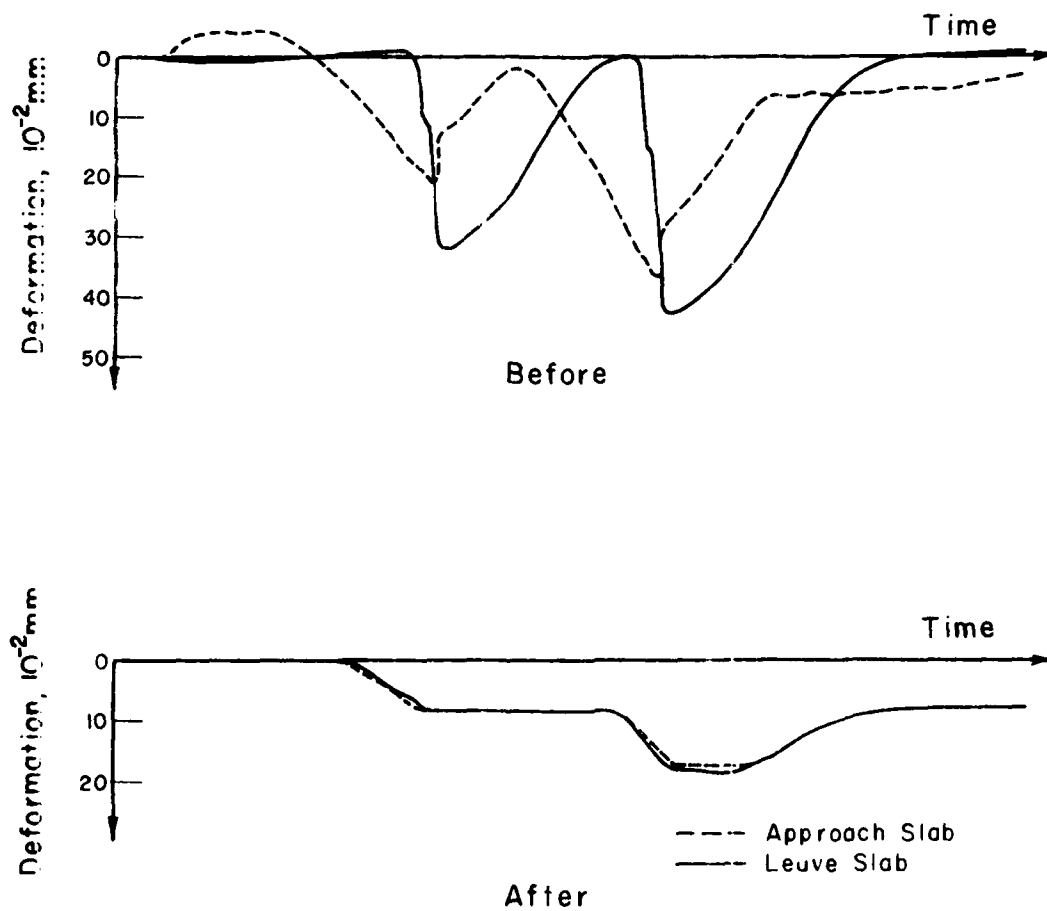


Figure 4-39. Effectiveness of French Keying Device on Joint Efficiency.

the first cold spell, they became detached and the repair was ruined. This drawback can be overcome by reducing the thickness of the tube. It appears that depending on the dimensions chosen and the axle loads used in France, it is possible to reduce thicknesses to about 1 or 1.2 mm. However, below 2.5 or 3 mm it is necessary to provide protection against corrosion by de-icing salt in particular. Solutions do exist but they are generally less reliable and more costly than an extra thickness of metal.

- (c) After 10 months of traffic (1500 commercial vehicles per day) and before failure of the gluing a joint was fatigue tested by means of the LPCP heavy vibrator. Fatigue failure occurred after  $0.8 \times 10^6$  cycles (sinusoidal loading of one slab end with a force of 0 to 6 t at a frequency of about 10 Hz).

## 2. Unglued Stressed Key

From the viewpoint of the operation of superhighways, the favorable period for maintenance work in France is in winter. The temperature is often low and water is practically always present in the pavement. Gluing is thus not an operation whose success is sufficiently certain in this period. We have been looking for a system which would make it possible to obviate gluing.

The new goal of research is to provide a link between the concrete and key by friction, without gluing. The potential advantages of this new process are the following:

- it is independent of weather conditions at time of installation
- it allows immediate re-opening to traffic
- it appears mechanizable and should thus allow installation rates compatible with work on the superhighways.

The following conditions should be fulfilled by the new keys in order to achieve this new goal:

- (1) They should always prevent the relative displacement of the two ends of the slabs.
- (2) They must always allow slab expansion and contraction without inducing significant longitudinal forces, in order to avoid any risk of structural blow-up.
- (3) To take up shearing by friction, they must develop a force perpendicular to the plane of the folds of at least 6 t (joint very open in winter for example) in order to support a vertical force of about 3 t (for 4 keys per joint on heavy traffic lane).
- (4) They must not develop forces greater than 15 or 20 t when the slabs expand, so as to avoid:
  - breakage of slab corners
  - slab displacement
  - blow-up of structure
  - longitudinal cracking by fatigue under traffic

Studies show that it is probably not possible to fulfill all these conditions with a metal key of the initial type. When the thickness is large, there is a sufficient spring force which is however extremely stiff. When the thickness is small the stiffness is suitable but the force is much smaller.

Several suggestions for resolving the problems listed above are suggested by Mr. Ray and co-workers. These will be considered at a later time.

Analysis of the French keying system with the finite element model also suggests the system to be a highly efficient load transfer system, but with

the only significant problems being the attachment of the system to the concrete, and that of selecting the appropriate stiffness for the key. Procedures for installation as a part of the longitudinal joint system in fresh concrete placed with a slip form paver must also be resolved. Cost of installation and long-term performance of the system have also not been resolved. Thus, while this jointing or keying system seems to have considerable potential, many factors affecting design of the system must still be resolved before it can be recommended for general use.

## CHAPTER 5

### SUMMARY, COSTS AND RECOMMENDATIONS

#### 5.a General Summary

Distress in rigid pavements caused by the longitudinal construction joints can be due to three major causes. These are: 1) deterioration of the concrete along the joints; 2) breakup of the slab due to cracking caused by stress concentrations due to loads applied near the slab edge; and 3) relative, vertical, permanent displacement of adjacent slab edges. Control of distress of the type listed in Items 2 and 3 above is normally accomplished by the use of some type of load transfer across the joint, whereas the type of distress listed in Item 1 may be caused by the load transfer system used, i.e., shearing of the keyway systems in many airport pavements.

The problem is to design pavement systems in general and the longitudinal joints in particular in a manner so that stresses near the edge are at an acceptable level, so the pavement will not develop any relative, permanent, vertical deformation across the joint, and so there will be no accelerated deterioration of the concrete around the joint. All such systems must be economical to construct, be easily maintained, and compatible with the use of slip form paving techniques.

There are a number of load transfer techniques which will provide adequate load transfer to reduce the edge load stress to a level below the maximum stress under the same load at an interior point in the slab. Reduction of edge stresses to a level significantly lower than those due to a load at an interior point would appear to be impractical. Conversely, if the stress under an edge load is significantly higher than that under an interior load, there is an imbalance in the pavement design regardless of

the level of edge stress developed. Since pavement edge deflection is always greater than interior load deflection, it follows that the edge load condition may always be critical to pavement performance even if the stresses in the slab under edge load are less than the maximum stress under an interior load. Thus, an optimum balanced design of a pavement slab is assumed to occur whenever the stress due to a load at an edge is equal to or slightly less than the stress under the same load at an interior point. This would normally occur with a load transfer efficiency of 75 percent or more.

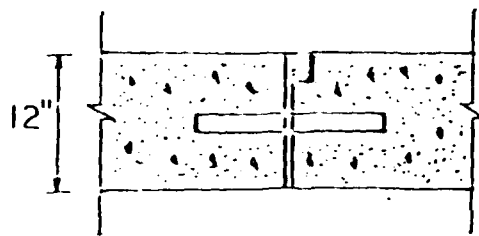
While balanced design would normally occur when the edge and interior load stresses are approximately equal, it may be more economical to achieve a reduced level of stress under edge loading through increased pavement sections rather than through improved load transfer efficiency across the joint. Increasing the total pavement cross section, either by increasing the slab thickness or by using a heavier subbase, may result in a less expensive pavement section than would a thinner pavement with expensive load transfer systems. Use of thicker pavement section to reduce edge stresses would also have the advantage of providing a greater factor of safety against failure at all points in the slab. Also, there is a great tendency for joints with efficient load transfer to lose efficiency with time. This reasoning would seem to suggest the use of sleeper slabs or thickened edge pavements as the obvious solution to this problem. These solutions were, in fact, critically analyzed and found to be impractical due to the extent of thickening or thickness of sleeper slab needed to produce the desired reduction in the edge stresses and deflections.

Also use of an increased pavement cross section either uniform or thickened edge, to reduce edge load stresses and deflections to an acceptable level may not completely eliminate the need for ties or load transfer

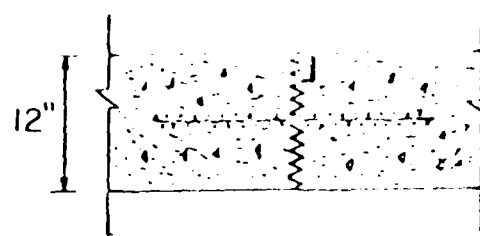
across the joint. Faulting is recognized as one of the most common types of joint distress in rigid pavements, and while faulting is usually associated with transverse joints, consideration must be given to the possibility of faulting along the longitudinal joints if all load transfer systems are eliminated and the majority of loads are applied on one side of the joint. It may be desirable to provide some load transfer or alignment devices to prevent faulting, even though such devices may not provide any significant level of load transfer. Keys and keyways could be used for alignment only, but failure of the keyways would always provide a potential maintenance problem.

In summary, load transfer devices can serve two distinct and separate functions. First, they can be used and designed to reduce the level of stresses and deflection at the pavement slab edges, and second, they provide a means of slab alignment to prevent permanent, relative displacement of the adjacent slab edges (faulting). Design considerations of the load transfer devices for these two functions are completely different and must be considered separately.

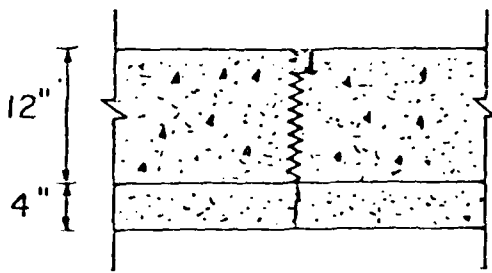
Figure 5-1 shows 6 pavement sections which have approximately the same level of edge stress due to a typical aircraft gear load applied near the pavement edge. These systems range from straight butt joints without any type of subbase or load transfer devices (Item f), to a combination of stabilized subbase and load transfer by aggregate interlock (Item c). These results are based on the theoretical pavement sections to produce adequate load transfer to limit the edge load to a specified level under a given load. These solutions do not take into account the need for a minimum subbase for use as a construction platform or for drainage and frost control purposes. These latter functions can be achieved with either bound or



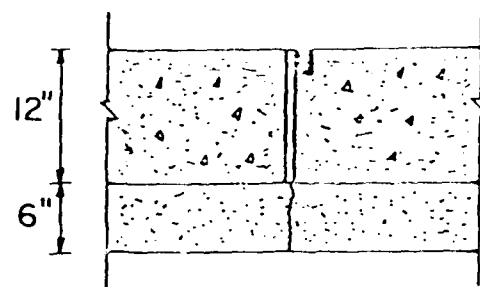
(a) Doweled Joint



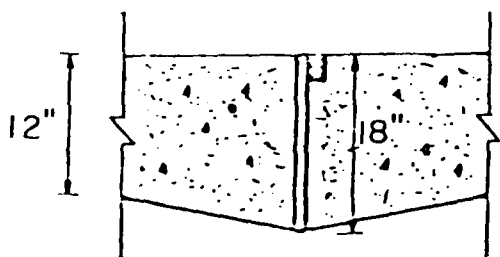
(b) Tied Joint With  
Aggregate Interlock



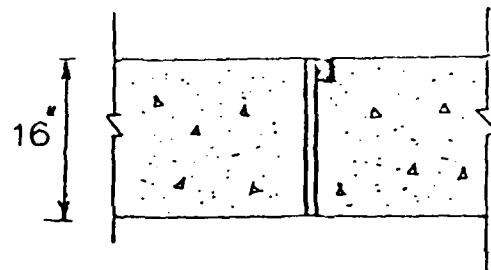
(c) Joint With Aggregate  
Interlock On Stab. Base



(d) Butt Joint On  
Stab. Base



(e) Thickened Edge Joint



(f) Butt Joint

Figure 5-1. Equivalent Pavement Systems Based on Maximum Edge Stress Criterion

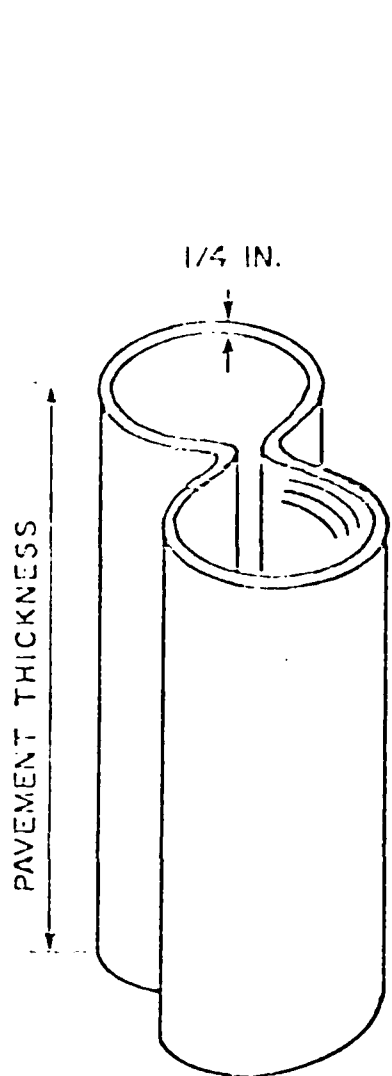


unbound granular subbases which add little or nothing to the structural capacity of the pavements, and for this reason were not included in these analyses.

In addition to the pavement sections shown in Figure 5-1, there are several other approaches to providing an adequate pavement section which are viable from an analytical and theoretical standpoint, but need further evaluation for cost and construction problems. These alternate load transfer systems are shown in Figures 5-2, 5-3, and 5-4.

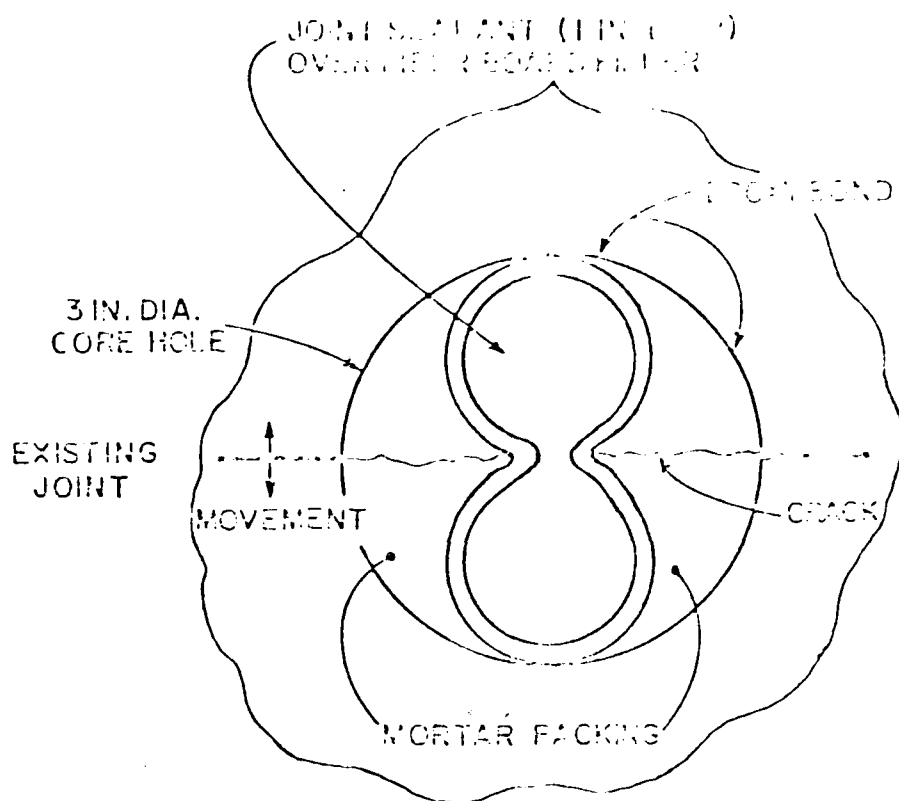
Figure 5-2 shows a load transfer system known as a "keying device" discussed earlier in Chapter 4. While these connectors will theoretically provide all the load transferability needed to keep the level of edge load stresses to an acceptable level there still remain serious questions with regard to how closely such connectors must be placed, how to install such connectors in a slip form paving operation, the long-term performance of pavements with the devices, and the cost of installing such units. These questions must all be evaluated before final decisions can be made with respect to the use of such a load transfer scheme. A number of these keying devices have been installed in France and the long-term performance of these devices should be closely followed before added work is done on them. Meanwhile, the constructability of joints with the keying devices with slip form pavers should be evaluated.

Figure 5-3 shows a joint system referred to in this analysis as a "Z" joint. Again, it can be demonstrated that this joint can theoretically transfer all necessary loads to keep the edge stresses and deflections to an acceptable level. It is noted, however, that all questions raised with regards to the French keying device are also applicable to the "Z" joint system. In addition, there is a problem of how many "Z" type joints can be

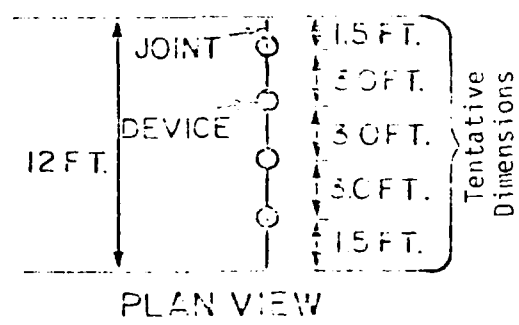


ISOMETRIC VIEW OF  
DEVICE

1 FT. = 0.3m  
1 IN. = 2.54cm



PLAN VIEW



PLAN VIEW

Figure 5-2. Figure Eight Steel Load Transfer Device (Schematic)

## ALTERNATE JOINT DESIGN

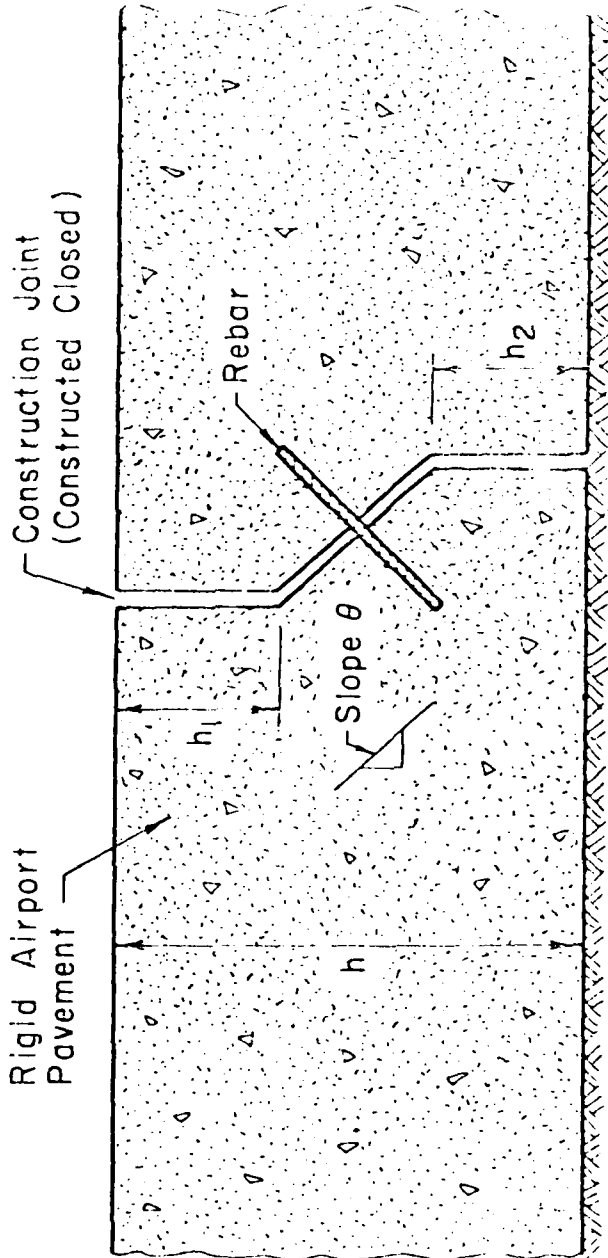


Figure 5-3. Alternate "Z" Joint for Longitudinal Joints with Slip-Form Paving Operations

No Scale

**Note :** Joint Showed Open For Showing Owners Only

## ALTERNATE JOINT DESIGN

Epoxy Bonded Construction Joint With  
Longitudinal Doweled Contraction Joints To  
Accommodate Temperature Changes And  
Provide Hinge Action

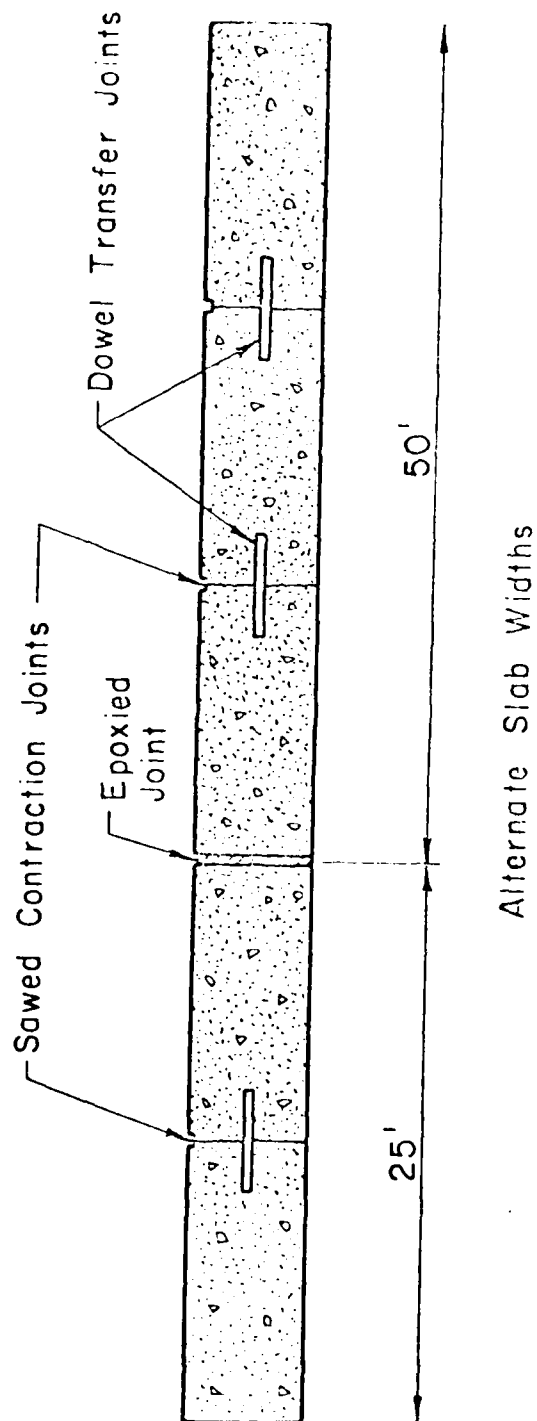


Figure 5-4. Alternate Construction Procedure for Installing Dowels at Longitudinal Joints with Slip-Form Paving Operations

used in adjacent joints. The "Z" type joint connection does not provide for free horizontal movement of the slab edges as the slabs shrink and expand due to temperature and moisture changes. This restraint may produce secondary cracking of the slabs if used on all joints across a 150 to 200 foot wide runway. It is noted, however, that with pavement slabs 14 inches or more in thicknesses, ties have been effective in pavement widths as great as 100 feet (4 - 25 foot lanes tied at 3 longitudinal joints). This 100 foot width would normally support almost 99 percent of all traffic on a runway and is greater than a typical taxiway system.

Figure 5-4 shows an alternate approach for getting the dowel load transfer systems into the pavements with slip form pavers. The major questions yet to be considered with this type of construction procedures are cost, permanence of the proposed bond, and the best adhesives and techniques to use for bonding the construction joints together.

In all of the joint load transfer systems shown in Figures 5-1 through 5-4 there is a question of the long-term durability of the load transfer approach. As demonstrated in Chapter 4 of this report, excessive bearing stresses between the dowels and the concrete can lead to elongation of the dowel sockets and thus to loss of load transfer efficiency of the dowels. Aggregate interlock can also be destroyed by repeated applications of high shear stresses across the joint. Loss of load transfer with aggregate interlock is most critical when the joints are allowed to open which can be eliminated by tying the joints together. Field results support this approach but there are insufficient documentation available to affect an acceptable design for joints with aggregate interlock.

Stabilized subbases can provide significant stress relief if made sufficiently thick and with adequate stiffness of the subbase material.

This approach can be designed to provide adequate structural capacity and efficient load transfer. If, however, the subbase and slab are bonded together then any cracks which develop in the subbase will reflect through the pavement slab. Conversely, if a bond breaker is used, then much of the efficiency of the total system is lost so it is usually cheaper to provide the equivalent structural capacity by increasing the thickness of the pavement slab than by increasing subbase thickness beyond the minimum required for construction, drainage and frost protection.

One method of longitudinal joint design which has been used with positive results is to use dowels as the load transfer systems. Such dowels are usually installed by constructing a butt joint and drilling sockets and grouting dowels in place. Gang drills for up to 7 holes at a time have been developed and have proven to be an economical way to install the dowels. Dowels are usually grouted into the fixed slab with an epoxy grout and the remaining end of the dowel coated to prevent bonding to the concrete. At least 4 airport pavements are known to have been constructed in this manner (Memphis, Nashville, Milwaukee, Salt Lake City). An alternate to the use of dowels in the longitudinal joint to install large diameter ties (#10 or #11 deformed bars) by grouting in the same manner as with the dowels.

#### 5.b Cost Analysis

The relative cost of the various pavement systems can be estimated from the cost data provided below. These cost data were selected from several sources which must remain confidential with the approximate range for each as listed. The values given are reasonable and current to the best of the author's knowledge, but it must be recognized that these

unit costs will vary with time, from location to location, and from job to job within a particular area. Such factors as the size of the project, the equipment the contractor has available and the general economics of a particular area will all affect the cost data shown. All costs shown represent "in-place" data.

Item	Unit Cost Range	Unit Used
Portland Cement Concrete	1.25-1.60	Per sq yd per inch
Subbase In Place		
Cement Stabilized Aggregate	0.70-0.80	Per sq yd per inch
Asphalt Stabilized Aggregate	0.80-1.10	Per sq yd per inch
Lime Fly Ash Aggregate	0.60-0.80	Per sq yd per inch
Crushed Stone	0.45-0.60	Per sq yd per inch
Gravel	0.40-0.50	Per sq yd per inch
Keyways in Long. Jt.	0.10-0.25	lineal ft
Dowels Installed in Basket (Fig. 5.4)	3.25-4.60	lineal ft
Dowels - Drilled and epoxied (5 to 7 holes per operation)	3.50-5.00	lineal ft
Tie Bars for Agg. Interlock	1.50-2.50	lineal ft
Keying Device (French)	No Data	
"Z" Joint	No Data - Est. same as Tie Bars	

Using the mean value for the cost data, and assuming a 25 foot wide paving lane the unit cost per square yard of pavement for the various load transfer systems can be estimated as follows.

Item (Fig. 5-1)	Cost per Square Yard of Pavement
a - 12" PCC + Doweled Joints	17.40 + 1.40 = 18.80
b - 12" PCC + Tied Joint	17.40 + .70 = 18.10
c - 12" PCC + 4" Stab. Subbase	17.40 + 3.00 = 20.40
d - 12" PCC + 6" Stab. Subbase	17.40 + 4.06* = 21.46
e - 12" PCC + 3" PCC (Ave)	17.40 + 4.35 = 21.75
f - 12" PCC + 4" PCC	17.40 + 5.80 = 23.20

\*(less \$1.00 per square yard for longitudinal joint sawing)

The above analysis indicates that the doweled joints and the tied joints are the most economical to construct. It must be kept in mind that some subbase will also be required of all pavements for a construction platform and for drainage and frost protection. For this analysis it is assumed that this is a constant cost factor to be added to all of the pavement sections analyzed.

The above analysis is based on first cost only and no attempt was made to evaluate the relative maintenance costs or relative performance of the various systems. It is known, however, that if inadequate dowel systems and too high a stress level is permitted on the aggregate interlock joints these systems will lose their ability to transfer load across joints. Design criteria will have to be developed to insure proper design of such systems. A suggested design based on the analyses presented in Chapter 3 and 4 of this report is presented below with design recommendations.



### 5.c Recommendations for Design

The design recommendations for longitudinal joints are based on the criteria of adequate load transfer to limit stresses and deflections along the edges and at the corners of the slab and must be economically constructable using either slip form or fixed form techniques. The procedures recommended have been used at several airports and while long term performance records are not available, short term performance records along with calculated values indicate the proposed designs should give good performance over a 20 year life.

Dowels and ties are the only proven methods of load transfer which can be constructed with both slip form or fixed form pavers. Both dowels and ties have been used extensively in airport pavements and while some problems have been observed with both methods, these problems can generally be attributed to inadequate design standards rather than to basic deficiencies in the system. The proposed designs should eliminate these deficiencies.

In developing a design for the longitudinal joint, the critical location is at the corners of the slabs. Furthermore, performance of the longitudinal joint is affected by the behavior and performance of the transverse joint. Thus, for an effective longitudinal joint design both the longitudinal and transverse joints must be designed as a unit, i.e., protected corners.

In general it is recommended that a 100 foot wide keel section of the runway be protected by ties or dowels for both the longitudinal and transverse joints. This can be accomplished by dowelling or tying the three central longitudinal joints and fully dowelling the 4 - 25 foot slabs in

the keel sections. Since slabs outside this 100 foot wide keel section will experience almost no traffic, no load transfer devices are required in the region outside the keel area. All longitudinal and transverse joints in taxiways should be protected with dowels or ties.

The efficiency of both ties and dowels are influenced by bearing stresses between the bars and the concrete. Both methods of load transfer decrease under repeated load application as the bearing stress increases. This problem appears to be more critical with transverse joints which experience complete stress reversal with each load application than with the longitudinal joints which experience unidirectional stresses with each pass of an aircraft. This problem is most crucial at the slab corners where the forces on the dowels and ties are greatest. Thus, for effective performance, the design of both longitudinal and transverse joints must be designed to keep the bearing stresses between the concrete and steel bars, either dowels or ties, at acceptable levels.

Bearing stress between the bars and the concrete is a function of bar diameter, concrete modulus and the magnitude of force transferred. Figure 4-11 shows how the critical bearing stress varies with the parameters of concrete modulus, bar diameter, slab thickness and subgrade support for a given magnitude of load transfer. From Figure 4-11 it is seen that slab thickness and subgrade support have almost no effect on this property. Consequently, the diameter of the ties and dowels for both longitudinal and transverse joints should be selected on the basis of the best estimate of the concrete modulus, and the magnitude and frequency of load applied near the joints.

Allowable bearing stresses between the bars and concrete have not been established precisely. Laboratory results reported by Cashell (35) indicate

that if the maximum bearing stress approaches the compressive strength of the concrete, a dowel looseness of around .005 inches could be anticipated after 600,000 load applications (Fig. 4-15). This amount of looseness is not excessive and joints with this magnitude of looseness can still provide an effective load transfer. Results from O'Hare Airport suggest that these values are realistic if good performance is to be achieved.

Figure 5-5 shows a typical failure pattern of a 15 inch jointed concrete slab at O'Hare Airport. It is noted that the load transfer of the longitudinal joint was negligible and that there was significant looseness of the dowels nearest the longitudinal joint. As the distance away from the longitudinal joint increased, the magnitude of bar looseness decreased, and near the center of the slab there was almost no discernable looseness in the dowels.

Bearing stresses between the bars and the concrete can be calculated from equation 4-6, to wit,

$$\sigma_{br} = \frac{(800 + .068E_c)}{D^{4/3}} \times (1 + 0.355W) \overline{LT}$$

where

D = bar diameter in inches

$E_c$  = Young's Modulus of the concrete in ksi

W = joint opening in inches

$\overline{LT}$  = maximum load transferred by a dowel in kips

Values for  $\overline{LT}$  are obtained from ILLI SLAB model for specific loading conditions. Table 5-1 gives some typical values which were obtained for  $\overline{LT}$  and  $\sigma_{br}$  for the O'Hare pavements assuming an  $E_c = 5 \times 10^6$  psi (3.5 GPa), W = 0.1 inches (2.5 mm), and D = 1 1/4 inches (31.15 mm).

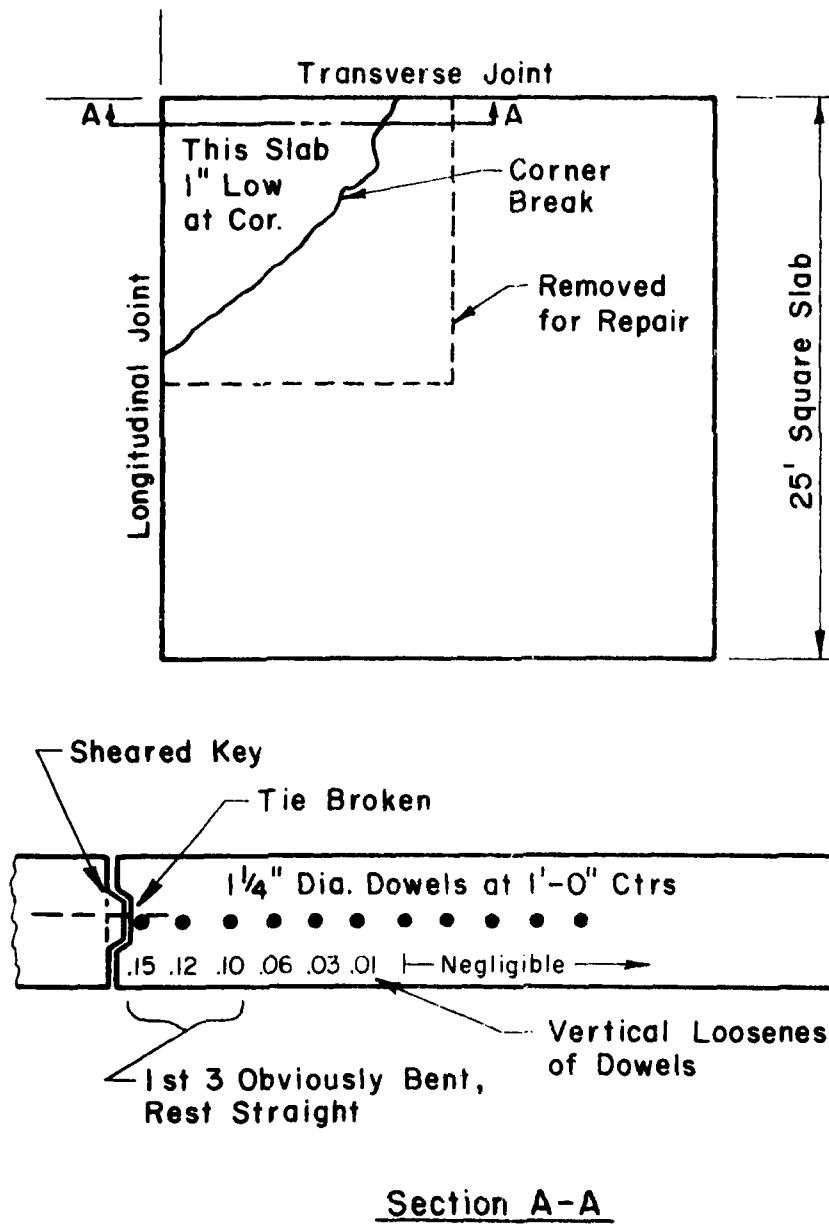


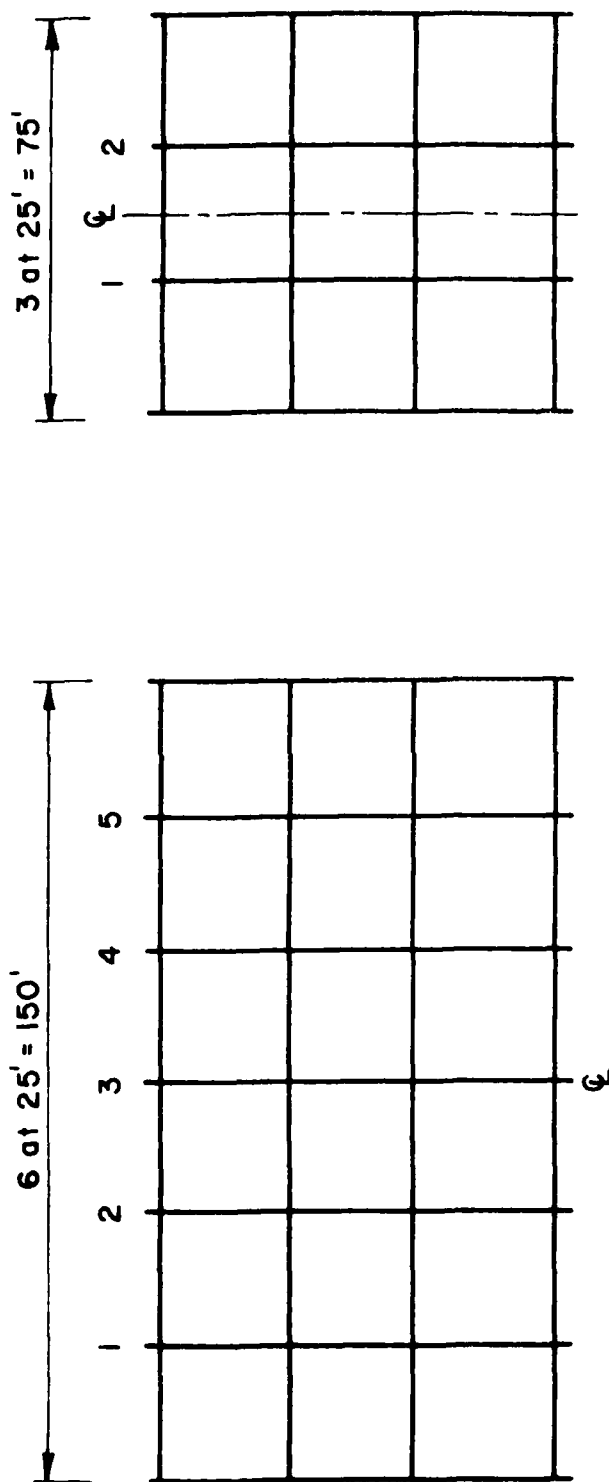
Figure 5-5. Typical Failure Patterns in Pavement Sections of O'Hare Airport.

Table 5-1. Loads and Bearing Stresses at Transverse Joints at O'Hare.

Aircraft/Gross Wt.	Location			
	Edge		Corner	
	LT	$\sigma_{br}$ (psi)	LT	$\sigma_{br}$ (psi)
DC 10-30/558 <sup>k</sup>	6.52	5,720	11.70	10,264
DC 10-30/403 <sup>k</sup>	3.40	2,982	8.45	7,413
747/778 <sup>k</sup>	6.06	5,316	10.93	9,589
747/600 <sup>k</sup>	4.70	4,123	8.43	7,395

From the bearing stresses in Table 5-1 it is seen that the potential bearing stresses near the corner, where significant looseness was experienced, was significantly higher than the anticipated strength of the concrete. Conversely, near the center of the joint where little looseness was observed, the maximum anticipated bearing stress was on the order of the compressive strength of the concrete.

Based on the results presented above, recommended joint designs for longitudinal and transverse joints for airport pavements are given in Figures 5-6, 5-7 and 5-8 based on design aircraft of 727, DC-8 or 707 and widebody aircraft. The load transfer devices indicated in these figures were determined to acceptably limit the bearing stresses between the concrete and the bar. Theoretically, it is possible to decrease the size of the dowels and ties away from the joint areas, but this refinement cannot be justified on the basis of the current technology. Current technology does not permit a further breakdown of these design values and construction costs would probably not justify a more detailed breakdown.



### RUNWAY

### DESIGN AIRCRAFT 727 Class

### TAXIWAY

#### Type Joint Recommended

Longitudinal

1 and 5

No Load Transfer - No Ties or Nominal Ties

2, 3 and 4

Tied - # 8 Deformed Bars at 12 in. Ctrs

Transverse

Dowelled Between Longitudinal Joints

1 and 5 with 1 1/4"  $\phi$  at 12 in. Ctrs

Undowelled Outside Joints 1 and 5

#### Type Joint

Longitudinal Joints

Tied - # 8 Deformed

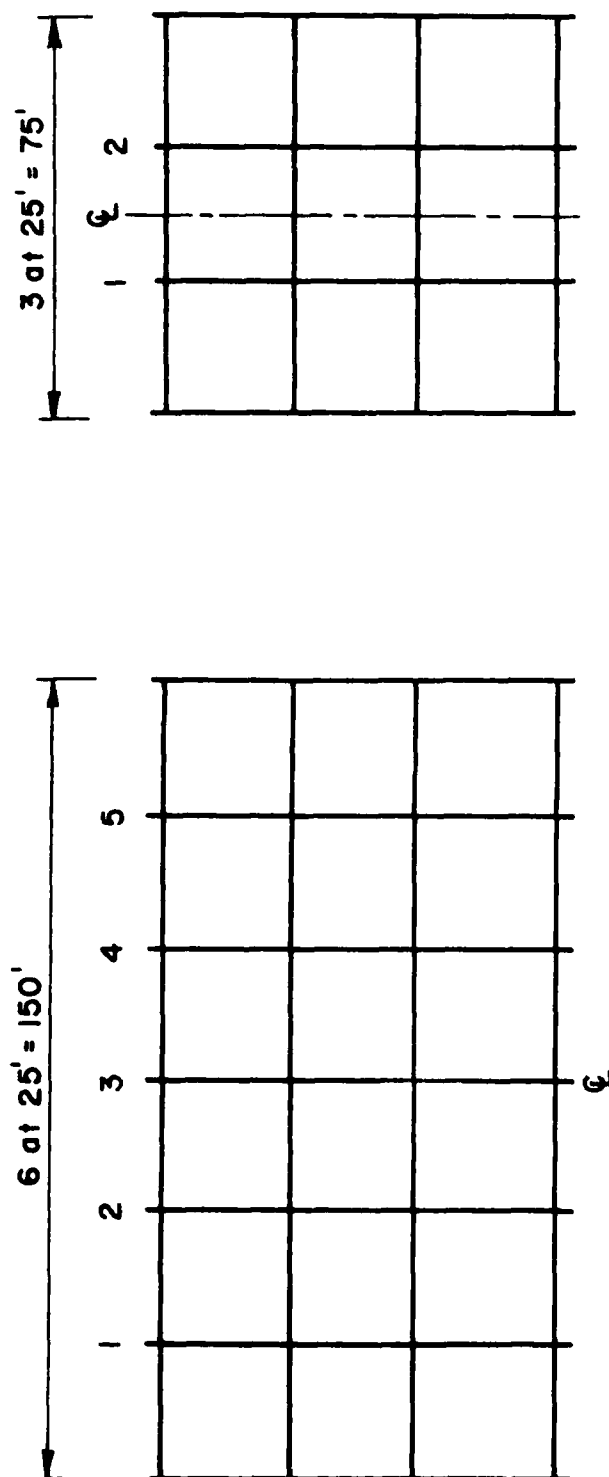
Bars at 12 in. on Ctrs

Transverse

Dowelled with 1 1/4"  $\phi$  at

12 in. Ctrs

Figure 5-6. Recommended Load Transfer Devices for Airport Pavements  
Designed for 727 Class Aircraft.



### DESIGN AIRCRAFT 707 & DC-8 Class

Type Joint Recommended  
Longitudinal

1 and 5

No Load Transfer - No Ties or Nominal Ties

2, 3 and 4

Tied - #10 Deformed Bars at 12 in. Ctrs

Transverse

Dowelled Between Longitudinal Joints

1 and 5 with 1 1/2"  $\phi$  at 12 in. Ctrs

Undowelled Outside Joints 1 and 5

Type Joint

Longitudinal Joints

Tied - #10 Deformed

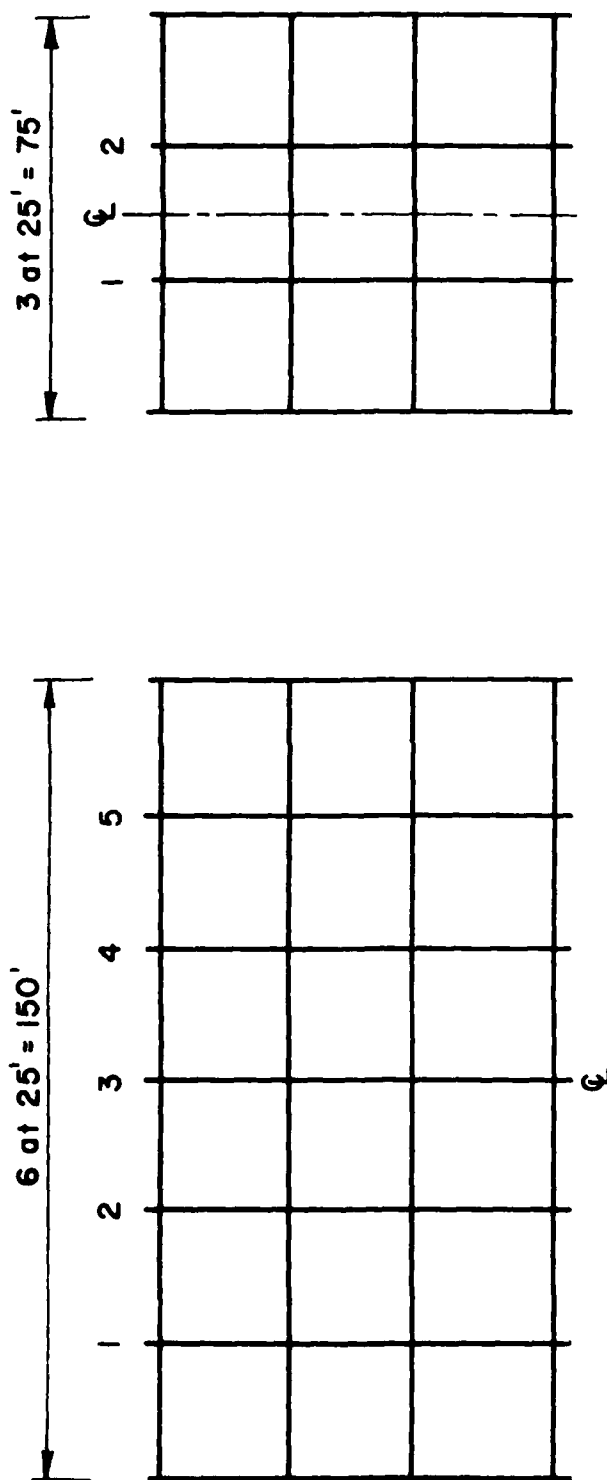
Bars at 12 in. on Ctrs

Transverse

Dowelled with 1 1/2"  $\phi$  at

12 in. Ctrs

Figure 5-7. Recommended Load Transfer Devices for Airport Pavements  
Designed for DC-8 Class Aircraft.



TAXIWAY

DESIGN AIRCRAFT  
Wide Bodied Aircraft  
(DC-10, 747, etc.)

- Type Joint
- Longitudinal Joints
    - Tied - # 11 Deformed Bars at 2 in. on Ctrs
  - Transverse
    - Dowelled with 1 1/2"  $\phi$  at 2 in. Ctrs

RUNWAY

- Type Joint Recommended
- Longitudinal
    - 1 and 5
    - No Load Transfer - No Ties or Nominal Ties
    - 2, 3 and 4
    - Tied - # 11 Deformed Bars at 12 in. Ctrs
  - Transverse
    - Dowelled Between Longitudinal Joints 1 and 5 with 2"  $\phi$  at 12 in. Ctrs
    - Undowelled Outside Joints 1 and 5

Figure 5-8. Recommended Load Transfer Devices for Airport Pavements Designed for Wide-bodied Aircraft.



The proposed joint design for the widebody aircraft (Fig. 5-8) is being installed in several pavement sections at O'Hare Airport. The proposed load transfer designs with 21 inch concrete pavement slabs and 6 inch stabilized subbase were compared with a recommended 18 inch slab and 18 inch stabilized subbase using conventional FAA load transfer patterns. The proposed designs were found to be superior based on both the stress and deflection criteria. Alternate bids for both the 21-6 with the proposed load transfer devices and the recommended 18-18 section were taken with the 21-6 section and the proposed load transfer plan bid at 11 to 15 percent below the standard 18-18 section. Thus, the proposed use of dowels and ties for load transfer in concrete pavements appears to be both effective and economical.

## CHAPTER 6

### RECOMMENDATIONS FOR FURTHER STUDY

As indicated in the introduction to this report, field validation of the analyses techniques developed were not a part of this study. Every attempt has been made to validate the models developed by comparison of the results from the models with results from classical theory when applicable, and comparison with results from earlier tests on pavements. Results from these comparisons indicate the models developed are valid and accurately predict the response of the pavements to load.

While the models presented herein appear valid for a wide range of loads and paving conditions, it must be borne in mind that the finite element modeling is a somewhat artificial method of representing the facility modeled. As a consequence, these models should be used with limitations, and while these limitations do not appear to be confining, they must be defined so that the constraints of use are not violated. In other words, the finite element model should be validated by comparison with field data for the specific applications intended.

In addition to field validation of the model there are also questions with respect to design criteria which must be addressed. Past and present design procedures were based on limiting stresses calculated using some assumed load transfer conditions across joints. With more precise methods for determining the effective load transfer across joints, and the effect of this load transfer on the responses of the pavement, new design criteria may be needed for reliable design.

Some of the load transfer procedures proposed herein have proven effective based on analysis of the systems, and some have even been validated by laboratory tests. The questions yet to be answered is how effective these

load transfer devices will be over the long term. For example, it has been clearly shown that dowels are very effective load transfer devices provided the dowels remain tight in the concrete sockets. Concrete sockets may elongate, however under repeated stress reversals if the bearing stress between the dowel and concrete are high. The level of stress at which the concrete dowel socket deterioration can be held to an acceptable level must be established before doweled joint systems can be designed with confidence.

Because of these and similar problems, studies must be undertaken to complement and validate the findings presented herein. These studies should include but not necessarily be limited to the items listed below:

1. Field validation of the finite element model presented herein and detailed in Volume III of this report. This should be done by instrumenting pavements in the field and comparing measured deflections and strains in the loaded pavements with results from the FEM model.

2. Validate the performance of the proposed load transfer systems both in the field and in the laboratory as indicated below:

- a. Dowels and tie bars with aggregate interlock have been demonstrated in the laboratory but must be validated under field conditions. This can be done by evaluating the performance of doweled and tied joints of pavements in service and comparing the bearing stresses between the bars and the concrete with the performance of these systems in service.

- b. The keying device shown in Figure 5-2 should be evaluated for constructability when used in conjunction with slip form paving, and its performance in service should be followed obtaining the appropriate data from the ongoing studies in France.

c. Load transfer systems shown in Figures 5-3 and 5-4 should be evaluated for constructability, and, if feasible, tested in the laboratory for effectiveness.

3. Cost effective studies of the various load transfer devices should be evaluated.

These are the most critical and potentially the most productive of the items requiring further study. Other concepts for improving the joint design of slip formed rigid pavements should also be evaluated as they are developed. For the immediate present, use of dowels and large diameter tie bars appears to be the most reliable. The use of the "Z" joint shown in Figure 5-5 appears to be a reasonable alternative but its cost, constructability, performance and reliability must be established through tests before this type joint can be specified on a routine basis.

## LIST OF REFERENCES

1. Packard, R. G., "Design of Concrete Airport Pavement," Report No. EB050.03P, Portland Cement Association, 1973.
2. Westergaard, H. M., "Computation of Stresses in Concrete Roads," HRB Proc. Vol. 6, 1926.
3. Pickett, G., and G. K. Ray, "Influence Charts for Concrete Pavements," Trans. ASCE, Vol. 116, 1951.
4. "The AASHO Road Test--Pavement Research," Special Report 61E, HRB, 1962.
5. Teller, L. W., and E. C. Sutherland, "The Structural Design of Concrete Pavements," Public Roads, Vol. 16, Nos. 3, 9, 10 (Oct., Nov., Dec., 1935); Vol. 17, Nos. 7, 8 (Sept., Oct., 1936); Vol. 23, No. 8 (Apr.-May-June 1943).
6. Barenberg, E. J., C. L. Bartholomew, and M. Herrin, "Pavement Distress Identification and Repair," Technical Report P-6, Department of Army, CERL, Champaign, Illinois, March 1973.
7. Spellman, D. L., J. R. Stoker, and B. F. Neal, "California Pavement Faulting Study," Res. Rep. 635167-1, California Division of Highways, 1970.
8. Spellman, D. L., J. H. Woodstrom, and B. F. Neal, "Faulting of PCC Pavements," HRR No. 407, 1972.
9. Gulden, W., "Pavement Faulting Study," Georgia Department of Transportation, Final Rep., 1975.
10. Stelzenmuller, W. B., L. L. Smith, and T. J. Larsen, "Load Transfer at Contraction Joints in Plain Portland Cement Concrete Pavements," Res. Rep. 90-D, Florida Dept. of Transp., April 1973.
11. "Design, Construction, and Maintenance of PCC Pavement Joints," NCHRP Synthesis 19, 1973.
12. Bryden, J. E., and R. G. Phillips, "Performance of Transverse Joint Supports in Rigid Pavements," Res. Rep. 12, New York State Dept. of Transportation, March 1973.
13. Smith, A. R., and S. W. Benhan, "Effect of Dowel Bar Misalignment Across Concrete Pavement Joints," Trans. ASCE, Vol. 103, 1938.
14. Segner, C., "A Study of Misaligned Dowels in Concrete Pavement," Alabama University and Alabama State Highway Department, 1967.

15. "Final Report of Model Tests to Determine Optimum Key Dimensions for Keyed Construction Joints," U.S. Army Engineers, Ohio River Division Laboratories, Mariemont, Ohio, June 1954.
16. Ball, C. G., and L. D. Childs, "Tests of Joints for Concrete Pavements," Portland Cement Association, Research and Development Bulletin RD-26, OIP, 1975.
17. Rice, J. L., "Keyed Joint Performance Under Heavy Load Aircraft," ASCE Transportation Engineering Journal, Vol. 98, No. TE4, Nov. 1972.
18. Grau, R. W., "Strengthening of Keyed Longitudinal Construction Joints in Rigid Pavements," Report No. FAA-RD-72-106, Aug. 1972.
19. Brown, P. B., and M. P. Jones, "Navy Experience in Eliminating Keys from Construction Joints of Concrete Airfield Pavements," Proc. of International Conference on Concrete Pavement Design, Purdue University, West Lafayette, IN., Feb. 15-17, 1977.
20. Timoshenko, S., and S. Woinowsky-Krieger, "Theory of Plates and Shells," 2nd ed., McGraw-Hill Book Company, New York, 1959.
21. Hogg, A. H. A., "Equilibrium of a Thin Plate Symmetrically Loaded, Resting on an Elastic Subgrade of Infinite Depth," Philosophical Mag., Series 7, Vol. 25, March 1938.
22. Holl, D. L., "Thin Plates on Elastic Foundations," Proc. 5th International Con. of Applied Mechanics, Cambridge, Mass., 1938.
23. Newmark, N. M., Numerical Methods of Analysis of Bars, Plates and Elastic Bodies, in L. E. Grinter (ed.), "Numerical Methods of Analysis in Engineering," The MacMillan Company, New York, 1949.
24. Hudson, W. R., and H. Matlock, "Analysis of Discontinuous Orthotropic Pavement Slabs Subjected to Combined Loads," HRR 131, 1966.
25. Vesic, A. S., and K. Saxena, "Analysis of Structural Behavior of AASHO Road Test Rigid Pavements," NCHRP Report 97, 1970.
26. Stilzer, F. C., Jr., and W. R. Hudson, "A Direct Computer Solution for Plates and Pavement Slabs," Res. Report S6-9, Center for Highway Research, University of Texas, Austin, 1967.
27. Abou-Ayyash, A., W. R. Hudson, and H. J. Treybig, "Effect of Cracks on Bending Stiffness in Continuous Pavements," HRR 407, 1972.
28. Pearre, C. M., III, and W. R. Hudson, "A Discrete-Element Solution of Plates and Pavement Slabs Using a Variable-Increment-Length Model," Res. Report No. S6-11, Center for Highway Research, University of Texas, Austin, April 1969.

29. Vora, M. R., and H. Matlock, "A Discrete-Element Analysis for Anisotropic Skew Plates and Grids," Res. Rept. No. 56-18, Center for Highway Research, University of Texas, Austin, August 1970.
30. Eberhardt, A. C., "Aircraft-Pavement Interaction Studies Phase I: A Finite-Element Model of a Jointed Concrete Pavement on a Non-Linear Viscous Subgrade," Rep. S-19, U. S. Army Eng. CERL, Champaign, Illinois, 1973.
31. Eberhardt, A. C., and J. L. Willmer, "Computer Program for the Finite-Element Analysis of Concrete Airfield Pavements," Technical Rept. S-26, U. S. Army Eng. CERL, Champaign, Illinois, 1973.
32. Huang, Y. H., and S. T. Wang, "Finite-Element Analysis of Concrete Slabs and Its Implications for Rigid Pavement Design," HRR 466, 1973.
33. Huang, Y. H., and S. T. Wang, "Finite-Element Analysis of Rigid Pavements with Partial Subgrade Contact," HRR 485, 1974.
34. Hung, Y. H., "Finite-Element Analysis of Slabs on Elastic Solids," Transportation Eng. Journal of ASCE, Vol. 100, No. TE2, May 1974.
35. Teller, L. W., and H. D. Cashell, "Performance of Dowels Under Repetitive Loading," Public Roads, Vol. 30, No. 1, April 1958.
36. Bradbury, R. D., "Design of Joints in Concrete Pavements," Proc. of the HRB, 12th Annual Meeting, 1932.
37. Timoshenko, S., and J. M. Lessels, "Applied Elasticity," Westinghouse Technical Night School Press, Pittsburg, PA., 1925.
38. Friberg, B. F., "Load and Deflection Characteristics of Dowels in Transverse Joints of Concrete Pavements," Proc. HRB, Vol. 18, Part 1, 1938.
39. Westergaard, H. M., "Spacing of Dowels," Proc. of the HRB, 8th Annual Meeting, 1928.
40. Kushing, J. W., and W. O. Fremont, "Design of Load Transfer Joints in Concrete Pavements," Proc. HRB, Vol. 20, 1940.
41. Sutherland, E. C., Discussion on "Design of Load Transfer Joints in Concrete Pavements," Proc. HRB, Vol. 20, 1940.
42. Friberg, B. F., "Design of Dowels in Transverse Joints of Concrete Pavements," Trans. ASCE, Vol. 105, 1940.
43. Finney, E. A., "Structural Design Considerations for Pavement Joints," Journal ACI, Vol. 53, No. 1, July 1956.

44. Marcus, H., "Load Carrying Capacity of Dowels at Transverse Pavement Joints," ACI Journal, Proc., Vol. 48, Oct. 1951.
45. Wilson, E. L., "Solid SAP, A Static Analysis Program for Three-Dimensional Solid Structures," SESM 71-19, Structural Engineering Laboratory, University of California, Berkeley, CA, 1969.
46. Zienkiewicz, O. C., "The Finite Element Method in Engineering Science," McGraw-Hill, London, 1971.
47. Cook, R. D., "Concepts and Applications of Finite-Element Analysis," Wiley, 1974.
48. Przemieniecki, J. S., "Theory of Matrix Structural Analysis," McGraw-Hill Book Company, 1968.
49. Yang, N. C., "Design of Functional Pavements," McGraw-Hill Book Company, 1972.
50. "Joint Spacing in Concrete Pavements," Highway Research Board, Research Rept. 17-B, 1956.
51. Darter, M. I., and E. J. Barenberg, "Design of Zero-Maintenance Plain Jointed Concrete Pavement," Technical Report Prepared for Federal Highway Administration, University of Illinois at Urbana-Champaign, June 1977.
52. Childs, L. D., "Test of Concrete Pavement Slabs on Cement-Treated Subbases," HRR No. 60, 1964.
53. Colley, B. E., and H. A. Humphrey, "Aggregate Interlock at Joints in Concrete Pavements," HRR No. 189, 1967.
54. Nosseir, S. B., S. K. Takahashi, and J. E. Crawford, "Stress Analysis of Multicomponent Structures," Naval Civil Engineering Laboratory Technical Report R-743, Port Hueneme, California, Oct. 1971.
55. Wilson, E. L., "Structural Analysis of Axisymmetric Solids," American Institute of Aeronautics and Astronautics, Journal, Vol. 3, No. 12, Dec. 1965.
56. Lokken, E. C., "Factors Influencing Joint and Sealant Designs for Concrete Pavement," Portland Cement Association, Report TA024, OIP, 1970.
57. "Thickness Design for Concrete Pavements," Concrete Information, Portland Cement Association, 1966.
58. Darter, M. I., and E. J. Barenberg, "Zero-Maintenance Design for Plain Jointed Concrete Pavements," Proc. of International Conference on Concrete Pavement Design, Purdue University, West Lafayette, IN, Feb. 15-17, 1977.



59. Melosh, R. J., "Basis for Derivation of Matrices for the Direct Stiffness Method," Journal, American Institute of Aeronautics and Astronautics, Vol. 1, No. 7, 1963, pp. 1631-1637.
60. Irons, B. M., "Engineering Application of Numerical Integration in Stiffness Methods," Journal, American Institute of Aeronautics and Astronautics, Vol. 4, No. 11, 1966, pp. 2035-2037.
61. Ang, A. H-S., and N. M. Newmark, "A Numerical Procedure for the Analysis of Continuous Plates," Proc. Second Conf. on Electronic Computation, Structural Division, ASCE, Sept. 1960.

APPENDIX A

TABULATION OF STIFFNESS MATRIX  
AND LOAD VECTOR

### A.1 Stiffness Matrix for Concrete Slab, Stabilized Base, and Overlay

Stiffness matrix for a rectangular, isotropic element, which is a symmetric 12x12 matrix is given as:

$$S(1,1) = (R)(60 G + 60 H + 30 V + 84 U)$$

$$S(2,1) = (R)(-60 H - 30 V - 12 U)B$$

$$S(2,2) = (R)(20 H + 8 U)C$$

$$S(3,1) = (R)(60 G + 30 V + 12 U)A$$

$$S(3,2) = (R)(-15 V)E$$

$$S(3,3) = (R)(20 G + 8 U)D$$

$$S(4,1) = (R)(30 G - 60 H - 30 V - 84 U)$$

$$S(4,2) = (R)(-60 H - 12 U)B$$

$$S(4,3) = (R)(30 G - 30 V - 12 U)A$$

$$S(4,4) = S(1,1)$$

$$S(5,1) = S(4,2)$$

$$S(5,2) = (R)(10 H - 2 U)C$$

$$S(5,3) = 0.$$

$$S(5,4) = -S(2,1)$$

$$S(5,5) = S(2,2)$$

$$S(6,1) = S(4,3)$$

$$S(6,2) = 0.$$

$$S(6,3) = (R)(10 G - 8 U)D$$

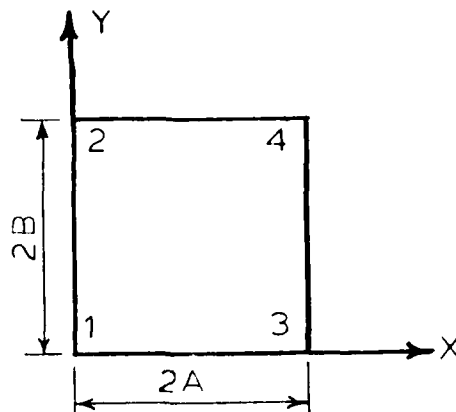
$$S(6,4) = S(3,1)$$

$$S(6,5) = -S(3,2)$$

$$S(6,6) = S(3,3)$$

$$S(7,1) = (R)(-60 G + 30 H - 30 V - 84 U)$$

$$S(7,2) = (R)(-30 H + 30 V + 12 U)B$$



$$\begin{aligned}
S(7,3) &= (R)(60 G + 12 U)A \\
S(7,4) &= (R)(-30G - 30 H + 30 V + 84 U) \\
S(7,5) &= (R)(-30 H + 12 U)B \\
S(7,6) &= (R)(-30 G + 12 U)A \\
S(7,7) &= S(1,1) \\
S(8,1) &= S(7,2) \\
S(8,2) &= (R)(10H - 8 U)C \\
S(8,3) &= 0. \\
S(8,4) &= -S(7,5) \\
S(8,5) &= (R)(5 H + 2 U)C \\
S(8,6) &= 0. \\
S(8,7) &= S(2,1) \\
S(8,8) &= S(2,2) \\
S(9,1) &= -S(7,3) \\
S(9,2) &= 0. \\
S(9,3) &= (R)(10 G - 2 U)D \\
S(9,4) &= -S(7,6) \\
S(9,5) &= 0. \\
S(9,6) &= (R)(5 G + 2 U)D \\
S(9,7) &= -S(3,1) \\
S(9,8) &= -S(3,2) \\
S(9,9) &= S(3,3) \\
S(10,1) &= S(7,4) \\
S(10,2) &= -S(7,5) \\
S(10,3) &= S(7,6) \\
S(10,4) &= S(7,1)
\end{aligned}$$

$$S(10,5) = -S(7,2)$$

$$S(10,6) = S(7,3)$$

$$S(10,7) = S(4,1)$$

$$S(10,8) = S(4,2)$$

$$S(10,9) = -S(4,3)$$

$$S(10,10) = S(1,1)$$

$$S(11,1) = S(7,5)$$

$$S(11,2) = S(8,5)$$

$$S(11,3) = 0.$$

$$S(11,4) = -S(7,2)$$

$$S(11,5) = -S(8,2)$$

$$S(11,6) = 0.$$

$$S(11,7) = S(5,1)$$

$$S(11,8) = S(5,2)$$

$$S(11,9) = 0.$$

$$S(11,10) = -S(2,1)$$

$$S(11,11) = S(2,2)$$

$$S(12,1) = S(9,4)$$

$$S(12,2) = 0.$$

$$S(12,3) = S(9,6)$$

$$S(12,4) = S(7,3)$$

$$S(12,5) = 0.$$

$$S(12,6) = S(9,3)$$

$$S(12,7) = -S(6,1)$$

$$S(12,8) = 0.$$

$$S(12,9) = S(6,3)$$

$$S(12,10) = -S(3,1)$$

$$S(12,11) = S(3,2)$$

$$S(12,12) = S(3,3)$$

where:

$S(i,j)$  = element at i-th row and j-th column

$2A$  = X-dimension of the element

$2B$  = Y-dimension of the element

$$C = 4B^2$$

$$D = 4A^2$$

$$E = 4AB$$

$$F = AB$$

$$G = (B/A)^2$$

$$H = (A/B)^2$$

$$R = \frac{1}{60 AB} \times \frac{Eh}{12(1 - \nu^2)}$$

$$U = \frac{1 - \nu}{2}$$

$E$  = modulus of elasticity

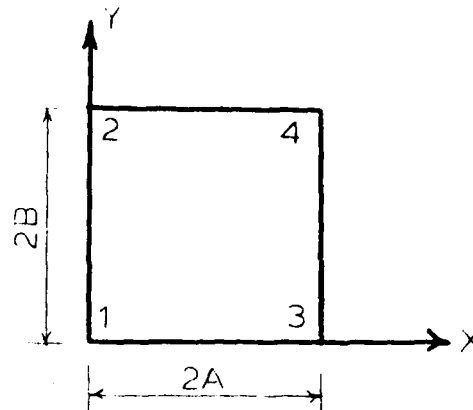
$\nu$  = Poisson's ratio

$h$  = thickness of the element

## A.2 Stiffness Matrix for Subgrade

Stiffness matrix for a rectangular subgrade element resting under concrete slab or stabilized base, which is a symmetric 12x12 matrix is given as:

$$\begin{aligned}
F(1,1) &= 24178 \ Q \\
F(2,1) &= -6454 \ BQ \\
F(2,2) &= 2240 \ B^2Q \\
F(3,1) &= 6454 \ AQ \\
F(3,2) &= -1764 \ ABQ \\
F(3,3) &= 2240 \ A^2Q \\
F(4,1) &= 8582 \ Q \\
F(4,2) &= -3836 \ BQ \\
F(4,3) &= 2786 \ AQ \\
F(4,4) &= 24178 \ Q \\
F(5,1) &= 3836 \ BQ \\
F(5,2) &= -1680 \ B^2Q \\
F(5,3) &= 1176 \ ABQ \\
F(5,4) &= 6454 \ BQ \\
F(5,5) &= 2240 \ B^2Q \\
F(6,1) &= 2786 \ AQ \\
F(6,2) &= -1176 \ ABQ \\
F(6,3) &= 1120 \ A^2Q \\
F(6,4) &= 6454 \ AQ \\
F(6,5) &= 1764 \ ABQ \\
F(6,6) &= 2240 \ A^2Q \\
F(7,1) &= 8582 \ Q \\
F(7,2) &= -2786 \ BQ \\
F(7,3) &= 3836 \ AQ \\
F(7,4) &= 2758 \ Q \\
F(7,5) &= 1624 \ BQ \\
F(7,6) &= 1624 \ AQ
\end{aligned}$$



$F(7,7) = 24178 \ Q$   
 $F(8,1) = -2786 \ BQ$   
 $F(8,2) = 1120 \ B^2Q$   
 $F(8,3) = -1176 \ ABQ$   
 $F(8,4) = -1624 \ BQ$   
 $F(8,5) = -840 \ B^2Q$   
 $F(8,6) = -840 \ A^2Q$   
 $F(8,7) = -6454 \ BQ$   
 $F(8,8) = 2240 \ B^2Q$   
 $F(9,1) = -3836 \ AQ$   
 $F(9,2) = 1176 \ ABQ$   
 $F(9,3) = -1680 \ A^2Q$   
 $F(9,4) = -1624 \ AQ$   
 $F(9,5) = -784 \ ABQ$   
 $F(9,6) = -840 \ A^2Q$   
 $F(9,7) = -6454 \ AQ$   
 $F(9,8) = 1764 \ ABQ$   
 $F(9,9) = 2240 \ A^2Q$   
 $F(10,1) = 2758 \ Q$   
 $F(10,2) = -1624 \ BQ$   
 $F(10,3) = 1624 \ AQ$   
 $F(10,4) = 8582 \ Q$   
 $F(10,5) = 2786 \ BQ$   
 $F(10,6) = 3836 \ AQ$   
 $F(10,7) = 8582 \ Q$   
 $F(10,8) = 3836 \ BQ$   
 $F(10,9) = -2786 \ AQ$



$$F(10,10) = 24178 Q$$

$$F(11,1) = 1624 BQ$$

$$F(11,2) = -840 B^2Q$$

$$F(11,3) = 784 ABQ$$

$$F(11,4) = 2786 BQ$$

$$F(11,5) = 1120 B^2Q$$

$$F(11,6) = 1176 ABQ$$

$$F(11,7) = -3836 BQ$$

$$F(11,8) = -1680 B^2Q$$

$$F(11,9) = 1176 ABQ$$

$$F(11,10) = 6454 BQ$$

$$F(11,11) = 2240 B^2Q$$

$$F(12,1) = -1624 AQ$$

$$F(12,2) = 784 ABQ$$

$$F(12,3) = -840 A^2Q$$

$$F(12,4) = -3836 AQ$$

$$F(12,5) = -1176 ABQ$$

$$F(12,6) = -1680 A^2Q$$

$$F(12,7) = -2786 AQ$$

$$F(12,8) = -1176 ABQ$$

$$F(12,9) = 1120 A^2Q$$

$$F(12,10) = -6454 AQ$$

$$F(12,11) = -1764 ABQ$$

$$F(12,12) = 2240 A^2Q$$

where:

$F(i,j)$  = element at i-th row and j-th column

$2A$  = X-dimension of the element

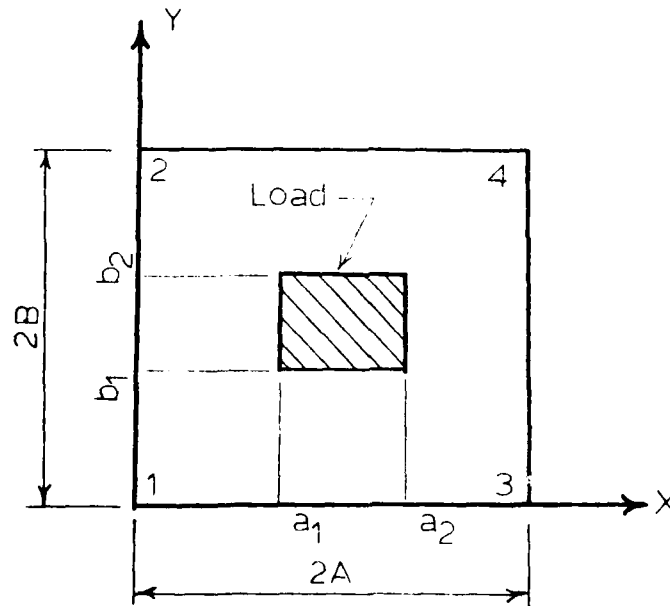
$2B$  = Y-dimension of the element

$$Q = \frac{k}{44100}$$

$k$  = modulus of subgrade reaction

### A.3 Equivalent Nodal Force Vector

The equivalent nodal forces for a uniformly distributed load ( $q$ ), over a rectangular section of the plate element which is a  $12 \times 1$  vector is given as:



$$\begin{aligned} P(1) = & R_1 - (0.75/A^2)R_4 - (0.25/AB)R_5 - (0.75/B^2)R_6 + (0.25/A^3)R_7 \\ & + (0.375/A^2B)R_8 + (0.375/AB^2)R_9 + (0.25/B^3)R_{10} \\ & - (0.125/A^3B)R_{11} - (0.125/AB^3)R_{12} \end{aligned}$$

$$\begin{aligned} P(2) = & -R_3 + (0.5/A)R_5 + (1/B)R_6 - (0.5/AB)R_9 - (0.25/B^2)R_{10} \\ & + (0.125/AB^2)R_{12} \end{aligned}$$

AD-A078 836

ILLINOIS UNIV AT URBANA-CHAMPAIGN DEPT OF CIVIL ENGIN--ETC F/G 13/2  
LONGITUDINAL JOINT SYSTEMS IN SLIP-FORMED RIGID PAVEMENTS. VOLU--ETC(U)  
NOV 79 A M TABATABAIE , E J BARENBERG DOT-FA-11-8474

FAA-RD-79-4-2

NL

UNCLASSIFIED

303

AL  
20 MAR 80



END

DATE

FILED

1 - 80

DOC

$$P(3) = R_2 - (0.5/A)R_4 - (0.5/B)R_5 + (0.25/A^2)R_7 + (0.25/AB)R_8 \\ - (0.125/A^2B)R_{11}$$

$$P(4) = (0.25/AB)R_5 + (0.75/B^2)R_6 - (0.125/A^2B)R_8 - (0.125/AB^2)R_9 \\ - (0.25/B^3)R_{10} + (0.125/A^3B)R_{11} + (0.125/AB^3)R_{12}$$

$$P(5) = (0.25/B)R_6 - (0.25/AB)R_9 - (0.25/B^2)R_{10} + (0.125/AB^2)R_{12}$$

$$P(6) = (0.5/B)R_5 - (0.5/AB)R_8 + (0.125/A^2B)R_{11}$$

$$R(7) = (0.75/A^2)R_4 + (0.25/AB)R_5 - (0.25/A^3)R_7 - (0.375/A^2B)R_8 \\ - (0.375/AB^2)R_9 + (0.125/A^3B)R_{11} + (0.125/AB^3)R_{12}$$

$$R(8) = -(0.5/A)R_5 + (0.5/AB)R_9 - (0.125/AB^2)R_{12}$$

$$R(9) = -(0.5/A)R_4 + (0.25/A^2)R_7 + (0.25/AB)R_8 - (0.125/A^2B)R_{11}$$

$$R(10) = -(0.25/AB)R_5 + (0.375/A^2B)R_8 + (0.375/AB^2)R_9 - (0.125/A^3B)R_{11} \\ - (0.125/AB^3)R_{12}$$

$$R(11) = (0.25/AB)R_9 - (0.125/AB^2)R_{12}$$

$$R(12) = - (0.25/AB)R_8 + (0.125/A^2B)R_{11}$$

where:

$P(i)$  = element at  $i$ -th row

$2A$  = X-dimension of the element

$2B$  = Y-dimension of the element

$$R_1 = q(a_2 - a_1) (b_2 - b_1)$$

$$R_2 = q(a_2^2 - a_1^2) (b_2 - b_1)/2$$

$$R_3 = q(a_2 - a_1) (b_2^2 - b_1^2)/2$$

$$R_4 = q(a_2^3 - a_1^3) (b_2 - b_1)/3$$

$$R_5 = q(a_2^2 - a_1^2) (b_2^2 - b_1^2)/4$$

$$R_6 = q(a_2 - a_1) (b_2^3 - b_1^3)/3$$

$$R_7 = q(a_2^4 - a_1^4) (b_2 - b_1)/4$$

$$R_8 = q(a_2^3 - a_1^3) (b_2^2 - b_1^2)/6$$

$$R_9 = q(a_2^2 - a_1^2) (b_2^3 - b_1^3)/6$$

$$R_{10} = q(a_2 - a_1) (b_2^4 - b_1^4)/4$$

$$R_{11} = q(a_2^4 - a_1^4) (b_2^2 - b_1^2)/8$$

$$R_{12} = q(a_2^2 - a_1^2) (b_2^4 - b_1^4)/8$$

$q$  = tire pressure

$a_1, a_2$  = X-dimensions of the loaded area

$b_1, b_2$  = Y-dimensions of the loaded area